1-1-2000

Luminesence study of polymer-copolymer blends using a carbazole/iodine probe/quencher system

Tammy Davis

LUMINESCENCE STUDY OF POLYMER-COPOLYMER BLENDS USING A CARBAZOLE/IODINE PROBE/QUENCHER SYSTEM

Tammy A. Davis

January 2000

A thesis submitted in partial fulfillment of the requirements for the degree of Master of Science in Chemistry

Approved: _____
Project Advisor

_____
Department Head

Department of Chemistry
Rochester Institute of Technology
Rochester, New York 14623

Copyright Release Form

LUMINESCENCE STUDY OF POLYMER-COPOLYMER BLENDS USING A CARBAZOLE/IODINE PROBE/QUENCHER SYSTEM

I, Tammy A. Davis, hereby grant permission to the Wallace Memorial Library, of R.I.T., to reproduce my thesis in whole or in part. Any reproduction will not be for commercial use or profit.

_____
Signature

4 February '00
Date

Abstract

The miscibility behavior of binary blends of polystyrene (PS), poly(methyl methacrylate) (PMMA) and their copolymers was re-evaluated using the luminescence of carbazole (Cz) and its quenching by 4-iodoaniline (I). The chromophore and quencher probes were polymerized into the polymers and copolymers to be blended. These experiments were conducted at room temperature, on thin films, and were compared to the published results of Braun, et. al.[13] Homopolymer/copolymer blend compositions were selected from regions of miscible, partially miscible, and immiscible phase behavior.

The quencher molecule, 4-iodoaniline, was derivatized to form the vinyl-functionalized monomer, N-(4-iodophenyl)maleimide (NIPMI). The synthesis of NIPMI was carried out in two steps: (1) nucleophilic attack and (2) dehydration.[61] The vinyl-functionalized chromophore, N-vinylcarbazole (VCz), was purchased through Aldrich. The polymers and copolymers used in this study were synthesized by free-radical polymerization using 2,2'-azobisisobutyronitrile (AIBN) to initiate the reaction. The polymers were characterized by proton nuclear magnetic resonance (^{1}H-NMR), differential scanning calorimetry (DSC), thermogravimetric analysis (TGA), and size exclusion chromatography (SEC).

Although there are several identifiable variations between the experimental luminescence results and what was expected based on the values published by Braun,et. al,[13] the results for the miscibility of the homopolymers, PS and PMMA, were as expected. The results for the phase behavior of the homopolymer-copolymer blend systems exhibit a larger deviation away from the results of Braun, et. al. The blends of poly[(methyl

methacrylate)$_{16}$-co-(styrene)$_{82}$-co-(vinylcarbazole)$_2$] ($P(MMA_{16}S_{82}VCz_2)$) and poly[(methyl methacrylate)$_{51}$-co-(styrene)$_{47}$-co-(vinylcarbazole)$_2$] ($P(MMA_{51}S_{47}VCz_2)$) with the quencher tagged PS homopolymer, PS_1, both gave 20-30% relative luminescence intensities rather than the predicted 100%. The blends of poly[(methyl methacrylate)$_{77}$-co-(styrene)$_{22}$-co-(vinylcarbazole)$_1$] ($P(MMA_{77}S_{22}VCz_1)$) and poly[(methyl methacrylate)$_{51}$-co-(styrene)$_{47}$-co-(vinylcarbazole)$_2$] ($P(MMA_{51}S_{47}VCz_2)$) with the quencher tagged PMMA homopolymer, $PMMA_1$, gave nearly 100% relative luminescence intensities rather than the predicted 0% results. Many of these discrepancies may be explained by the polydispersity and the properties of the polymers used in the study. We found, the preparation conditions, specifically regarding oxygen contamination, also play an important role in determining the luminescence characteristics. Taking these factors into account, this luminescence method was found to be a valuable tool in probing the phase behavior of blends on the molecular level, which is a limitation of many methods currently in use.

Acknowledgments

This research could not have been completed if it were not for the support and guidance of those around me. First and foremost, I must thank Dr. Andreas Langner, for his endless supply of wisdom and encouragement. I would also like to thank my committee members, Dr. Paul Craig, Dr. Massoud Miri, and Dr. Kay Turner, for their continued support. I would also like to express my deep appreciation to Dr. Thomas Mourey and Kim Le of Eastman Kodak Company for their guidance in their SEC lab.

On a more personal level, I would like to thank my family and friends. It is their love and faith in me that has sustained me through the darkest hours and given me the strength to achieve my goals.

Table of Contents

List of Figures

List of Tables

I. Introduction

Polymers are continually becoming more specialized and versatile. One method applied to increase the range of available properties for a given polymer or copolymer is the creation of blends. A blend is defined as a mixture of two or more polymers with no covalent bonds between them. With a few exceptions, the existence of a single-phase system is necessary to the usefulness of the blend. Polymers which combine to form a single-phase system are said to be miscible. Polymers which phase separate are termed immiscible.

Polymers have become an integral part of modern industry. Their applications have become extremely diverse and specialized. As the number of specific commercial applications grows, the demand for the development of polymers with specific properties or characteristics also grows. One obvious example of the need for very specific properties may be found in the field of medicine, where polymers are used for coatings on surgical implements,[1] orthopedic repair,[1-3] organ transplants,[3,4] and implants.[2,5,6]

Since the discovery of macromolecules, polymer scientists have focused their attentions on their properties, and how to manipulate or enhance them. In the earlier years, the desire to achieve varied properties manifested itself in the discovery of many new polymers. Soon, it was realized that properties could be altered by using more than one monomer at a time. Copolymerization offers a wider range; however in many cases a compromise, of properties.[7] In recent years, the focus has been shifted to the use of more than one polymer at a time, as polymer blends.

Blends offer a greater range of properties with no change to the compositions of their constituents. An increased range of properties has lead to a greater diversity of

applications. This has provided manufacturers with a broad range of price-per-performance characteristics, giving the blends a high level of value and commercial importance. However, polymer blends must, with a few exceptions, be miscible to assure mechanical compatibility and attain the desired properties. For these reasons, the miscibility of polymer blends has become an important research focus.

Miscibility describes the "solubility" of one polymer or copolymer in another. However, it is important to note that solubility is not synonymous with miscibility since ideal, or random, mixing may not adequately describe the true nature of a blend even if physical properties may suggest solubility.[7] Immiscible polymers exist as a two-phase, heterogeneous system. An immiscible system will exist as various domains within a given system. The domains may include regions of amorphous or crystalline phases, or areas of differing composition. Some immiscible polymer systems have exhibited definite advantages if mechanical compatibility could be achieved. A few examples include high impact polystyrenes and ABS. A high impact polystyrene (HIPS) is a melt blend of polystyrene and rubber, usually polybutadiene. ABS represents acrylonitrile-butadiene-styrene, one type being a mix of styrene/acrylonitrile copolymer with butadiene rubber. In general, however, since the usefulness of polymer blends is based primarily on achieving "blended" properties, miscibility is crucial to the usefulness of the multicomponent system. Most miscible polymers exist as a single, homogeneous phase. Miscibility assures the achievement of mechanical compatibility, with a superposition of properties of the components in a blend.[7]

Several characteristics must be considered when engaging in miscibility studies. These may be classified into two general groups: mechanical compatibility and

polydispersity. Mechanical compatibility is associated with the following properties: (1) good adhesion between substituents; (2) average mechanical properties; (3) behavior of a two-phase block or graft copolymer; and (4) ease of blending.[7] All polymers and copolymers exhibit varying types and degrees of polydispersity. Five areas of polydispersity which may affect the miscibility of a system will be addressed: (1) Molecular weight is the most obvious source of polydispersity. Even those samples which are marketed as mono-disperse contain a measurable molecular weight distribution. (2) Microstructure describes the manner in which repeating units are added to a chain. Several variations are possible with respect to the microstructure of a polymer. Structural isomerism (i.e. cis, trans, racemic, and meso) and sequence isomerism (i.e. head-to-head, head-to-tail) are two examples of differences in microstructure. (3) The degree of branching affects the way a polymer or copolymer arranges itself. Consequently, its other properties depend strongly upon it. A common example is polyethylene, which may be prepared in high and low density forms varying in the amount of branching. Aspects which must be considered include the number, length, and position of the branches. (4) Composition refers to the ratios of the incorporated comonomers. In cases of differing reactivity ratios, the composition of the copolymer may change drastically as the polymerization proceeds. In a severe case, the distribution may be so broad that the copolymer itself will phase separate into two domains of different average composition. (5) The configuration describes the pattern of comonomer arrangement. The order in which the comonomers arrange in the chain has a significant effect on the properties of the copolymer and, therefore, its miscibility. Random, alternating, block, and graft copolymers provide examples of the different sequence types

which may occur. Each of the five characteristics mentioned above contribute to the polydispersity of a polymer system and complicate the evaluation of its miscibility interactions with another unique polymer system.[8] Several studies have been conducted to evaluate the effects of molecular weight,[9, 10] microstructure,[11, 12] composition,[10, 13-17] and sequence type[17-19] on the phase behavior of blends.

There are numerous methods for assessing the miscibility of blends. The simplest of which is the method of direct observation. Miscible polymers with no crystalline phases form thin films that are transparent and homogeneous. However, this method can give ambiguous results. One example of this is the fact that immiscible, completely amorphous polymers also form transparent films if their refractive indices are the same. Another cause of ambiguity occurs when the refractive indices of the amorphous component polymers are different, yet the film appears transparent when the solvent evaporates. Typically, closer examination will reveal that it has actually formed two uniform layers. Another disadvantage of using optical clarity to assess the miscibility of a system is that it is not useful for the study of semi-crystalline polymers.

An improvement to direct observation is the use of microscopy. It is used to visually seek out domains of varying composition using some mode of amplification.[7, 13, 19] As was the case for direct observation, the existence of regions of heterogeneity indicates immiscibility. Prepared films, used in microscopy studies, should be less than five micrometers in thickness to ensure accurate measurements. Visual and phase contrast microscopy require a minimum difference in refractive index to differentiate the domains. Contrast may be enhanced using polarized light or by staining with a chemical agent such as osmium tetroxide.[20] Significant developments were made in phase contrast

microscopy in the 1960's making it a popular method for miscibility studies.[20-23] Transmission Electron Microscopy (TEM) utilizes differences in electron beam intensity passing through a sample to image different domains. Selective chemical reactions or annealing in the electron beam provide the electron opacity factors required for the detection of domains in TEM.[24-26] However, there is always a danger that using chemical agents or temperature changes to enhance image contrast will induce a phase change in the film. Scanning Electron Microscopy (SEM) contrasts a sample's surface topography, or texture. The contrast may be emphasized by breaking the sample in its glassy state and imaging the fracture surface.

Other commonly practiced methods include the measurement of the glass transition temperature (T_g) or melt temperature (T_m).[13, 17, 18] T_g is the temperature at which the long range motion of polymer chains stop and amorphous regions take on glassy properties, like brittleness and rigidity. T_m refers to the melting point of crystalline polymers. Miscible polymer blends exhibit one T_g value, while those which are immiscible exhibit two unique values. However, this method cannot be used when the T_g values are too similar in magnitude to be resolved, or when the heterogeneous domains are smaller than 10 nm.[27, 28] Most sample miscibilities vary over the temperature range being investigated. This is a problem especially when it occurs at $T > T_g$ of all phases.[8] This method is also complicated by the high viscosity of polymers, even well above the T_g values. At low temperatures, polymer interactions are dominated by enthalpy. At high temperatures, the interactions are entropy-dominated. Therefore, at high temperatures, there is a tendency for the long chain coils to exclude other polymers which may have been miscible at lower temperatures. An example of this is the blend of

polystyrene (PS) and a copolymer of poly[(methyl methacrylate)$_{0.15}$-co-(styrene)$_{0.85}$] ($P(MMA_{15}S_{85})$). A thin film of the blend exists as a clear, single phase at temperatures below 25°C and a cloudy, two-phase film at 180°C. As the film is heated above 25°C, it becomes cloudy. The temperature of the onset of phase separation is referred to as the upper critical solution temperature (UCST). The film remains cloudy until it reaches a temperature (above 180°C) referred to as the lower critical solution temperature (LCST). At this temperature a single phase emerges. These features are demonstrated in the phase diagram in Figure 1. There are numerous methods for measuring T_g and T_m values. All of which probe the sample over a large temperature range. Differential scanning calorimetry (DSC) is the most commonly applied method for determining T_g and T_m.

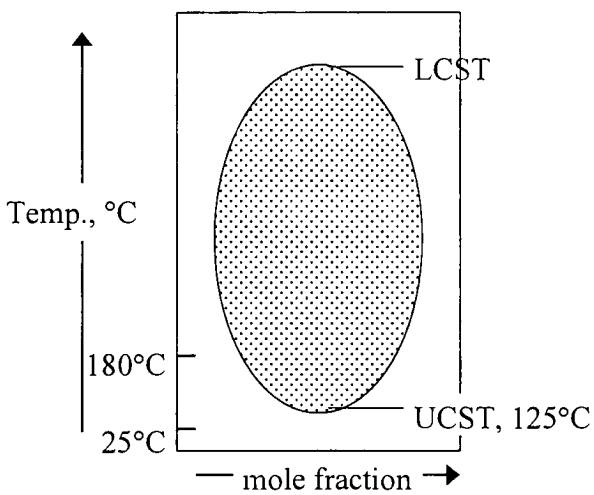

Figure 1. Phase diagram for $P(MMA_{15}S_{85})$/PS blend with upper (UCST) and lower critical solution temperatures (LCST). The white region represents a single phase, the gray region represents a two-phase system.

Cloud point measurement is just one of many scattering methods available.[13, 15] It is used to determine the transition point from the stable, homogeneous state to the turbid state. The transition points or "cloud" points are brought on by changes in temperature, pressure, and composition of the mixture. For example, using the temperature as the variable, an experiment would proceed by heating slowly to a few degrees above the cloud point and cooling back at an equally slow rate to a few degrees below the clearing. The temperatures of first indication and final disappearance of cloudiness are recorded and averaged to obtain each cloud point value. The procedure is repeated for a series of blend compositions, to give enough information to generate a Temperature-Composition Plot.

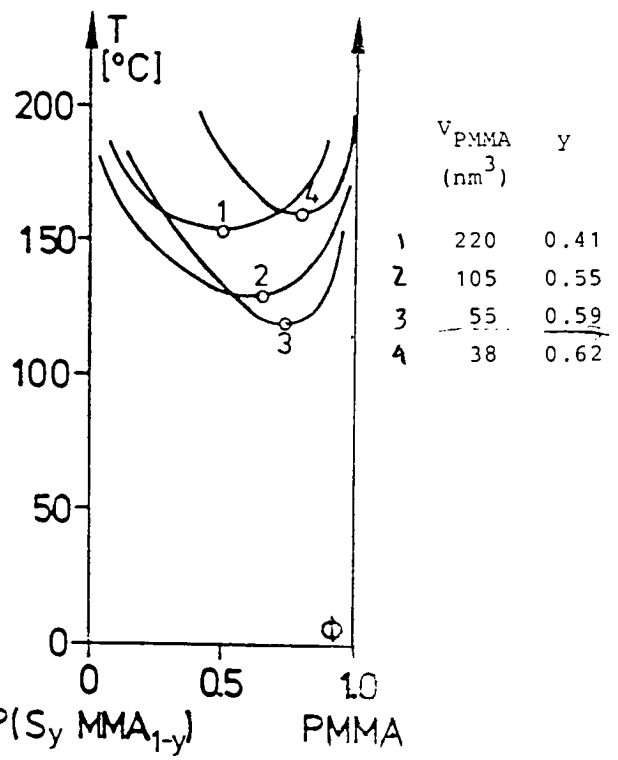

Figure 2. Cloud point diagram for blends of PMMA with varying copolymer compositions of $P(S_yMMA_{1-y})$.[13] The numbered curves represent decreasing chain volumes of PMMA.

This is shown in Figure 2 for the system of poly[(methyl methacrylate)-co-(styrene)] and poly(methyl methacrylate) where V_{PMMA} is the molar volume of PMMA used.[13] V_{PMMA} increases with molecular weight. ϕ represents the volume fractioning or blend ratio composition and y is the mole fraction of styrene incorporated into the copolymer. The area above each of the curves corresponds to a two-phase region. The area below the curves corresponds to a single-phase region. The open circle, where each curve is numbered, represents the UCST for that particular polymer-copolymer blend system. For example, curve 3 for the blend of poly[(methyl methacrylate)$_{0.41}$-co-(styrene)$_{0.59}$] with PMMA (V_{PMMA} = 55 nm^3), the UCST is approximately 125°C.

Dilute solution viscometry is an indirect method for predicting polymer miscibility based on the interactions of two polymers in a dilute solution (ternary system).[29] A problem arises, however, when the data is extrapolated to a binary system (no solvent). Through a series of derivations, two mathematical approaches have been developed. The approaches vary only by the definition of the two-component value of the interaction parameter, b_{12}. Krigbaum & Wall[30] define its value as the geometric mean:

$$b_{12}^{*} = (b1 \times b2)\text{^}0.5 \qquad (1)$$

where b1 and b2 are coefficients that describe homogeneous interactions of polymer molecules that make up the binary blend. Catsiff & Hewett[31] define its value as the arithmatic mean:

$$b_{12}^{**} = (b1 + b2) / 2 \qquad (2)$$

By using the following equation, both define the region of miscibility.

$$(\eta_{sp})_M = \{[\eta]_1 w_1 + [\eta]_2 w_2 + (b_1 w_1^2 + b_2 w_2^2 + 2\, b_{12} w_1 w_2) c_M\} c_M \qquad (3)$$

where $(\eta_{sp})_M$ is the specific viscosity, $[\eta]$ is the limiting viscosity number, w_1 and w_2 are the relative mass fractions of the polymers in the blend, and c_M is the total mass concentration of the polymers. The limiting viscosity number is a viscometric parameter that reflects polymer-solvent interactions based on the chemical nature of the media, the temperature, molecular weight, and molecular weight distribution.[29]

The difference in these theories is most clearly demonstrated by Figure 3. While both approaches agree that a positive deviation from the calculated specific viscosity indicates a miscible system, and a negative deviation indicates immiscibility, there is still a significant difference in the results. Although the Krigbaum & Wall model has more basis in theory, experimental data fits the Catsiff & Hewett model more closely.

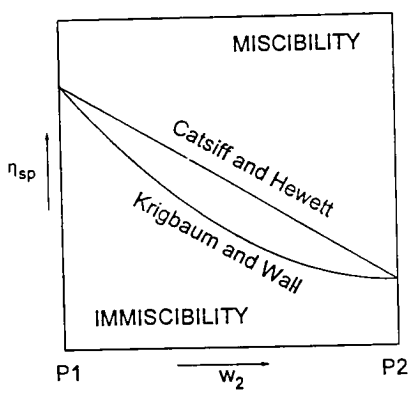

Figure 3. Plot of η_{sp} vs. w_2.[29]

High resolution solid-state NMR has also been used to detect domains of heterogeneity in polymeric mixtures.[32, 33] This is possible due to recent advances in NMR technology involving magic angle spinning . Using a combination of dipolar decoupling, cross-polarization, and rotation of the probe at the "magic angle", the spin

lattice relaxation time, $T_{1\rho}$ (^{1}H), can be used to determine the local environment of a spin within ~2 nm spatial resolution.[32] $T_{1\rho}$ (^{1}H) is measured separately for molecules A and B and is interpreted based on their relative values. If A and B are miscible, $T_{1\rho}^{A}(^1H) = T_{1\rho}^{B}(^1H)$, indicating a single- phase environment. If A and B are immiscible, $T_{1\rho}^{A}(^1H) \neq T_{1\rho}^{B}(^1H)$, indicating a multi-phase environment. While the high resolution of MAS-^{13}C-NMR is an enormous benefit in this work, it suffers from the disadvantage of a poor signal/noise ratio due to the small abundance of ^{13}C.

Inverse gas chromatography can be used to predict the miscibiity of a system.[34, 35] The theory is based on the interaction of miscible polymers to give an exothermic heat of mixing (ΔH_{mix}), which results from the exchange interactions and the free-volume differences between the component materials (ΔV_f). In a polymer-polymer system, the contribution of ΔV_f is small relative to the exchange interaction. Therefore, the focus is on the latter. It has been proposed that ΔH_{mix} of low molecular weight polymer analogues approximate the ΔH_{mix} of polymers in a blend.[34] Inverse gas chromatography is applied to calculate the non-combinatorial free energy of the mixing parameter (or exchange interaction parameter), X_{12}, based on the Flory-Huggins theory of polymer solution thermodynamics. The modeled blend system is predicted to be miscible when X_{12} is negative. The analogues used are typically hydrogenated monomer units of one of the component polymers of the blend, while the second blend component comprises the stationary phase. In simpler terms, the method compares the effective boiling point (BP_{eff}) of the analogue in contact with the second polymer to its single-component boiling point(BP). If $BP_{eff} > BP$, then ΔH_{mix} is negative and the system is considered

miscible. This method is only an approximation based on certain assumptions concerning the behavior of the analogue.

There have been a number of miscibility studies reported in the literature which utilized luminescence.[36-39] This is largely due to the high level of sensitivity that may be achieved by this technique. Two types of photoluminescence may be employed: fluorescence and phosphorescence. A benefit of phosphorescence over fluorescence is that the area probed is larger due to the longer lifetime of the phosphorescent species, allowing larger phase domains to be identified. However, the range of the effective radius must be small enough to probe structure at the molecular level. Since luminescence is of primary interest to this project, it is useful to discuss the theory on which it is based.

Photoluminescence occurs when a photon of light is absorbed by a molecule and, as a consequence, light is emitted. The absorption of light promotes the molecule to a higher energy state by transferring an electron of the highest occupied molecular orbital (HOMO) to its corresponding lowest unoccupied molecular orbital (LUMO), as depicted in Figure 4. Each orbital also has several vibrational states of higher energy which a molecule may be excited to. The molecule relaxes to the lowest vibrational level of each exited state prior to any luminescence. Before the molecule is excited, it is said to be in the ground state (a), which is designated by S_0. In the ground state, the electrons are paired in the HOMO. This pairing leads to a diamagnetic molecule, with a net spin of zero. The term singlet corresponds to the spin multiplicity, which is one. Upon absorption of a photon, the excited singlet state (b), designated S_1, is produced by the promotion of one of the electrons to the LUMO with no change in spin. Therefore the

total spin and multiplicity remain the same as that of the ground state. The triplet state (c), designated T_1, is populated via the mixing of the singlet and triplet wave functions. This is called intersystem crossing. The change in spin of the electron in the LUMO leads to a three fold degeneracy in energy for a total spin of unity. The triplet is said to be paramagnetic. It is highly unlikely that the triplet state will be populated directly from the ground state due to the change in spin. Therefore, it is often referred to as a spin forbidden transition.

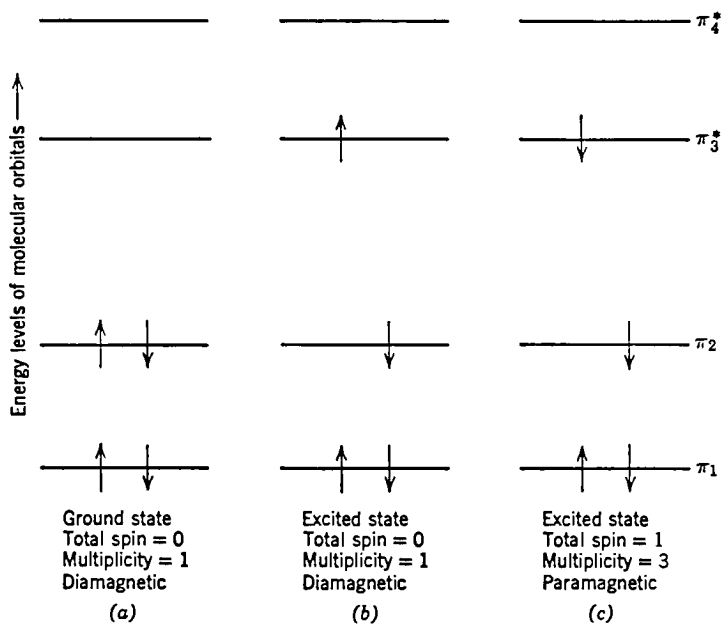

Figure 4. Molecular orbital diagram for butadiene.[40] The HOMO is represented by the π_2 bonding orbital. The LUMO is represented by the π_3^* anti-bonding orbital.

Once excited, the molecule can lose energy in two competing mechanisms: non-radiative and radiative transitions. These are depicted in Figure 5. These processes may

occur in several ways, always resulting in a relaxation to the ground state singlet. Non-radiative processes include vibrational relaxation, internal conversion, intersystem crossing, and chemical reaction. Radiative processes include fluorescence and phosphorescer--

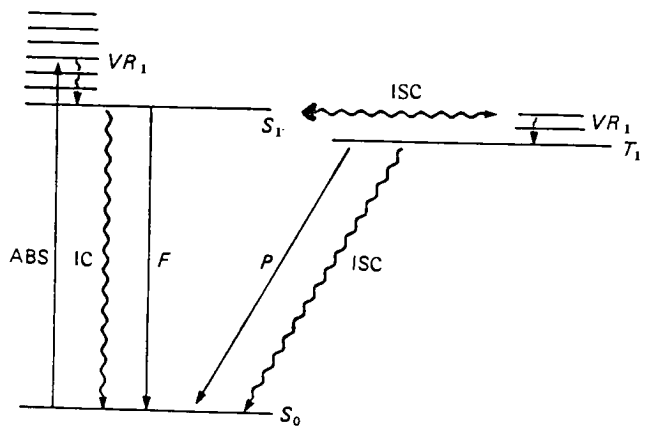

Figure 5. Energy level diagram showing deactivation pathways for a typical organic chromophore.[41]

Non-radiative processes do not result in the emission of a photon as a result of deactivation. The energy is released as thermal energy or heat. Vibrational relaxation (VR_1) is characterized by the loss of energy of a molecule in the excited state due to collisions with other molecules in solution or the solvent. In VR_1, the molecule relaxes from a higher energy vibrational level to a lower energy vibrational level of the same excited state. Internal conversion (IC) refers to the process by which an excited molecule may relax to other states of the same spin quantum number (e.g. $S_1 \rightarrow S_0$). Intersystem crossing (ISC) refers to the process of moving to a state of a different spin quantum number (e.g. $S_1 \rightarrow T_1$).

Radiative processes are those that result in the emission of photons of light having energy, hυ. The expression, hυ, which was proposed by Einstein, describes energy in the form of light where h is Planck's constant, 6.6261 x 10^{-34} joule second, and υ is the frequency in $second^{-1}$. Fluorescence (F) occurs when a photon is released due to transitions which occur between an excited singlet state and the ground state (e.g. $S_1 \rightarrow S_0 + h\upsilon$). Phosphorescence (P) refers to the release of a photon due to a transition between triplet excited states and the singlet ground state of the molecule (e.g. $T_1 \rightarrow S_0 + h\upsilon$). The wavelength of phosphorescent emission is generally longer than that of fluorescence emission. This is due to the lower energy of the triplet state relative to the excited singlet. The lifetime of the fluorescent species is in the range of 10^{-7}-10^{-10} s. Phosphorescent lifetimes are significantly longer, 10^{-3}-10 s. Due to the longer lifetime, there is more opportunity for interactions of the excited molecule with its environment. This allows partial depletion of the triplet state population before a photon can be given off.

Aside from phosphorescence, there is another type of emission which depletes the triplet population.[40-43] Jablonski first proposed the phenomenon of delayed fluorescence (DF) in the mid-1930's, suggesting that it's mechanism involves higher vibrational states of excited triplets and the addition of external thermal energy to encourage the intersystem crossing to an excited singlet.[44] The excited singlet would then relax by fluorescence emission. Delayed fluorescence demonstrates the same spectroscopic character as "spontaneous" fluorescence, but exhibits a significantly longer lifetime.

There are two main types of delayed fluorescence: E-type and P-type. E-type is named for the dye, eosin, which Parker and Hatchard used in many of their studies.[45] It was determined that E-type delayed fluorescence results from the intersystem crossing of

the first excited triplet, T_1, to the first excited singlet, S_1, when the energy difference (ΔE) between the two excited states is small. This is demonstrated in the expression below. The small ΔE corresponds to the activation energy (E_a) of the transition, that must be supplied thermally. If ΔE is greater than 40 kcal/mol, E-type emission is negligible at normal temperatures. E-type DF is not characteristic of unsaturated aromatic hydrocarbons. This is because at the temperature the transition from the excited triplet state to the excited singlet state occurs, quenching processes are more likely.[46] The lifetime, τ_{DF}, of E-type delayed fluorescence is the same as that of the phosphorescent triplet. This is a common diagnostic test for determining if the delayed fluorescence is E-type.[41]

E-type delayed fluorescence:

$$S_0 \xrightarrow{h\nu} S_1 \xrightarrow{ISC} T_1 \xrightarrow{\Delta}_{ISC} S_1$$
$$\downarrow \qquad\qquad \downarrow \qquad\qquad \downarrow$$
$$F \qquad\qquad P \qquad\qquad DF$$

The second type of delayed fluorescence was first observed, by Kautsky, in a fluorescence study, at low temperatures, conducted in the presence of oxygen.[47, 48] Since the temperature was too low for E-type delayed fluorescence, a new mechanism was proposed. Kautsky hypothesized that the transition was bi-photonic in nature. One triplet takes energy from a second triplet, promoting the first to the excited singlet state and reducing the other to the ground state. This is demonstrated in the relationship below.

Oxygen was proposed to absorb the excess energy. The interaction of the two triplets became known as triplet-triplet annihilation when Kautsky's theory was later verified by

P-type delayed fluorescence:

$$T_1 + T_1 \text{ - - - - -> } S_1 + S_0$$

Parker and Hatchard.[49] This type of delayed fluorescence was labeled P-type for the pyrene used in their work. Triplet-triplet annihilation actually proceeds as a resonance interaction, that is quantum mechanical in nature.[50] It was also demonstrated that, since it is a bi-photonic process, the intensity of the delayed fluorescence should vary as the square of the intensity of the excitation beam.[50] This is the diagnostic test commonly used to identify the presence of P-type delayed fluorescence. Kinetic analysis has indicated that the lifetime of P-type emission exhibits first order decay and is half that of the corresponding phosphorescence.[41]

Of particular interest in this application of luminescence is the work of Lin Qiao, who used a phosphorescent probe/quencher system to evaluate the miscibility properties of the homopolymers, polystyrene (PS) and poly(methyl methacrylate) (PMMA).[39] The polymers were modified by incorporating the chromophore, benzophenone, into one polymeric component of the binary polymeric mixture to be studied. A signal modifier was incorporated into the second polymer of the blend. The modifier in this experiment was the quencher molecule, 4-iodoaniline. The iodine of the quencher molecule facilitates the quenching of the phosphorescent emission by a mechanism known as the heavy atom effect. This will be discussed in detail later. In a miscible system, the

luminescent probe approaches the quencher probe within its quenching radius, thus quenching the signal. In an immiscible system, the quencher and the chromophore cannot approach each other, and therefore there is no affect on the phosphorescent emission.

The purpose of the present research is to evaluate the applicability of a different phosphorescent probe system for miscibility studies of known polymer blends. This research parallels that of Qiao in many ways, but with several major differences. Carbazole is the incorporated chromophore for this project. Carbazole is known to exhibit P-type delayed fluorescence. The signal modifier, 4-iodoaniline, remains the same. The experiments are performed at room temperature using thin films of the polymer blends. First, the experiment is conducted on the homopolymers, PS and PMMA, both with themselves and with each other. This is done to demonstrate the effectiveness of the probe system on the simplest system. Next, copolymer compositions (S_x MMA_{1-x}) were selected in regions corresponding to their miscibility, immiscibility, and partial miscibility with PS and PMMA. These are presented in Table 1. The selections were made based on the miscibility diagram of Braun (Figure 6), determined using light microscopy and DSC to evaluate cast films at high and low temperatures.

N-ethylcarbazole is considered to be the best analog of the polymerized N-vinyl-carbazole. Upon incorporation into the copolymers, the double bond of N-vinylcarbazole becomes saturated. The emission spectra of N-ethylcarbazole at two temperatures are given in Figure 7.[52] The fluorescence is exclusively ultraviolet in nature. It is analogous to fluorene with the additional influence of the imido group on the fluorescence of the benzene rings.[43] The fluorescent lifetime (τ_F) of carbazole is 15-16 ns in solution.[51] Delayed fluorescence commonly occurs in the carbazole system due to triplet-triplet

annihilation. This type of delayed fluorescence is referred to as P-type. Several characteristic trends of P-type delayed fluorescence have been observed in carbazole luminescence, such as $\tau_F = \frac{1}{2} \tau_P$ and that the delayed fluorescence intensity increases with the excitation intensity. The temperature has little effect on the fluorescence bands.

Table 1. Selected blend systems for study.

Miscible	PS / $P(S_{0.95}MMA_{0.05})$	PMMA / $P(S_{0.25}MMA_{0.75})$
Partially Miscible	PS / $P(S_{0.85}MMA_{0.15})$	PMMA / $P(S_{0.50}MMA_{0.50})$
Immiscible	PS / $P(S_{0.50}MMA_{0.50})$	PMMA / $P(S_{0.85}MMA_{0.15})$

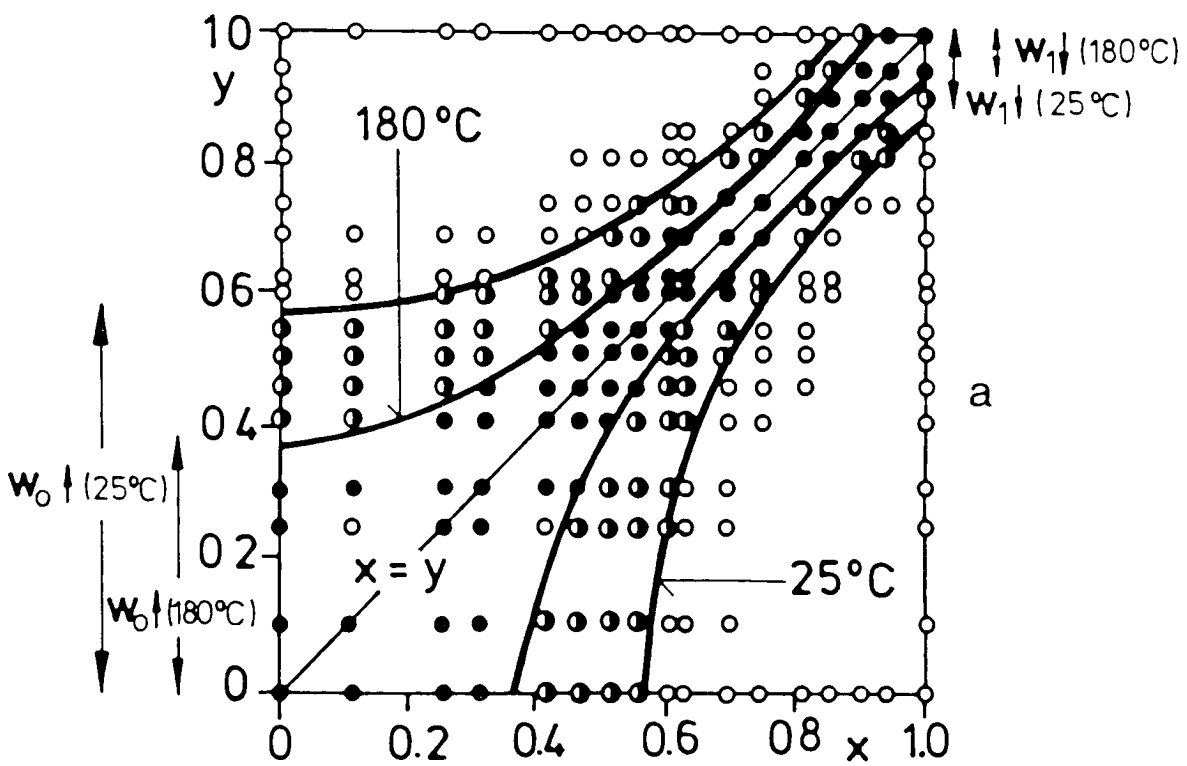

Figure 6. Phase diagram of copolymer blends of $P(S_xMMA_{1-x}) / P(S_yMMA_{1-y})$.[13]
● : one phase, ○ : two phases, ◑ : one phase at 25°C, but two phases at 180°C.

The phosphorescence spectrum of carbazole lies at shorter wavelengths than those of many corresponding hydrocarbons. It also exhibits a longer lifetime. The phosphorescent lifetime (τ_P) of a rigid solution at 77 K is 7-8 seconds.[53] At room temperature, the phosphorescence is quenched, as demonstrated in Figure 7, due to collisions with other molecules in solution and solvent molecules. Therefore, it is necessary to consider carbazole in a solid state, such as the polymer matrix applied in this research. The study by Williamson and MacCallum, however, revealed that the phosphorescence lifetime of carbazole in a polymer matrix is sensitive to the identity of the matrix.[54] They determined that τ_P of carbazole is ~2.2 seconds at a concentration of 0.182 M in PS and ~2.8 seconds at a concentration of 0.2467 M in PMMA. The matrix effect will be discussed in detail later.

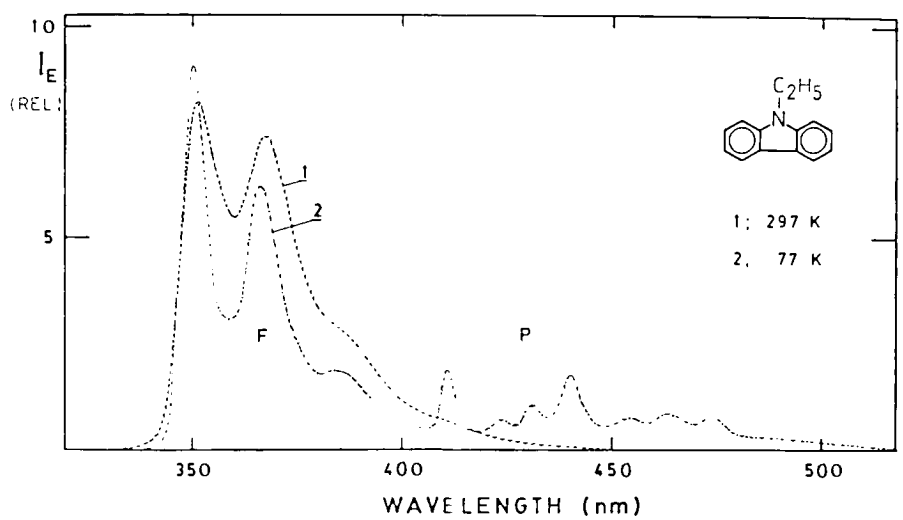

Figure 7. Emission spectra of N-ethylcarbazole at 297 K (λ_{ex} = 293) and at 77 K (λ_{ex} = 295).[52] The concentration is 1 x 10^{-5} M in the mixed solvent, ethyl ether : iosopentane : ethanol (5:5:2 by volume).

Since the (0,0) bands of the carbazole spectrum are intense, and typically display totally symmetrical vibrations, the population of the excited triplet state is not considered to be symmetry forbidden. This is demonstrated by the vibrational structure and intensity distribution of the phosphorescence emission spectrum. The energy level diagram and vibronic transition energies based on the absorption and luminescence spectra at 77K are given in Figure 8 for N-ethylcarbazole.[52]

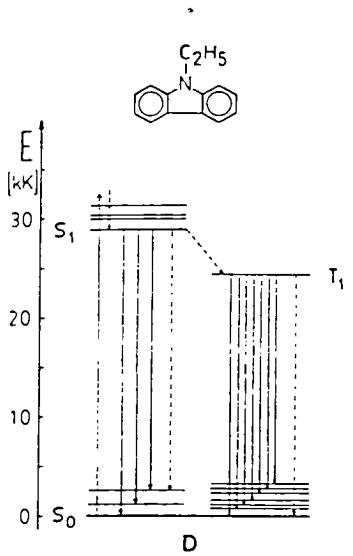

Vibronic transitions	υ (± 50 cm^{-1}) cm-1	nm
$S_0 \rightarrow S_1$		
0 → 0	28820	347
0 → 1	29850	335
0 → 2	30210	331
0 → 3	31250	320
$S_0 \rightarrow S_2$		
0 → 0	33960	294
0 → 1	34780	288
0 → 2	35460	282
$S_1 \rightarrow S_0$		
0 → 0	28570	350
0 → 1	27320	366
0 → 2	25970	385
$T_1 \rightarrow S_0$		
0 → 0	24330	411
0 → 1	23590	424
0 → 2	23150	432
0 → 3	22730	440
0 → 4	21980	455
0 → 5	21600	463
0 → 6	21100	474

Figure 8. Energy level diagram and vibronic transition energies of N-ethylcarbazole.[52]

Carbazole has been the subject of numerous luminescence studies.[52, 54-60] Another spectroscopic study was conducted by Johnson on carbazole and four of its N-substituted

derivatives, including N-vinylcarbazole, using photoselection techniques.[55] Measurements were made in polar and nonpolar solutions at room temperature and at 77K. Johnson demonstrated that the absorption spectrum of carbazole gives four distinct bands at 345, 295, 264, and 246nm. This was also true of N-ethylcarbazole and N-isopropylcarbazole, whose spectra were very similar to that of carbazole. However, Johnson noted that the absorption band at 264nm is not present in the unsaturated derivatives, N-vinylcarbazole and N-phenylcarbazole. They gave similar spectra to each other. The polarity of the solvent had no effect on the intensities of the absorption and emission spectra. Carbazole was not soluble in the nonpolar solvent at 77 K and was therefore not studied under these conditions. A study of the N-substituted derivatives revealed the general trend that the unsaturated systems did not phosphoresce at 77 K. It is believed that this is because the unsaturation is α to the carbazole.

Williamson and MacCallum, in an effort to evaluate the usefulness of polymer matrices as substrates in phosphorescence experiments, used the lifetimes of carbazole and N-ethylcarbazole as their standard of comparison.[54] Polymer solutions containing various concentrations of carbazole were prepared and cast as films. The lifetime measurements were made over the broad temperature range of 80-298 K. Polystyrene and poly(methyl methacrylate) were the matrices tested. Williamson and MacCallum found that the phosphorescence lifetime of a chromophore in a homopolymer matrix is influenced by several factors, including concentration, temperature, and the identity of the matrix. Delayed fluorescence was observed at 380 nm, with $\tau_{DF} < \tau_P$. They found that the polymer matrix deactivates the excited triplet state via non-radiative decay (NR) and

energy transfer to the matrix. NR is more pronounced at higher temperatures, due to the temperature-dependent term of the derived equation,

$$k_{NR} = k^0_{NR} + A \exp(-E/RT). \quad (4)$$

At lower temperatures the temperature-dependent term is negligible. An increase in the concentration of chromophore also lead to a decreased lifetime. This was explained in terms of delayed fluorescence and T_1-T_1 annihilation. The triplet population is increased due to the increased concentration, providing more opportunity for triplet-triplet collisions to occur.

Another study was designed to evaluate solvent penetration and site accessibility of labeled copolymers. Carlier used carbazole as an energy transfer donor to probe the micro-environment of these systems by measuring the non-radiative fluorescence energy transfer (NRET), or quenching in the presence of an acceptor.[56] Anthracene, the energy transfer acceptor, was dispersed in the solvent for these experiments. NRET occurs by the transfer of energy form the donor to the acceptor by a dipole-dipole resonance mechanism. The efficiency of NRET is dependent on the overlap of the emission spectrum of the donor and the absorption spectrum of the acceptor, the distance between the dipoles, and the dipole orientations. Given that the overall energy transfer constant, K, is sensitive to solvent and polymer structure, information about the system may be obtained from them. Carlier applied the Stern-Volmer equation to extract the K values for the systems studied. The Stern-Volmer equation is given by:

$$I_{F(0)} / I_{F(DA)} = 1 + k_T \tau_{F(0)} [A] \quad (5)$$

where $I_{F(0)}$ is the fluorescence intensity of the isolated donor, $I_{F(DA)}$ is the fluorescence intensity of the donor in the presence of the acceptor, k_T is the rate of energy transfer, $\tau_{F(0)}$

is the lifetime of the isolated donor, and [A] is the concentration of acceptor. The equation may also be expressed as:

$$I_{F(0)} / I_{F(DA)} = 1 + K [A] \quad (6)$$

The overall energy transfer constants may be derived from a series of measurements by plotting the ratio of intensities vs. the acceptor concentration, with K as the slope.

The carbazole/anthracene pair is effective in probing the local environment of the probe for a range of 2-3nm. This is equivalent to the scale of polymer-solvent molecular interactions.

If the interaction between the probe and the quencher leads to the coupling of the orbitals and the spin motions of electrons, the spin multiplicities are altered resulting in a perturbation of the electronic states. This is the mechanism by which a triplet acquires some singlet character and, conversely, a singlet acquires some triplet character. This process may occur in both radiationless and photoactive transitions between the singlet and triplet states, (i.e. intersystem crossing and phosphorescence, respectively.) For "light" elements or molecules made up of light elements, such as carbon and hydrogen, the spin-orbit coupling is small. For "heavy" elements, like iodine and bromine, there is a high degree of spin-orbit coupling interactions. These interactions facilitate the modification of spin states for the processes mentioned above. This is commonly referred to as the heavy atom effect. There are two other factors that may affect spin-orbit coupling. The first is similar to the heavy atom effect. Paramagnetic molecules exhibit heterogeneous magnetic fields. This increases spin-orbit coupling. Finally, spin-orbit coupling is enhanced through the formation of complexes by charge transfer. These

factors may work together to alter the spin states of the molecules, however, typically one is dominant.

Spin-orbit coupling increases the occurrence of all three spin state transitions; (1) intersystem crossing ($S_1 \leftrightarrow T_1$), (2) phosphorescence ($T_1 \rightarrow S_0 + h\upsilon$), and (3) radiationless relaxation to the ground state ($T_1 \rightarrow S_0$) to different degrees. The dominant mechanism under a given set of experimental conditions must be determined for each chromophore individually. Some common criteria for the determination of the enhancement of each of the transitions is as follows:

(1) Intersystem crossing ($S_1 \rightarrow T_1$) is characterized by an increase in quantum yield, ϕ_P, of phosphorescence and a corresponding decrease in the fluorescence quantum yield, ϕ_F. This results in a greater value for ϕ_P/ϕ_F.

(2) Phosphorescence ($T_1 \rightarrow S_0 + h\upsilon$) is characterized by a decrease in the phosphorescent lifetime and an increase in the strength of triplet-singlet absorption.

(3) Radiationless relaxation to the ground state ($T_1 \rightarrow S_0$) is characterized by a decrease in quantum yield, ϕ_P, of phosphorescence and a decrease in phosphorescence lifetime.

Abbott and Vo-Dinh used room temperature phosphorescence (RTP) in the selective analysis of azaarenes in the presence of homocyclic polyaromatic hydrocarbons (PAH).[57] The selectivity of the method was based on the influence of mercury(II)chloride on the components of a mixture of polynuclear aromatic (PNA) compounds or heterocyclic PAHs. RTP of azaarenes, compounds containing nitrogen in a six-member aromatic ring, was enhanced in the presence of mercury(II) chloride, while the mercury

had a quenching effect on the PAHs. Carbazole was among the PNAs studied. This indicates that not all nitrogen-containing heterocyclics have enhanced emission in the presence of Hg(II). Carbazole has a nitrogen in its five-member indole-type ring. It was suggested that nitrogen heteroatoms behave as Lewis bases and, therefore would complex with transition metals. It was further suggested that the heterocyclic PAHs are poor donors and may not be sufficiently basic to promote coordination to the Hg(II) cation.

In a previous study, Vo-Dinh and Hooyman demonstrated the effect of six heavy atom salts on the phosphorescence emission of various PNAs, including carbazole.[58] Table 2 gives the six heavy-atoms whose effects were evaluated and the corresponding heavy-atom enhancement factors for two common phosphores. The heavy-atom enhancement factor, f_s^{HA}, is defined as the ratio of the phosphorescence emission with the heavy-atom (HA) to the phosphorescence emission without:

$$f_s^{HA} = [(i_s^{HA} - i_b^{HA}) / (i_s - i_b)] * c_s / c_s^{HA} \quad (7)$$

where i_s and i_b are the RTP signal of the sample S and the blank B respectively, c_s is the concentration of the sample. The phosphorescence spectra of carbazole adsorbed on filter paper in the presence of most of the heavy atoms of Table 2 are shown in Figure 9.[57]

Table 2. Phosphorescent Enhancement Factor f_s^{HA} for carbazole and quinoline.[57]

Compound	Conc. M	$AgNO_3$ 0.5 M	CsI 0.2 M	NaI 2 M	NaBr 2 M	$Pb(OAc)_2$ 0.5 M	$LiClO_4$ 2 M
Carbazole	10^{-4}	0	72	75	18	35	2
Quinoline	10^{-4}	40	15	12	75	210	4

Iodide salts function as heavy-atom perturbers by increasing the rate of ISC and population of the excited triplet state resulting in the enhancement of carbazole

phosphorescence. However, iodo-compounds function as heavy-atom perturbers by increasing the rate of radiationless relaxation of excited state triplets to the ground state, resulting in a decrease in carbazole phosphorescence intensity.

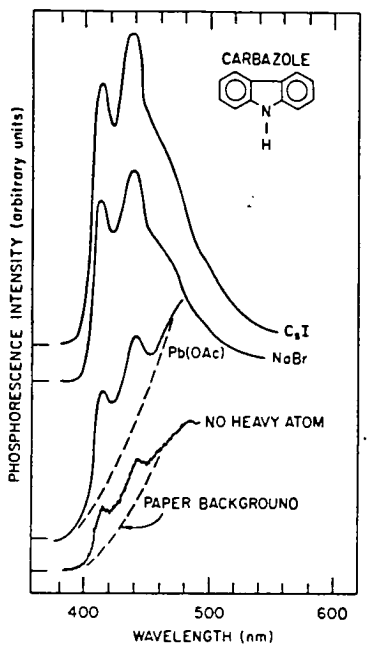

Figure 9. RTP spectra of carbazole with various heavy atoms.[57]

The miscibility of known binary blend systems of PS, PMMA and their copolymers is evaluated by the phosphorescence of carbazole and its quenching by 4-iodoaniline, incorporated into the polymers and copolymers in the experiments that follow. These experiments are designed with specific questions in mind: Is the carbazole/iodine chromophore/quencher system effective in probing the miscibility of binary blends of PS/PMMA homopolymers? of P(S-MMA) copolymers? What role, if any, will delayed fluorescence play in the study?

II. Experimental

A. Materials and Synthesis

Solvents. Chloroform was dried over anhydrous calcium chloride. The 1,4-dioxane and benzene were used as received and blanketed with nitrogen between uses.

Reagents. Sodium acetate, acetic anhydride, 2,2'-azobisisobutyro-nitrile (98%) (AIBN), 4-iodoaniline (98%), and maleic anhydride (99%) were purchased from Aldrich. All reagents were used as received with the exception of maleic anhydride which was sublimed and stored in a dessicator prior to use.

Monomers. Styrene (99+ %) (S) was purchased from Aldrich. It was run through a disposable inhibitor removal column (Aldrich) to remove the inhibitor, 10-15 ppm 4-tert-butyl catechol (TBC), which acts as a free radical trap to prevent polymerization during storage. Methyl methacrylate (99%) (MMA) was purchased from Aldrich and run through a disposable inhibitor removal column (Aldrich) to remove 10-100 ppm monomethyl ether hydroquinone (MEHQ). N-Vinyl carbazole (98%) (VCz) was purchased from Aldrich and stored in a dessicator prior to use.

N-(4-iodophenyl)maleimide (NIPMI) was synthesized in a two step process developed by Searle.[61] The first step is the nucleophilic attack of nitrogen of 4-iodoaniline on one of the carbonyls of maleic anhydride to form the N-(4-iodophenyl) maleamic acid (NIPMA) intermediate. NIPMA is dehydrated in the second step to form NIPMI. The synthetic route is shown in Figure 10.

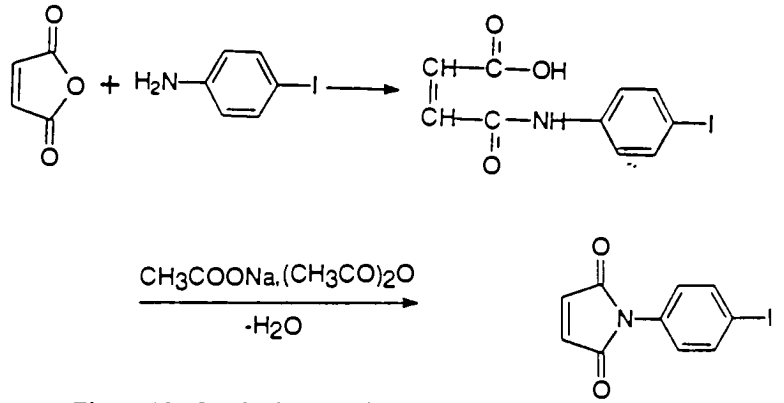

Figure 10. Synthetic route for N-(4-iodophenyl)maleimide.

In a dry 250-mL round bottom flask, 0.9806 g (10 mmol) maleic anhydride was dissolved in 10 mL chloroform. In an addition funnel, 2.1903 g (10 mmol) 4-iodo-aniline was dissolved in 10 mL chloroform. The contents of the addition funnel were added dropwise with vigorous stirring. Using an ice bath, the temperature was maintained below 10°C for 30 minutes to form NIPMA. It was not isolated. The dehydration of the acid resulted through the addition of approximately 0.41 g (5 mmol) anhydrous sodium acetate, 10.21 g (100 mmol) acetic anhydride, and 10 mL chloroform to the reaction. With stirring, the reaction is heated at 70 °C for 2 hours. Afterward, the reaction was washed several times with water. The washes were extracted with cyclohexane to recover lost product. The cyclohexane and chloroform were evaporated and the residue was recrystallized twice by heating and cooling in cyclohexane. The product was dried in a vacuum oven at 40 °C for 24 hours. The process gave a 63.06 % percent yield. The melting point was 160-161 °C.

Polymers and Copolymers. There are three controls in this study: polystyrene (PS) and poly(methyl methacrylate) (PMMA), and a 50:50 copolymer of methyl methacrylate and styrene ($P(MMA_{50}S_{50})$). An additional reference used was a

commercial high molecular weight PS. The homopolymers, PS and PMMA, were used as received. The PS controls, one with a M_w of ~127,000 g/mol (labeled "med. molecular weight") and the other labeled "high molecular weight", were made by Monomer-Polymer and Dajac Laboratories, Inc. The PMMA control, with a M_w of ~120,000 g/mol, was purchased from Aldrich. The PMMA contained 5% toluene. The third control, $P(MMA_{50}S_{50})$, was copolymerized by the procedure described below, omitting the tag. The feed ratio for the 50/50 copolymer was 0.4850 mol (4.8858 g) MMA and 0.5150 mol (5.3637 g) S based on the reactivity ratios, r1 and r2, of 0.54 and 0.43, respectively.[62]

Tagged Copolymers. The tagged polymers were synthesized by free radical polymerization. The monomer feed ratios for each targeted copolymer were determined by the following equation from Painter:

$$
\begin{aligned}
& d[M_1]:d[M_2]:d[M_3] = \\
& [M_1]\left\{\frac{[M_1]}{r_{31}r_{21}} + \frac{[M_2]}{r_{21}r_{32}} + \frac{[M_3]}{r_{31}r_{23}}\right\}\left\{[M_1] + \frac{[M_2]}{r_{12}} + \frac{[M_3]}{r_{13}}\right\} \\
& :[M_2]\left\{\frac{[M_1]}{r_{12}r_{31}} + \frac{[M_2]}{r_{12}r_{32}} + \frac{[M_3]}{r_{32}r_{13}}\right\}\left\{[M_2] + \frac{[M_1]}{r_{21}} + \frac{[M_3]}{r_{23}}\right\} \\
& :[M_3]\left\{\frac{[M_1]}{r_{13}r_{21}} + \frac{[M_2]}{r_{23}r_{12}} + \frac{[M_3]}{r_{13}r_{23}}\right\}\left\{[M_3] + \frac{[M_1]}{r_{31}} + \frac{[M_2]}{r_{32}}\right\}
\end{aligned}
\qquad (8)
$$

where [M] is a concentration of monomer and r is a reactivity ratio.[65]

The reactivity ratios employed in the calculations are tabulated in Table 3 and Table 4. Table 3 refers to the reactivity ratios for the monomers of the copolymers containing the luminescent probe. Table 4 corresponds to the reactivity ratios for the monomers of the copolymers containing the quencher probe. An assumption was necessary in the selection of the reactivity ratios for NIPMI. These values were not found

Table 3. Reactivity Ratios for Ternary Copolymers of S, MMA, and VCz

M_1	Methyl methacrylate
M_2	Styrene
M_3	N-Vinyl carbazole

		Reference
r_{12}	0.54	62
r_{13}	2.00	63
r_{21}	0.43	62
r_{23}	5.7	63
r_{31}	0.04	63
r_{32}	0.035	63

Table 4. Reactivity Ratios for Ternary Copolymers of S, MMA, and NIPMI

M_1	Methyl methacrylate
M_2	Styrene
M_3	N-(4-iodophenyl)maleimide [N-phenyl maleimide]

		Reference
r_{12}	0.54	62
r_{13}	0.91	64
r_{21}	0.43	62
r_{23}	0.07	64
r_{31}	0.30	64
r_{32}	0.01	64

Table 5. Summary of the calculated feed ratios for the synthesized polymers. (F = incorporation, f = feed, MW = molecular weight in g/mol, d = density in g/mL, mol = quantity in moles, g = weight in grams, vol = volume in mL)

F		f			
MMA : S : VC_z(NIPMI)		MMA	S	VC_z	NIPMI
	MW	100.12	104.15	139.20	299.07000
	d	0.936	0.909		
49:49:02	mol	0.0428	0.0488	0.0084	
	g	4.2851	5.0825	1.1693	
	vol	4.58	5.59	-	
74:24:02	mol	0.0772	0.0172	0.0056	
	g	7.7293	1.7914	0.7795	
	vol	8.26	1.97		
14:84:02	mol	0.0070	0.0830	0.0100	
	g	0.7008	8.6445	1.3920	
	vol	0.75	9.51	-	
04:94:02	mol	0.0020	0.0880	0.0100	
	g	0.2002	9.1652	1.3920	
	vol	0.21	10.08		
98:00:02	mol	0.0960	0.0000	0.0040	
	g	9.6115	0.0000	0.5568	
	vol	10.27	0.00		
00:98:02	mol	0.0000	0.0900	0.0100	
	g	0.0000	9.3735	1.3920	
	vol	0.00	10.31	-	
49:49:(02)	mol	0.0478	0.0518		0.00400
	g	4.7857	5.1862		1.19628
	vol	5.11	5.71		-
98:00:(02)	mol	0.0980	0.0000		0.00200
Run synth 2X	g	9.8118	0.0000		0.59814
	vol	10.48	0.00		-
00:98:(02)	mol	0.0000	0.0999		0.00015
Run synth 2X	g	0.0000	10.3994		0.04486
	vol	0.00	11.44		-

in the literature. Since iodine behaves similarly to hydrogen, in terms of electron-withdrawing ability, it was assumed that the reactivity ratios of NIPMI would closely resemble those of N-phenyl maleimide.

Table 5 summarizes the calculated feed ratios for each of the targeted copolymers. The mole ratios are scaled to produce 0.1000 moles of product.

Prior to the synthesis, the glassware was dried in an oven set above 150 °C. The set-up shown in Figure 11 was assembled in a hood and purged with dry nitrogen for 15 minutes prior to the charging of the monomers. The inhibitors were removed as needed and the monomers were charged to the reaction vessel with 100 mL 1,4-dioxane and 0.02 g AIBN (1.2×10^{-4} mol). A bubbler containing mineral oil was used to maintain a positive pressure of nitrogen in the reaction flask throughout the synthesis. The reaction was carried out at 70 °C and was run for 8 hours. The polymers were then precipitated in a large amount of cold methanol, filtered, washed, and reprecipitated. The reprecipitation was performed in 1,4-dioxane with a cold methanol drownout.

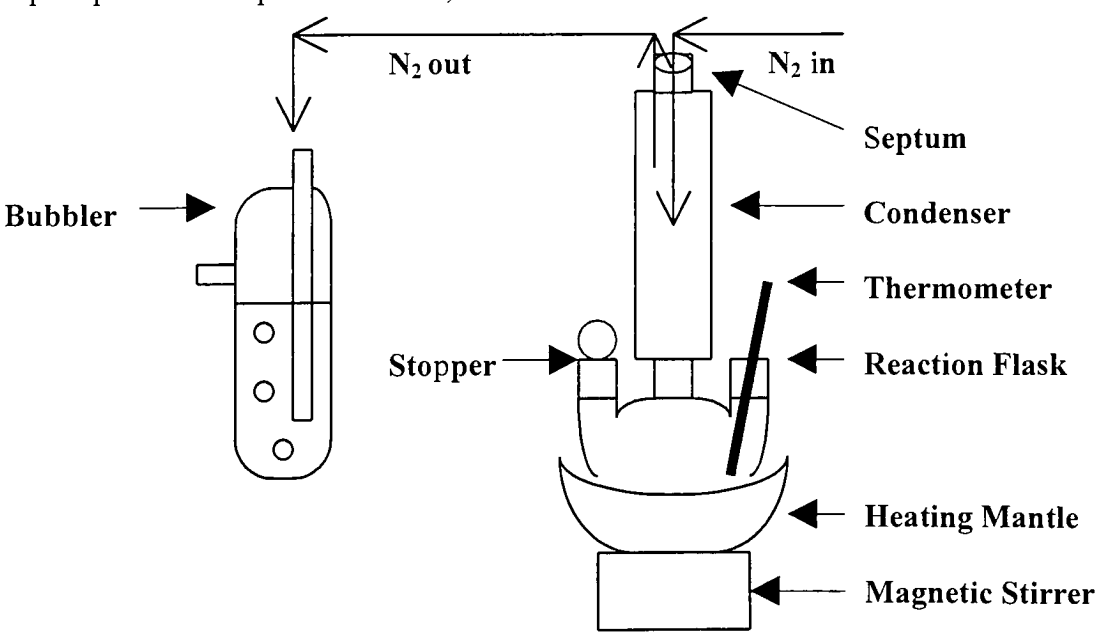

Figure 11. Polymerization reaction set-up.

B. Characterization

Fourier Transform Infrared Spectroscopy (FTIR). Infrared spectroscopic analysis was performed on a Bio-Rad Excalibur Series FTS 3000 FTIR spectrometer. The software employed was Bio-Rad Merlin, Bio-Rad Laboratories, Version 1.1A, ©1993-1998. Samples were prepared in the form of potassium bromide (KBr) pellets. Data was collected in transmission mode from 4000-400 cm^{-1}, at a resolution of 4 cm^{-1}. The air background and sample scans represent an average over 20 scans.

Proton-Nuclear Magnetic Resonance (^{1}H-NMR). NMR spectra were collected using a Bruker 300 spectrometer. The solvent used was deuterated dichloromethane. The NMR frequency is 299.9 MHz. Chemical shifts are reported in parts per million (ppm). Instrument control and data collection are performed via the UNIX based software, ICON-NMR 1.3.a.4, © Bruker Analytik GmbH 1997. The gathered data is analyzed by XWIN-NMR 1.3, © 1996.

Differential Scanning Calorimetry (DSC). DSC was performed using a TA Instruments DSC-2010 Differential Scanning Calorimeter. Ten milligrams of polymer were weighed into a sealed aluminum pan. A nitrogen (Air Products) atmosphere was maintained throughout the experiment at a flow of 50 mL/min. A sealed empty pan was used as the reference. The samples were equilibrated at 150 °C and cooled to 50 °C at a rate of 10 °C/min. After this temperature was held constant for five minutes, the temperature was then ramped back up to 150 °C at a heating rate of 10 °C/min. Instrument control was achieved via Thermal Advantage 1.0F, © 1999 TA Instruments, Inc. The thermograms were analyzed by Universal Analysis for Windows 95/98/NT, Version 2.5H, © 1998-1999.

Thermogravimetric Analysis (TGA). TGA was performed on a TA Instruments TGA-2050 Thermogravimetric Analyzer equipped with a TA Instruments Gas Switching Accessory. A nitrogen (Air Products) atmosphere was maintained throughout the experiment at a flow of 90 ml/min. A platinum sample pan was used to contain the polymer samples. The furnace chamber was equilibrated at 50°C and data was collected as the temperature was increased to 600°C at a rate of 10°C/min. The gas was then switched to air (Air Products) and the temperature held at 600°C to ensure the removal of all residues from the sample pan. Instrument control and data analysis were performed using the same software as was used for the DSC.

Size Exclusion Chromatography (SEC). The SEC data was collected using three Polymer Laboratories Plgel mixed-C, 7.5 x300 mm SEC columns and a multidetector system to monitor the separation. The detectors employed were ultraviolet (UV), differential viscometry (DV), differential refractive index (DRI), and light scattering (LS) at 15 and 90 degrees. The UV detector, Spectroflow 757 Absorbance Detector, recorded the intensity at 270 nm. The DV detector, Viscometer Detector H502a, was supplied by Viscotek Corporation. The DRI detector was a Waters model 410. The LS detector, KMX-6 LALLS photometer, was supplied by LDC Analytical. The columns and LS, DV, DRI detectors were operated at 35.0 °C. HPLC-grade tetrahydrofuran (THF) (J.T.Baker) was the eluent, pumped at a flow rate of 1.0 mL/min. Flow rate corrections were made using acetone as a flow marker. Acetone was present in the sample solvent, THF, at 0.2% levels. The samples were prepared at concentrations of 2 mg/mL and injected as 100 μL volumes. A universal calibration method was used to interpret the results, based on a narrow molecular weight distribution polystyrene standard of MW 280,000 g/mol.

Data collection and processing were completed using local software from Eastman Kodak Company, Kodak UCAL Version 5.0 and Kodak LS4 REV 4.00.

C. Luminescence Experiments

Blend Preparation. Blends of the selected copolymers were prepared using 50/50 wt/wt % of the two polymeric components of the binary system. One component contained the chromophore probe, while the other contained the quencher probe. The polymers were swollen as a 10% solution in THF. The viscous solutions were sonicated for several hours. The blends were then cast as smears on glass substrates in sets of five. The evaporation of the solvent was affected in two steps. (1) The films were placed in a dessicator at room temperature for 12 hours. (2) Then the films were heated in a vacuum oven, set at 115 °C, for 24 hours. The vacuum oven was purged with nitrogen several times. These steps were deemed necessary to prevent the THF from leaving the films too quickly, causing bubbling and irregular surfaces on the films.

Luminescence Measurements. Luminescence measurements were performed and recorded using a Perkin-Elmer LS-50B Luminescence Spectrometer. The software used to collect and store the data was FL WinLab, Version 3.00, © 1994-1999 by the Perkin-Elmer Corporation. Fluorescence and phosphorescence emission spectra were collected for each film. The films were excited at 295 nm and emission data was recorded from 320-550 nm. A front-face arrangement was used to minimize reabsorption of the emission signal. A schematic of this set-up is shown in Figure 12. The excitation slit was set at 2.5 nm. The emission slit was set at 2.5 nm for fluorescence and 7.5 nm for

phosphorescence measurements. A 290 nm emission cutoff filter was installed to minimize the amount of scattered light reaching the detector.

Conditions for the phosphorescence measurements were as follows: gate = 2.00 ms, cycle = 33 ms, flash count = 1, and delay = 0.02 ms. Due to the low intensity and, therefore, poor signal to noise ratio, the phosphorescence scans were averaged over 5 scans.

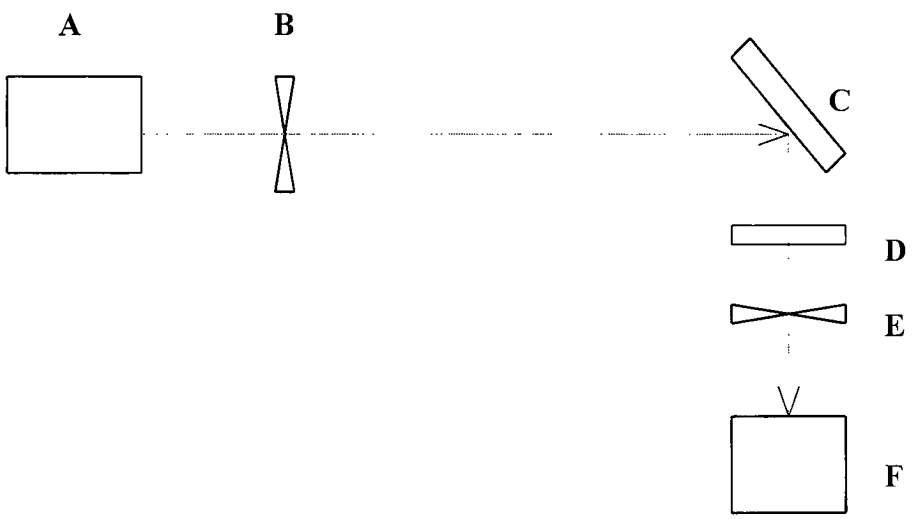

Figure 12. Schematic diagram of front-face optical arrangement.
A: Tungsten lamp, B: Excitation monochromator, C: Sample film,
D: Cutoff filter, E: Emission monochromator, F: Detector

III. Results and Discussion

A. Materials and Synthesis

Synthesis of N-(4-iodophenyl)maleimide. The synthesis of the polymerizable quencher probe was performed in two steps.[61] The first step is the imidization of maleic anhydride and 4-iodoaniline. The imidization occurs by nucleophilic attack of the amine group on a carbonyl of maleic anhydride. The product of this step is N-(4-iodophenyl)maleamic acid (NIPMA)

The second step is the dehydration of N-(4-iodophenyl)maleamic acid. This step closes the ring to produce N-(4-iodophenyl)maleimide (NIPMI). Sodium acetate is used as a catalyst in this step.

The final product was characterized by FTIR and ^{1}H-NMR.[66] The FTIR spectrum in Figure 13 provides evidence that the maleamic acid has been converted to the maleimide. The absence of the strong, broad O-H stretch in the region of 3300-2500 cm^{-1} indicates that the dehydration step has occurred. The missing N-H stretching band, around 3300 cm^{-1}, is additional evidence of the ring closure. The amide carbonyl is present at 1710 cm^{-1}. The C=C stretch is also observed at 1500 cm^{-1}.

The ^{1}H-NMR spectrum in Figure 14 provides more conclusive evidence of the formation of the desired product, NIPMI. Three signals characteristic of the product are detected, each of which are integrated for two protons. The signal designated "a" is a singlet at 6.75 ppm, corresponding to the vinyl protons in the 5-member ring. These protons are deshielded by the neighboring amide carbonyls and are, therefore, located farther downfield than other vinyl protons in a 5-member ring (~6.10 ppm). The doublets

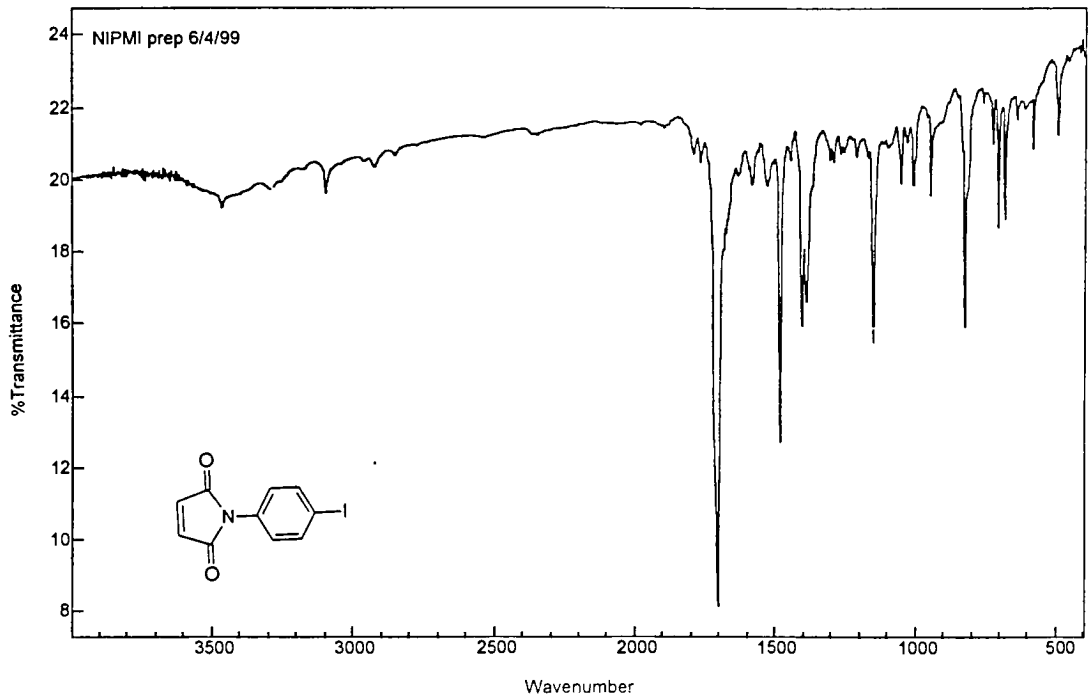

Figure 13. FTIR Spectrum of NIPMI.

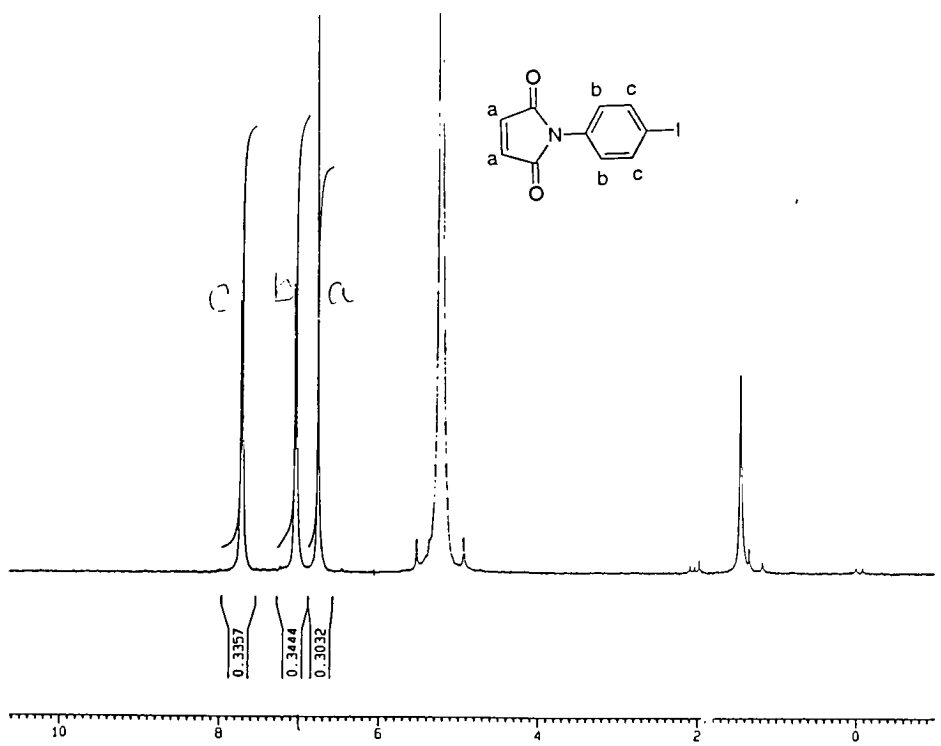

Figure 14. ^{1}H-NMR Spectrum of NIPMI. (299.9 MHz)

designated "b" and "c", at 7.00 and 7.70 ppm respectively, correspond to the aromatic protons. The protons at "b" are meta to the iodine, while the protons at "c" are at ortho positions. The deshielding nature of the iodine pushes the "c" protons farther downfield than "b". Due to the strong electrical quadrupole moment of iodine, the splitting of the signal at "c" is unaffected by its close proximity.

B. Characterization

Synthesis of the Copolymers. The polymerization reactions proceeded by a free radical mechanism. The chemical initiator, AIBN, was used to start the synthesis. To avoid complications due to a drift in the compositions of the copolymers, the polymerizations were taken only to approximately ten percent conversion.

Since specific binary and ternary copolymers were targeted, it was necessary to first calculate the required feed ratios to accurately achieve the targeted incorporation of each monomer. The operating equation and results of these calculations were discussed in the synthesis section.

The synthesized copolymers were characterized by ^{1}H-NMR, DSC, TGA, and SEC. The ^{1}H-NMR spectra of the probes, carbazole (Figure 15) and NIPMI (Figure 14), are helpful in the characterization of the polymerized products. It was noted that the signals farthest downfield (> 7.2 ppm) for each of the probes could be used to quantify the probe's incorporation in the copolymers. In the case of vinyl carbazole, the two aromatic protons designated "d" could be integrated, while the other six aromatic carbazole protons overlap the signals due to the five aromatic protons of styrene. The signals from the three vinyl protons, which are now saturated and part of the backbone,

are located upfield. They overlap the three protons due to the styrene backbone segments and all eight of the protons of methyl methacrylate. Using this information, it was possible to determine the composition of the synthesized copolymers containing as little as one percent of a given monomer.

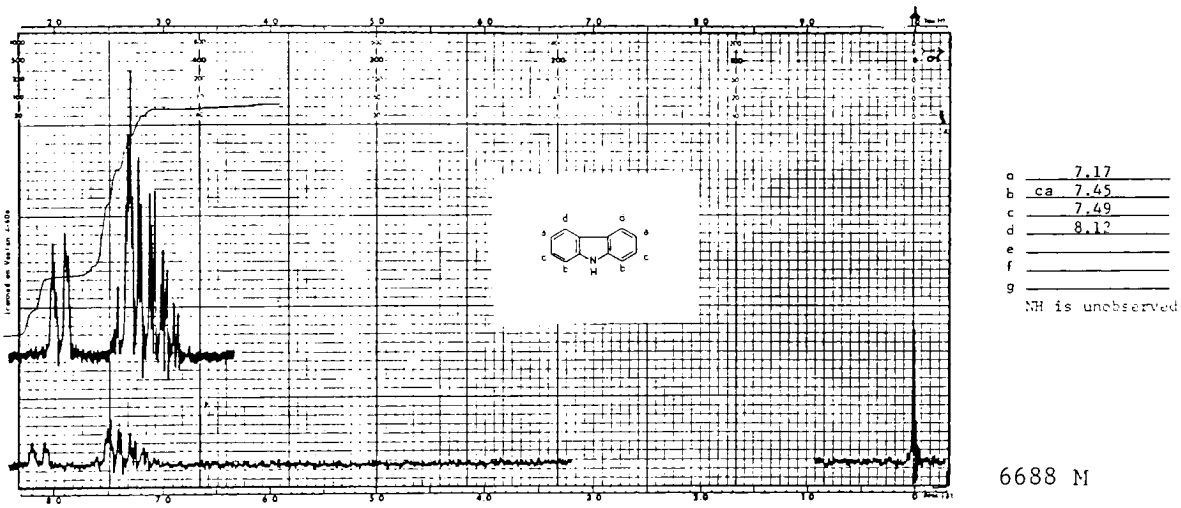

Figure 15. ^{1}H-NMR of carbazole.[67] (300 MHz)

Similarly, the NIPMI content was determined by integrating the peaks due to the two aromatic protons designated "c". The other two aromatic protons were not deshielded enough by the iodine to avoid overlap with the five aromatic protons of styrene. The backbone protons in the 5-member ring would be observed around 3.00 ppm, if not for the overlap with the three protons of the styrene backbone and the eight protons of methyl methacrylate. Example spectra for the 50/50 copolymers with and without probes are given in Figure 16. Table 6 provides a summary of the calculated incorporation percentages for each of the copolymers. The complete set of ^{1}H-NMR spectra are provided in Appendix A.

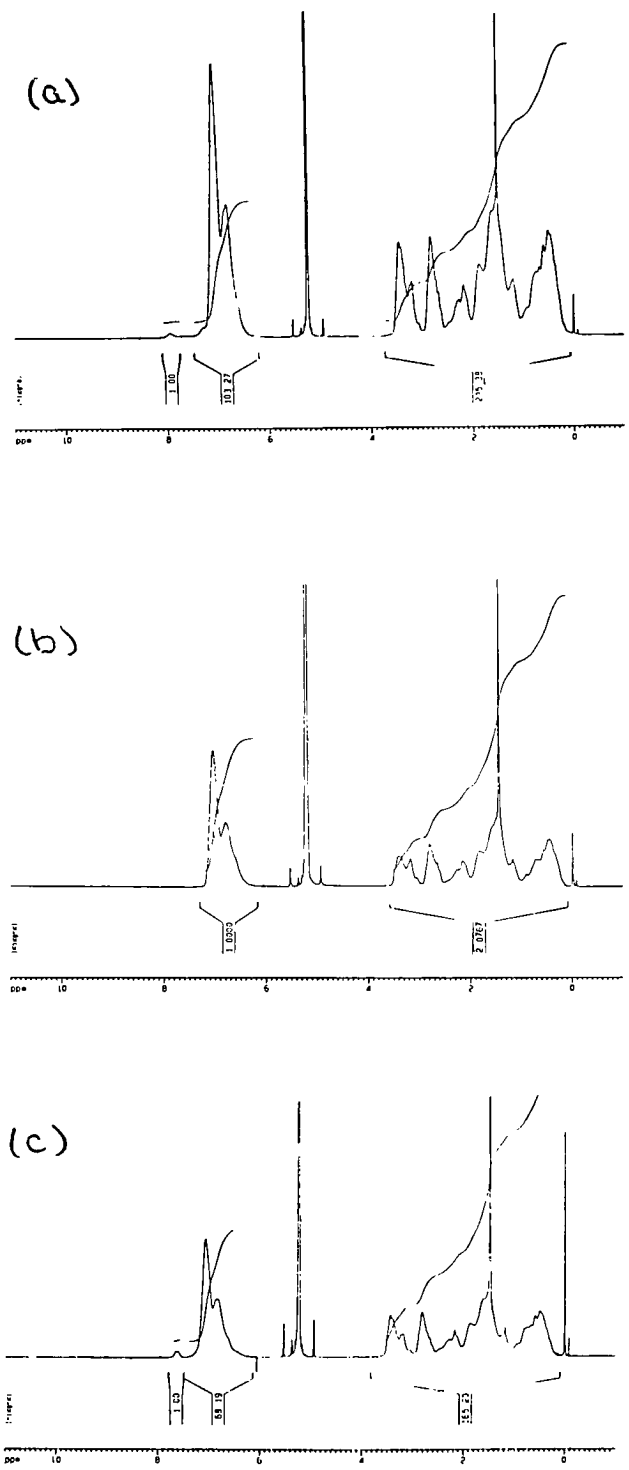

Figure 16. ^{1}H-NMR spectra of 50/50 copolymers
with and without the incorporated probes. (299.9 MHz)
(a) $MMA_{49}S_{49}VCz_2$ (b) $MMA_{50}S_{50}$ (c) $MMA_{49}S_{49}NIPMI_2$

Table 6. Summary of polymer compositions as determined by ^{1}H-NMR.

F (intended) (mole %)	NB ref.	F (actual) (mole %)
MMA : S : VCz (NIPMI)		MMA : S : VCz (NIPMI)
49:49:02	63	51 : 47 : 02
74:24:02	64	77 : 22 : 01
14:84:02	66	16 : 82 : 02
04:94:02	67	09 : 89 : 03
98:00:02	68	97 : 00 : 03
00:98:02	69	00 : 97 : 03
49:49:(02)	75	53 : 46 : (01)
98:00:(02)	60	98 : 00 : (02)
00:98:(02)	72	00 : 98 : (02)
50:50:00	73	48 : 52 : 00

Data collected from the DSC and TGA are necessary to demonstrate that the incorporation of the luminescent and quencher probes at low percentages does not alter the physical properties of the polymers and copolymers to be studied. Provided the physical characteristics are the same, it may be assumed the probe-containing blend system models the behavior of the original probeless system. The physical characteristics used to determine this invariance were the glass transition temperature (T_g) and the decomposition temperature (T_d). Values of T_g were determined from the data collected from the DSC. The glass transition temperature was measured at the midpoint of the extrapolated tangents as demonstrated in Figure17. The values of T_d were determined from the data collected from the TGA. The decomposition temperature was defined as the extrapolated onset as shown in Figure 18. Three commercially produced samples were run as a reference.

Literature values of T_g and T_d for PS are 100 °C and 399 °C, respectively.[68,69] The literature T_d values were determined for 50% loss at a heating rate of 10 °C/min. It was determined experimentally that the commercially produced polystyrene has a T_g of

103 °C and a T_d value of 401 °C. The synthesized polystyrene containing the luminescent probe, 9-VCz, (00:98:2) was determined to have a T_g of 104 °C and a T_d value of 400 °C. The synthesized polystyrene containing the quencher probe, NIPMI, (00:98:(2)) was determined to have a T_g of 108 °C and a T_d value of 395 °C. These values are within the experimental precision of the instruments and the variability of the method of data analysis. Therefore, the tagged copolymers of PS are considered to maintain the properties of polystyrene with the minor incorporation of the given probes.

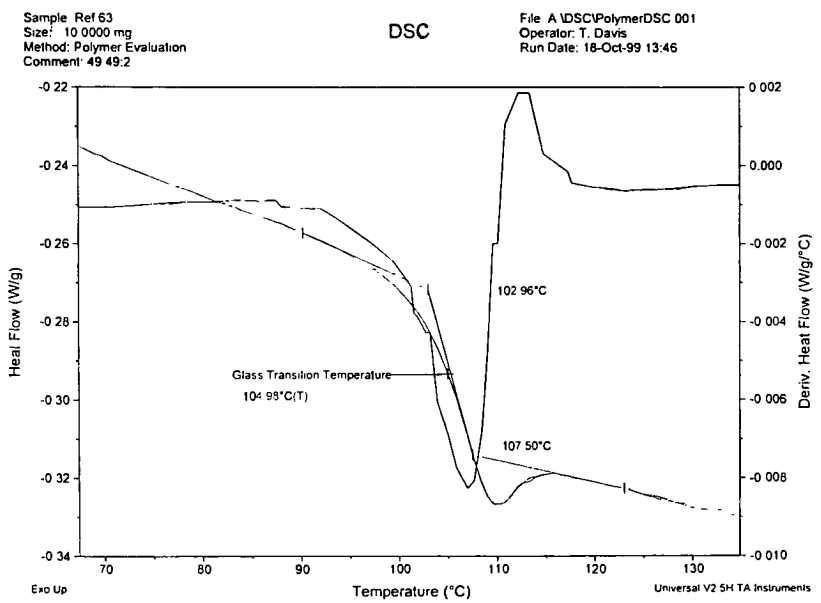

Figure 17. DSC thermogram used to determine the T_g value for $P(MMA_{51}\ S_{47}\ VCz_2)$

It was determined that the commercially produced PMMA has a T_g of 102 °C and a T_d value of 382 °C. The literature quotes the T_g to be 125.6 °C for a 64% syndiotactic PMMA[70] and 41.5 °C for a 95% isotactic PMMA[71]. The decomposition temperature of PMMA for a half life of 30 min, is given as 330 °C in literature.[72] Therefore, the low T_g of the experimental reference PMMA may be attributed to a more isotactic arrangement.

This may also explain the slightly high T_d value. The synthesized PMMA containing the luminescent probe, 9-VC, (98:00:2) was determined to have a T_g of 125 °C and a T_d value of 334 °C. The synthesized PMMA containing the quencher probe, NIPMI, (98:00:(2)) was determined to have a T_g of 129 °C and a T_d value of 343 °C. The variation in these values is within the precision of the methods used. Therefore, the tagged copolymers of PMMA are also considered to maintain the properties of the untagged polymers.

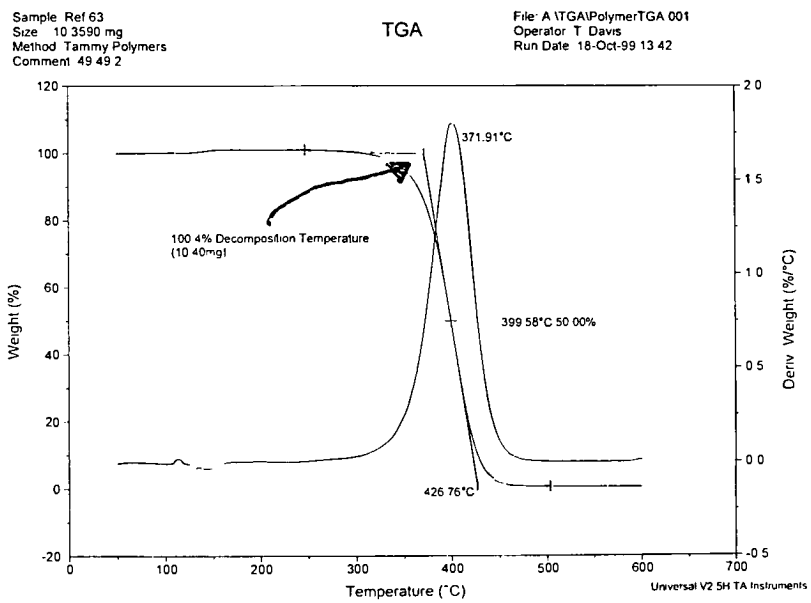

Figure 18. TGA thermogram used to determine the T_d value for $P(MMA_{51}\ S_{47}\ VCz_2)$

Examination of the data for the copolymers, for which no reference was analyzed, reveals a clearly identifiable pattern. As demonstrated in the temperature vs. composition plots of Figure 19, the trend is evident. As the percentage of MMA increases, the T_g

increases and the T_d decreases. This trend indicates that the copolymers of compositions intermediate to the PS and PMMA are also behaving as if the tag were not present.

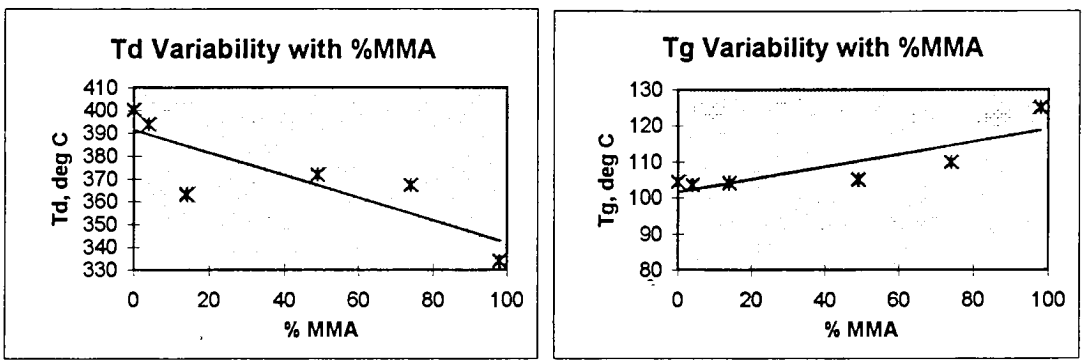

Figure 19. Trend plots of Tg and Td changes with increasing MMA composition.

Given that the physical characteristics, T_g and T_d, of the model compounds are consistent with their respective parent polymers and copolymers, it is assumed that the blends of the above mentioned polymers will also behave consistently. The results of all the thermal analyses are tabulated in Table 7. Complete sets of DSC and TGA thermograms may be found in Appendices B and C respectively.

SEC data was gathered using four types of detectors: DRI, DV, UV, and LS. This yielded a wealth of information including molecular weight, polydispersity, molecular weight distribution, and residual monomer content. The weight averaged molecular weights (M_w) were calculated by two methods, universal calibration and light scattering. The values obtained appear to be very consistent from method to method. The number-averaged molecular weights (M_n) were also calculated using the universal calibration

method. The results of these analyses are tabulated in Table 8. Sample SEC data is shown in Figure 20.

Table 7. Summary of results of thermal analyses.

Polymer	Ref	Tg, C	Td, C
49:49:02	63	105	372
74:24:02	64	110	367
14:84:02	66	104	363
04:94:02	67	104	394
98:00:02	68	125	334
00:98:02	69	104	400
49:49:(02)	75	110	376
98:00:(02)	60	129	343
00:98:(02)	72	107	395
50:50:00	73	104	378
00:100:00	Med PS	ND	382
100:00:00	PMMA	102	342
00:100:00	High PS	103	401

The polydispersity ratio (PDR) was calculated for each copolymer. The values range from 1.53 to 2.01. This range indicates that two methods of termination took place to varying degrees in the polymerization process. Termination by combination will give a polydispersity ratio of 1.5.[73] Termination by disproportionation gives a polydispersity ratio of 2.0. Slow reaction rates favor termination by combination.

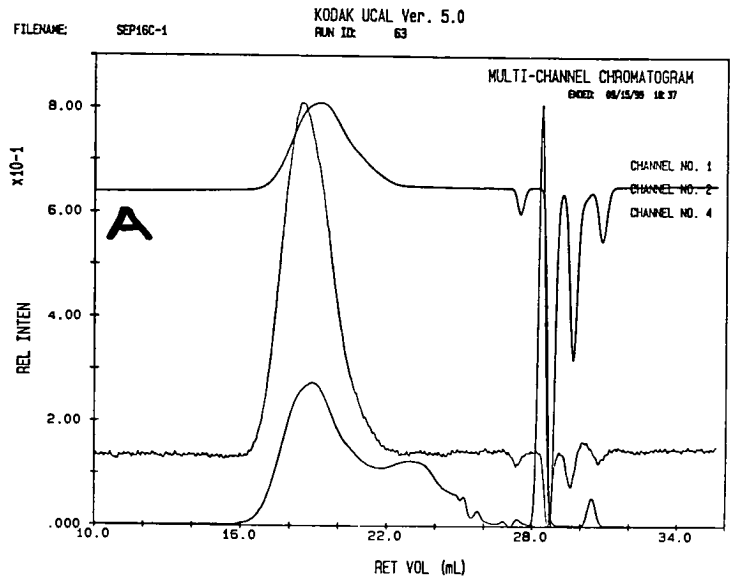

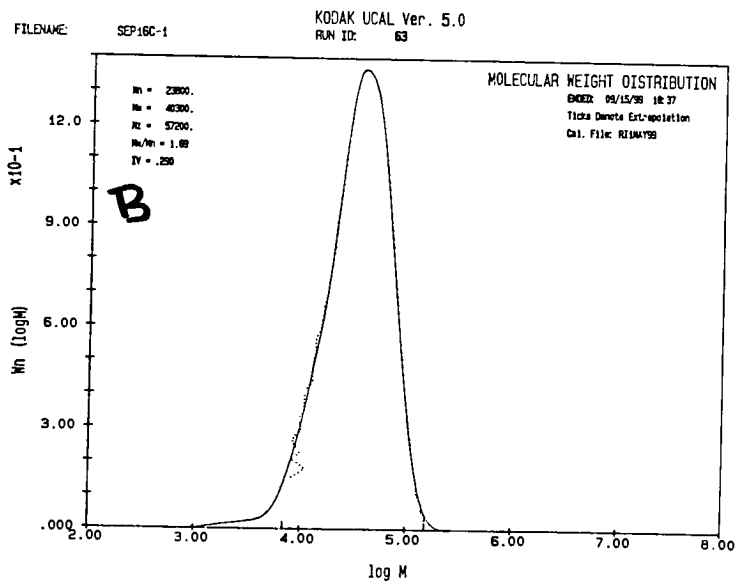

Figure 20. SEC data used to determine the molecular weight averages for $P(MMA_{51}\ S_{47}\ VCz_2)$ A: Chromatograms of three detectors, channel 1: differential viscometry, channel 2: differential refractive index, channel 4: ultraviolet; B: Molecular weight distribution based on refractive index and viscosity differences.

Table 8. Summary of SEC data and results.

				Universal Calibration			Light Scattering
Polymer	Ref	dn/dc	[IV] dL/g	Mn	Mw	PDR	Mw
98:00:(02)	60-B	0.0909	0.4085	69150	113500	1.64	112000
49:49:02	63-C	0.1367	0.292	22300	40200	1.80	41550
74:24:02	64-D	0.1231	0.3515	28050	56450	2.01	57600
14:84:02	66-E	0.1707	0.213	17200	27550	1.60	27400
04:94:02	67-F	0.1795	0.213	14950	27700	1.85	28250
98:00:02	68-G	0.0942	0.376	48550	87750	1.81	88850
00:98:02	69-H	0.1819	0.268	22500	40600	1.80	42750
00:98:(02)	72-I	0.1803	0.252	22700	39950	1.76	41750
50:50:00	73-J	0.1492	0.454	38250	64800	1.69	66900
49:49:(02)	75-K	0.1354	0.276	27350	41950	1.53	43700

The molecular weight distributions in all of the synthesized polymers are narrow. PDR is less than 2. However, in the polymers containing N-vinyl carbazole, a bimodal distribution was revealed by UV detection. The lower molecular weight fraction was more concentrated in the luminescent probe.[74] This low molecular weight fraction, $M_n \sim$ 3000 g/mol is seen as a tail on the main peak when observed with the RI or viscosity detectors. Figure 20 demonstrates these qualities. The seemingly large quantity of this fraction is apparently due to the larger molar absorptivity of N-vinyl carbazole. Table 8 summarizes the SEC results. Complete sets of SEC data, including chromatograms from all four detectors and the analyzed molecular weight distribution, may be observed in Appendices D and E, respectively.

C. Luminescence Experiments

Evaluation of the luminescence spectra indicated that the systems under study are quite complex. The numerous variations which may be present in the samples, the numerous processes that affect the energy levels and the spin states of luminescent molecules, and the properties of the systems themselves must be considered both individually and simultaneously.

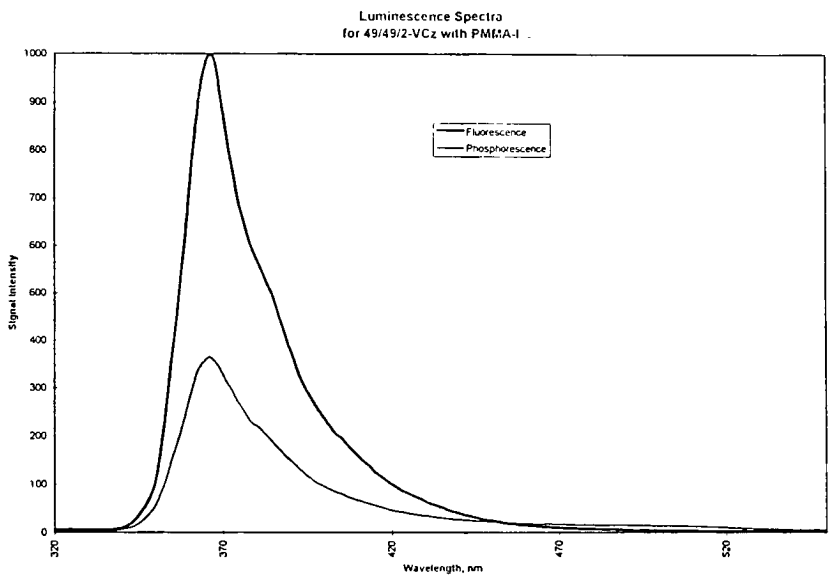

Figure 21. Fluorescence and phosphorescence spectra for a thin film of a blend of $PMMA_I$ with $P(MMA_{51}\ S_{47}\ VCz_2)$

Qualitative and quantitative analyses were evaluated and graphed to reveal trends in the luminescence data. An example of the spectral data obtained for a representative film is given in Figure 21. The luminescent copolymers, those containing N-vinyl carbazole (VCz), were blended with homopolymers containing NIPMI quencher (PS_I, $PMMA_I$). The blends were considered in two series: blends with PS_I and blends with $PMMA_I$. Each series demonstrated obvious trends, similarities, and differences. A plot of signal

vs. % diluent (Figure 22) indicated that the signal, for both fluorescence and phosphorescence, increased with % diluent. The signal values represent the sum of the signal intensities from 340 to 550 nm at 1 nm intervals. The % diluent represents the incorporated percentage of the monomer in the copolymers complementary to that of the homopolymer in the blend. For example, in the series blended with $PMMA_I$, the diluent is styrene (S). In both series, the fluorescence, as expected, is a larger signal than that of the phosphorescence. However, in the $PMMA_I$ series, the intensity of the fluorescence and phosphorescence trendlines are of greater signal intensity than those of their respective PS_I trendlines. Two possible explanations for this are considered. They include the effects of the matrices themselves and the potential for residual oxygen in the thin films. These topics will be discussed in detail later in this paper.

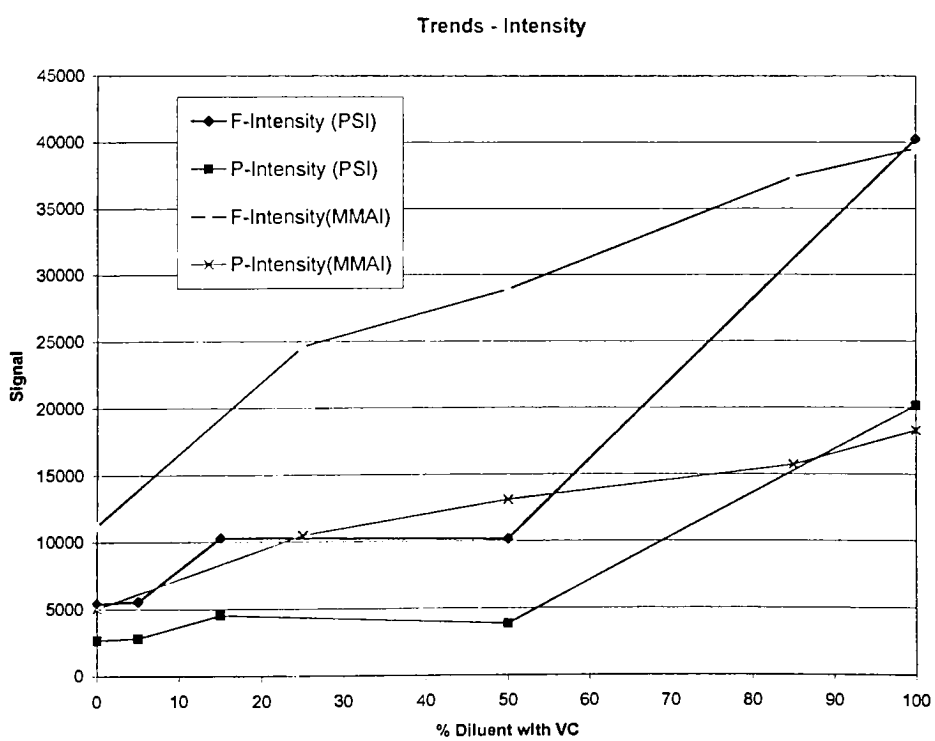

Figure 22. Plot of signal vs. % diluent.

Figure 23 presents a similar plot to that depicted in Figure 22. Here the signal responses have been normalized by the percent incorporation of VCz in each copolymer. As can be seen, the signals do not vary linearly. This normalization step was necessary to

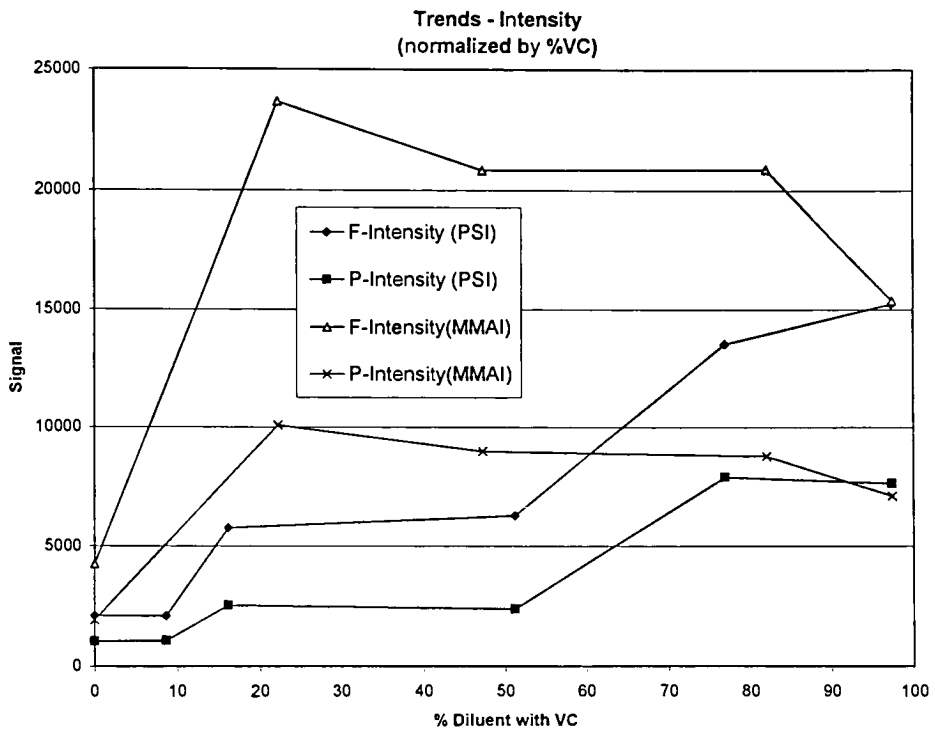

Figure 23. Plot of signal intensities (normalized by % VCz) vs. % diluent

account for variations in signal due to the [VCz]. The luminescent signals of the control films were not effective comparisons. The controls were made by blending the VCz-containing copolymers with commercially produced homopolymers containing no quencher. The controls were found to be unacceptable based on the thermal analysis data of the homopolymers. Thermal analysis revealed that the PS control had no clear T_g and the PMMA control was determined to be more isotactic than the $PMMA_I$ used in the study. This assessment is based on the lower T_g value of the control. The $PMMA_I$

control also demonstrated a two-step decomposition in the TGA thermogram, indicating that oxygen had permeated the polymer surface. In consideration of these findings, it was decided that the controls may not behave in the same manner as the synthesized systems being probed. Thus the controls were discounted in the analysis. The control spectra and the average spectra of all of the blends studied are presented in Appendix F.

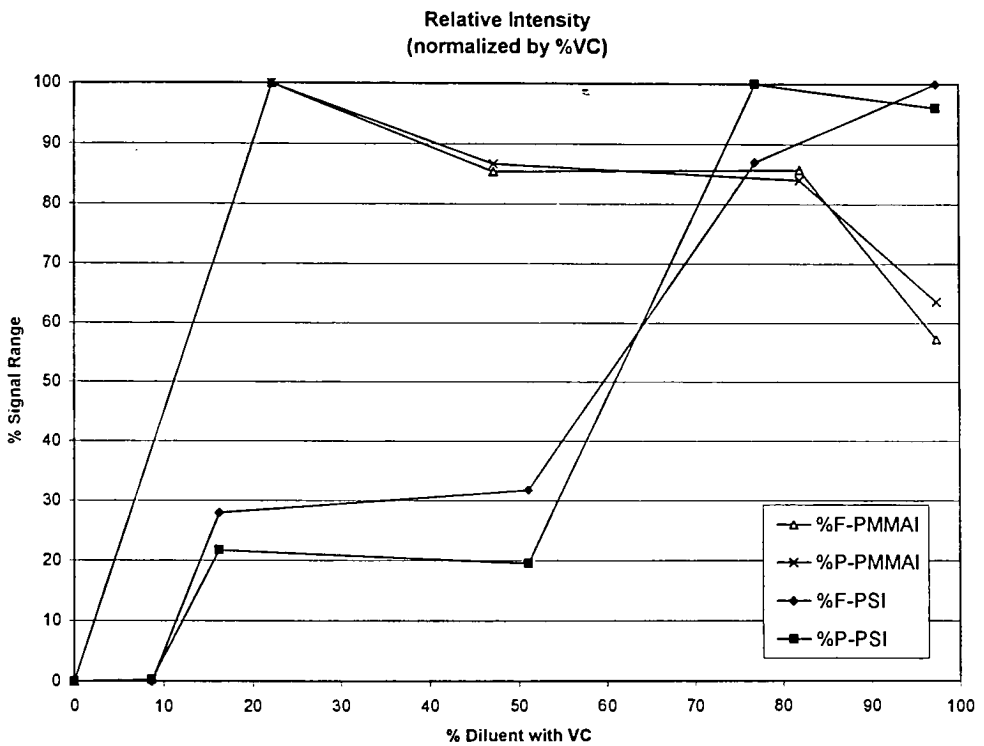

Figure 24. Plot of relative signal intensities normalized by % VC vs. % diluent.

Reduction of the signal intensities of the fluorescence and the phosphorescence to the same relative scale, Figure 24, revealed that the fluorescence and phosphorescence signal intensities parallel each other for both blend series. Therefore, it is only necessary to refer to one or the other in the remainder of this analysis. At this point, the assumption

must be made that the normalized signal minimum of Figure 23 represents a single phase system, where the VCz probe of the copolymer is able to approach the NIPMI probe of the homopolymer within an effective quenching radius. This signal height is defined as the zero point on Figure 24. For example, PS_{VCz} is miscible with PS_I giving a relative signal of zero percent. This data also indicates that the iodine of NIPMI quenches the signal rather than enhancing it in these materials. The assumption is also made that the normalized maximum corresponds to the resultant signal of a two-phase system, where the probes are not permitted to approach each other and, therefore, no quenching is observed. For example, PS_{VCz} is completely immiscible with $PMMA_I$, leading to the maximum luminescent signal intensity at 100% diluent. The data points which lie intermediate to the completely miscible minimum and the completely immiscible maximum demarcations are not consistent with the expected results. These inconsistencies, however, may be explained in several contexts, which will be addressed.

Based on the assumptions defined above, Figure 24 may be used to define the phase diagram of the PS-PMMA system. The results are tabulated in Table 9, along with the determinations made by Braun, et. al. using light microscopy and DSC. A plot of the expected trends is shown in Figure 25.

Braun used light microscopy and DSC to study the miscibility trends of the PS-PMMA system over a broad temperature range.[13] Both optical techniques and T_g monitoring methods have limitations. These were discussed in the introduction section of this paper. Limitations aside, the luminescence study was conducted at room temperature (23°C). At this temperature the "partially miscible" blends are expected to exhibit a

single-phase system. However, upon heating, a two-phase system emerges, as indicated in Figure 25.

Table 9. Experimental and published results of miscibility studies of $P(S_xMMA_{x-1})$ blends. M = miscible, PM = partially miscible (M @ 25°C, I @ 180°C), I = immiscible.

Blends			Miscibility Properties	
Polymer I	Polymer2 (MMA/S/VCz)	Target Pol 2	Experimental	Published[13]
PS_I	00/97/03	00/98/02	M	
	09/89/03	04/94/02	M	
	16/82/02	14/84/02	*	
	51/47/02	49/49/02	*	PM(target), I (actual)
	77/22/01	74/24/02	I	I
	97/00/03	98/00/02	I	I
$PMMA_I$	97/00/03	98/00/02	M	M
	77/22/01	74/24/02	I	M
	51/47/02	49/49/02	I	PM
	16/82/02	14/84/02	I	I
	00/97/03	00/98/02	I	I

* Indicates inconsistency of defining parameters.

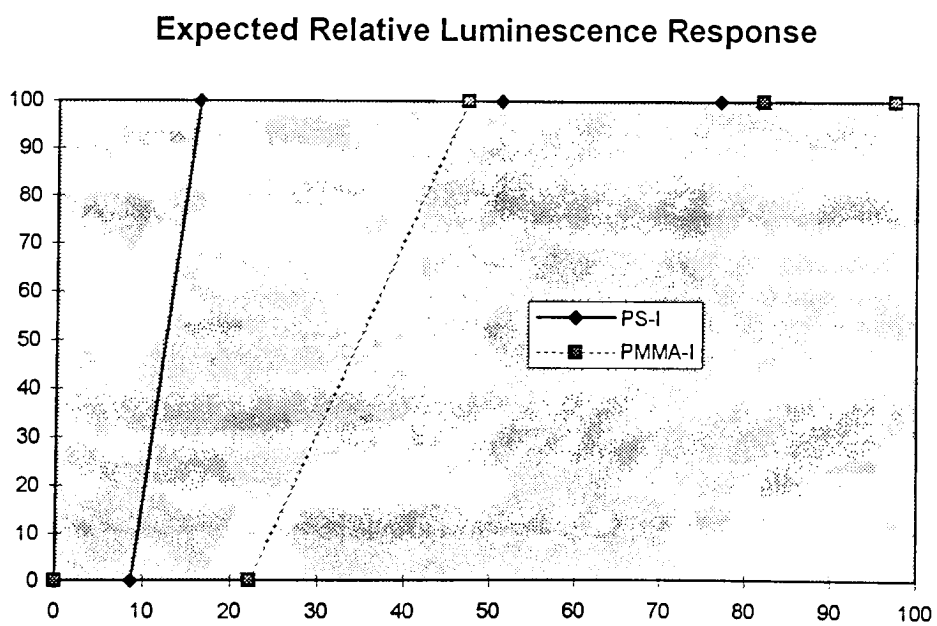

Figure 25. Plot of expected trends, relative signal intensity vs. % diluent

Although many of the blends behave as expected in comparison to the values published by Braun, there are several identifiable variations. While the extreme data points of each series behave as expected, the center points defy the predictions. The blends of $P(MMA_{16}S_{82}VCz_2)$ and $P(MMA_{51}S_{47}VCz_2)$ with PS_I both gave relative luminescence intensities near 20-30%. These blends were predicted to be immiscible and, therefore, give maximal relative signal intensities. The blend of $P(MMA_{77}S_{22}VCz_1)$ with $PMMA_I$ gave a relative luminescence intensity at or near 100%. This blend was predicted to be miscible and, therefore, give a minimal relative signal intensity.

Many factors may have contributed to these differences. These factors may be placed into four main categories. The first category of concern relates to the polydispersity of the synthesized polymers used in the study. The second category addresses the pathways for energy transfer in these materials. The third category considers the effects of oxygen contamination. The fourth category relates to the properties of the polymer matrices themselves, and how they affect the luminescence of the carbazole system.

As discussed in the introduction, all synthetic polymers are polydisperse with respect to molecular weight, microstructure, degree of branching, composition and sequence type. The SEC data demonstrated a narrow and uniform molecular weight distribution for each of the copolymers in this study. The distributions of the VCz-containing copolymers were slightly skewed due to the presence of a bimodal distribution of the carbazole-containing fraction of the copolymer. Still, the polydispersities ranged from approximately 1.5 to 2.0, (Braun, 1.6-2.0) which is considered to be relatively narrow even in the presence of the bimodal distribution in the VCz-containing polymers.

Other studies found in the literature indicate that molecular weight is generally only a concern at significantly lower values than those of this study. Since the weight-averaged molecular weights of the polymers of this study were greater than 27000 g/mol and measurements were made at room temperature, molecular weight was most likely not a contributing factor in the miscibility of the majority of the polymers produced. Although it is possible that the lower molecular weight fractions could have increased the miscibility of partially miscible systems or penetrated the phase boundaries of otherwise immiscible systems, it is unlikely. The molecular weight of this fraction is substantial at 2000-3000 g/mol. Still, the presence of the fraction must be considered as one possible explanation for the observed variations. The lower molecular weight portion of the bimodal distribution indicated by the SEC data may have increased miscibility in the homopolymers due not only to the molecular weight differences, but also due to the change in composition of the copolymers containing VCz. The fraction becomes more significant with increasing PS content in the copolymers. This may have resulted in the trend of decreasing signal intensities with changing % diluent, favoring an increase in [PS].

Microstructure is another contributing aspect of the multicomponent nature of the polymers in a blend. In this study, DSC data was used as an indicator of differences in microstructure. Microstructure features may include differences in sequence isomerization (head-to-tail), structural isomerization or tacticity (syndiotactic, isotactic). The only obvious indication of these features is the high T_g value of the synthesized PMMA samples. This increased value indicates that the PMMA is more syndiotactic in nature. Diad analysis could not be performed on the polymer samples.

A third contributor to a multicomponent polymeric system is the degree of branching. Although it is possible that branching may have occurred in the polymerization reactions, it is highly unlikely due to the bulky nature of the aromatic ring of PS and of the methyl acrylate group of PMMA. The possibility of branching will not be considered further.

There are two other factors in the "polydispersity" of a polymeric system which involve copolymers specifically. They are composition and sequence type. It is clear that the copolymer composition has a direct affect on the phase behavior of their resulting blends. For this reason, the work published by Braun, et.al. was very important for this study. A phase diagram for blends of varying compositions of $P(S_xMMA_{x-1})$ / $P(S_yMMA_{y-1})$, resulting from Braun's research, was presented in Figure 6. The copolymer compositions used in our study were selected from each of the miscibility regions of his phase diagram. These were employed to evaluate the utility of the luminescence probe/quencher system for determining the miscibility of polymer blends.

Steps were taken during the polymerization to prevent the creation of copolymers of differing copolymer compositions. The polymerization reactions were carried out to an estimated 10% conversion of monomer to polymer. This precaution was intended to eliminate the possibility of the depletion of one or more of the monomers. If this depletion were to occur, the available monomer or feed ratios would be altered, resulting in a drift in the copolymer compositions during the course of the reaction. Evidence that this step was successful was provided by the NMR scans of duplicate sample preparations. However, the SEC data indicates that VCz tends to concentrate in the low molecular weight fraction of the polymerization batch. This disparity was not observed in

the NMR data. As stated in the characterization section, the low molecular weight mode observed in the SEC UV-chromatogram appears large due to the larger molar absorptivity of the VC component. The relative size of the lower molecular weight signals in the UV-chromatogram increases with PS content in the copolymers. This indicates that the effect is more pronounced in the case of PS than with PMMA. This is explained by the reactivity ratios presented in Table 3: r_{31} and r_{32} are 0.04 and 0.035, respectively, where M1 = MMA, M2 = S and M3 = VCz.[63] A reactivity ratio is a ratio of a monomer's affinity to react with itself to a monomer's affinity for the other monomer. Therefore, the reactivity ratios indicate a slightly higher affinity of VCz for styrene than methyl methacrylate. The tendency of VCz to react with a monomer other than itself is likely the result of steric hindrance.

The reactivity ratios of NIPMI indicate that it prefers to combine in an alternating manner with styrene and randomly with methyl methacrylate. An alternating arrangement is indicated by a product of the reactivity ratios equal to zero. The product of r_{23} and r_{32}, is 0.0007, where r_{23} and r_{32} are 0.07 and 0.01 respectively.[64] The random arrangement is indicated by the product of the reactivity ratios indicating neither alternating nor block patterns. However, there will be more MMA incorporated due to its greater reactivity. The reactivity ratios, r_{13} and r_{31}, are 0.91 and 0.30 respectively.[64]

The reactivity ratios for MMA and S in P(MMA-S) copolymerization are approximately equal at values of 0.54 and 0.43 respectively.[62] These reactivity ratios indicate that each monomer is twice as likely to react with the other monomer rather than itself. This indicates that they will combine in an essentially random fashion. Once

again, diad analysis would provide more conclusive evidence, however it was not deemed necessary at this point.

Figure 5 demonstrates the many ways in which an excited molecule can exchange energy before eventually returning to the ground state. These processes may be radiative or non-radiative. Non-radiative processes include vibrational relaxation, internal conversion, intersystem crossing, and reaction. Radiative processes include fluorescence and phosphorescence.

Delayed fluorescence is also an important process for the carbazole system. As discussed in the introduction of this paper, the delayed fluorescence of carbazole occurs by a mechanism known as triplet-triplet annihilation. This process is non-radiative, but leads to a fluorescent transition having a lifetime comparable to that of phosphorescence. Triplet-triplet annihilation is a biphotonic process where one triplet absorbs energy from a second triplet, promoting the first to the excited singlet state and reducing the other to the ground state singlet. Triplet-triplet annihilation is sensitive to the local concentration of the chromophore. In theory, the more concentrated the system, the more excited triplets are present, and therefore the higher the probability that the excited triplets will interact. Delayed fluorescence is concentration-dependent and, therefore, may explain the inconsistencies between some of the data points in the fluorescence and phosphorescence trendlines where they do not track each other well. Moment analysis determined that PS has more phosphorescent character than PMMA. However, these concepts do not explain the inconsistent behavior between the PS_I and $PMMA_I$ series intensities.

It was noted in this study that the phosphorescence lifetime was especially short for a carbazole species, making the delayed fluorescence difficult to observe. The

expected phosphorescence lifetime of carbazole at room temperature in PS or PMMA is on the order of 2-3 seconds.[54] In these experiments, the phosphorescence lifetime was observed to be on the order of 0.01 ms. It is suspected that the decreased lifetime is the result of oxygen trapped in the polymer matrices. The triplet state of oxygen non-radiatively deactivates the excited triplet of carbazole.[75] The experimental oxygen permeabilities at room temperature for PS and PMMA are 450 and 17.0 D.U., respectively.[76] Dow units (D.U.) are cc mil / [day (100 inches^2) atm], where mil is one thousandth of an inch. The permeability is calculated by the equation:

$$P = Q\,t / A\,\tau\,\Delta p \qquad (9)$$

where Q is the quantity of penetrant molecules, t is the thickness, A is the surface area, τ is a fixed amount of time, and Δp is the partial pressure difference between the two surfaces of the specimen. The fact that oxygen is more soluble in PS than PMMA explains the much lower signal intensities of the PS_I series in comparison to the $PMMA_I$ series. Within each series, the % diluent changes and, therefore, the % PS in the copolymers must also be considered. As the PS content increases in the VCz containing polymer, the intensity decreases. In the $PMMA_I$ series (Figure 24), the signal of the second data point is at the maximum relative value. As the % PS (or diluent) proceeds towards 100%, the intensity decreases as a result of increasing $[O_2]$ in the matrix. In the PS_I series, the PS and, therefore, the $[O_2]$ decreases as you proceed toward 100% diluent (100% $PMMA_{VCz}$).

An exploratory experiment was performed to determine if the reduced lifetime is in fact due to the presence of oxygen.[77] New sample films were prepared using THF sparged with nitrogen and THF sparged with oxygen. The luminescent signals of the films prepared in the nitrogen environment were five times as great as those prepared in the oxygen system. Another consequence of the presence of oxygen is that there are less carbazole triplets available to produce delayed fluorescence, explaining again why the delayed fluorescence signal is also less intense.

There is evidence that the polymer matrices themselves have a marked influence on the luminescence of the system.[54] Williamson and MacCallum, working with carbazole, determined that the phosphorescence lifetime of a chromophore in a homopolymer matrix is influenced by several factors including concentration, temperature, and the identity of the matrix. Williamson and MacCallum also observed delayed fluorescence at 380 nm, with $\tau_{DF} < \tau_{P}$. This indicates that the fluorescence is less likely to be affected by the matrix. Williamson and MacCallum also observed that the phosphorescence lifetime of carbazole was greater in a PMMA matrix than that in a PS matrix. Based on their observations, they proposed that the excited triplet state of carbazole is deactivated by the polymer matrix via non-radiative decay (NR) and energy transfer to the matrix. The energy transfer to the PS matrix was observed to be exothermic, while transfer to the PMMA matrix was endothermic. This is evidence that the deactivation of the excited triplets is thermodynamically favorable in the styrene matrix due to the lower energy level of the excited triplet of the matrix relative to that of the chromophore. Energy transfer to the PMMA matrix is less favorable since the

excited triplet state of PMMA lies at a higher energy than that of the carbazole triplet, and would require the addition of energy to be populated.

A fourth factor may explain the differences in experimental and the expected literature phase behavior in the binary blend systems. The primary methods employed by Braun, et. al. to determine the miscibility properties were DSC and light microscopy.[13] As discussed in the introduction of this paper, these methods are limited by the relative differences in the T_g values and the relative differences in the refractive indices of the components of the binary blends. Another limitation is the methods' dependence on the size of the phase domain. It is possible that the $P(MMA_{77}S_{22}VCz_1)$ copolymer is actually completely immiscible with $PMMA_1$ on the molecular level. Perhaps the phase boundaries were not sharp enough to be detected by visual methods such as light microscopy. This reinforces the scientific need for a method that is capable of probing the phase behavior of polymeric blends on the molecular level.

Conclusion

Although there are several identifiable variations between the experimental luminescence results and what was expected based on the values published by Braun,et. al., the predictions of the miscibility of homopolymers of PS and PMMA systems based on these results generally were as expected. The largest variation occurred for predicting the phase behavior of homopolymer-copolymer blend systems. The blends of $P(MMA_{16}S_{82}VCz_2)$ and $P(MMA_{51}S_{47}VCz_2)$ with PS_1 both gave 20-30% relative luminescence intensities rather than the predicted 100%. The blends of $P(MMA_{77}S_{22}VCz_1)$ and $P(MMA_{51}S_{47}VCz_2)$ with $PMMA_1$ gave nearly 100% relative luminescence intensities rather than the predicted 0% results.

The variations in the PS_1 series may be explained in several ways. The lower molecular weight portion of the chromophore-containing copolymers may have increased the miscibility of the blend systems. The increased $[O_2]$ in the PS portion of the copolymer may have non-radiatively deactivated the excited triplet of the carbazole probe.[75] The excited state triplet of Cz may have been deactivated by the PS matrix via non-radiative decay and energy transfer to the matrix.[54] All of these effects lead to a decrease in the carbazole luminescence in polystyrene-rich systems.

Only with careful control and monitoring of the above mentioned variables can this luminescence probe/quencher method be applied to successfully determine the miscibility of PS-PMMA blend systems. The polydispersity of the polymers and copolymers to be studied must be avoided as much as is possible. In the case of low molecular weight fractions, dialysis may be performed to eliminate the troublesome portion. Solvents should be sparged with dry nitrogen prior to use. A glove box would

also help to minimize oxygen contamination during film preparation. Careful screening of controls would allow effective comparisons to compensate for matrix effects. Along with these precautions, a study of the concentration effects of carbazole would be useful, especially in interpreting the effects and benefits of delayed fluorescence. Since the delayed fluorescence quantum yield is greater than the phosphorescence quantum yield, delayed fluorescence provides more signal and greater sensitivity to the study.

References

1. Magerl, Fritz; Wintermantel, Erich; Mayer, Joerg; Tognini, Roger; Thomas, Andreas; Spirig, Walter; *PCT Int. Appl.*, 17 pp.
2. Felt, Jeffrey C.; *PCT Int. Appl.*, 37 pp.
3. Shea, Lonnie D.; Bonadido, Jeffrey; Mooney, David J.; *PCT Int. Appl.*, 144 pp.
4. Kataoka, Kazunori; Harada, Atsushi; Ikeda, Shuichi; Sakurai, Yasuhisa; Okano, Mitsuo; Aoyagi, Takao; *Jpn. Kokai Tokkyo Koho*, 7 pp.
5. Bao, Qi-Bin; Yuan, Hansen; *PCT Int. Appl.*, 41 pp.
6. Geertsema, A. A.; Schutte, H. K.; Van Leeuwen, M. B. M.; Rakhorst, G.; Schakenraad, J. M.; Van Luyn, M. J. A.; Verkerke, G. J.; *Biomaterials*, **20**, 1997 (1999).
7. Olabisi, Olagoke; *Polymer-Polymer Miscibility*, Academic Press: New York, 1979.
8. Krause, Sonja; *Pure and Appl. Chem.*, **58**, 1553 (1986).
9. Callaghan, T. A.; Paul, D. R.; *Macromolecules*, **26**, 2439 (1993).
10. Thompson, Edward V.; Klempner, Daniel; Frisch, Kurt C. (Eds.); *Polymer Alloys II: Blends, Blocks, Grafts, and Interpenetrating Networks*, Plenum Press: New York, 1980.
11. Liu, H. Z.; Lin, K. J.; *Macromolecules*, **1**, 157 (1968).
12. Liquori, A. M.; Anzuino, G.; Coiro, V. M.; D'Alagni, M.; DeSantis, P.; Savino, M.; *Nature (London)*, **206**, 358 (1965).
13. Braun, D.; Yu, D.; Kohl, P.R.; Gao, X.; Andradi, L.N.; Manger, E.; Hellman, G.P.; *Journal of Polymer Science, Part B: Polymer Physics*, **30**, 577 (1992).

14. Ikawa, Kiyoshi; Hosoda, Saturu; *Polymer Journal*, **22**, 643 (1990).

15. Brannock, G. R.; Barlow, J. W.; Paul, D. R.; *J. Polym. Sci.*, **29**, 413 (1991).

16. Hino, Toshiaki; Song, Yuhua; Prausnitz, John. M.; *Macromolecules*, **28**, 5717 (1995).

17. Galvin, Mary E.; *Macromolecules*, **24**, 6354 (1991).

18. Galvin, Mary; Heffnen, Sharon; Mirau, Peter; *Polym. Prepr. (Am. Chem. Soc., Div. Polm. Chem)*, **33**, 1174 (1992).

19. Winey, Karen I.; Berba, Maria Luisa; Galvin, Mary E.; *Macromolecules*, **29**, 2868 (1996).

20. Inoue, T.; Soen, T.; Hashimoto, T.; Kawai, H.; *Polym. Prepr. (Am. Chem. Soc., Div. Polm. Chem)*, **10**, 538 (1969).

21. Marsh, P. A.; Voet, A.; Price, L. D.; Mullens, T. J.; *Rubber Chem. Technol.*, **41**, 344 (1968).

22. Vasile, C.; Schneiderm L. A.; *Eur. Polym. J.*, **7**, 1205 (1965).

23. Walters, M. H.; Keyte, D. N.; .; *Rubber Chem. Technol.*, **38**, 62 (1965).

24. Smith, R. W.; Andries, J. C.; .; *Rubber Chem. Technol.*, **47**, 64 (1974).

25. Matsuo, M.; Nozaki, C.; Jyo, Y.; *Polym. Eng. Sci.*, **9**, 197, (1969).

26. McMaster, L. P.; *Adv. Chem. Ser.*, **142**, 43 (1975).

27. Tsitsilianis, C.; Staikos, G.; *Macromolecules*, **25**, 910 (1992).

28. Miles, I. S.; Rostami, S. (Eds.); *Multicomponent Polymer Systems*, Longman Scientific and Technical: England, 1992.

29. Rogosic, M.; Mencer, H. J.; *European Polymer Journal*, **33**, 621 (1997).

30. Krigbaum, , W. R.; Wall, F. T.; *J. Polym. Sci.*, **5**, 505 (1950).

31. Catsiff, E. H.; Hewett, W. A.; *J. Appl. Polym. Sci.*, **6**, S30 (1962).

32. Voelkel, R.; *Angewante Chemie*, **27**, 1, 1468 (1988).

33. Kelts, L.W.; Landry, C.J.T.; Teegarden, D.M.; *Macromolecules*, **26**, 11, 2941 (1993).

34. Dutta, S.; Chakraborty, S.S.; Mandal, B.M.; Bhattacharyya, S.N.; *Polymer*, **34**, 16, 3499 (1993).

35. Feraz, Fatima; Hamou, Assia Siham Hadj; Djadoun, Said; *Eur. Polym. J.*, **31**, 665 (1995).

36. Horie, K.; Mita, I.; *Polym. J.*, **8**, 227 (1976).

37. Tao, W.C.; Frank, C.W.; *Macromolecules*, **23**, 13, 3275 (1990).

38. Haines, D.J.; Wilson, G.J.; Ghiggino, K.P.; Hill, D.J.; *Polymer International*, **26**, 4, 267 (1991).

39. Qiao, Lin; *Miscibility Study of Polymer Blends by a Novel Phosphorescent Quenching System*, M.S. Thesis, RIT, 1998.

40. Becker, Ralph S.; *Theory and Interpretation of Fluorescence and Phosphorescence*, John Wiley & Sons, Inc.: New York, 1969.

41. Guillet, James; *Polymer Photophysics and Photochemistry*, Cambridge University Press: New York, 1985.

42. Zander, M.; *Phosphorimetry*, Academic Press: New York, 1968.

43. Pringsheim, Peter; *Fluorescence and Phosphorescence*, Interscience Publishers, Inc.: New York, 1949.

44. Jablonski, A.; *Nature*, **131**, 839 (1933); *Z. Physik*, **94**, 38 (1935).

45. Parker, C. A.; Hatchard, C. G.; *Trans Faraday Soc.*, **59**, 284 (1963).

46. Kautsky, H.; Merkel, H.; *Naturwissenschaften*, **27**, 195 (1939).

47. Kautsky, H.; Muller, G. O.; *Naturwissenschaften*, **29**, 150 (1941).

48. Kautsky, H.; Muller, G. O.; *Z. Naturforsch.*, **2a**, 167 (1947).

49. Parker, C. A.; Hatchard, C. G.; *Proc. Roy. Soc.*, **A269**, 574 (1962).

50. Azumi, T.; McGlynn, S. P.; *J. Chem. Phys.*, **38**, 2773 (1963); **39**, 1186 (1963).

51. Harvey, P.; Durocher, G.; *J. Luminescence*, **33**, 175 (1985).

52. Zelent, B.; Ganguly, T.; Farmer, L.; Gravel, D.; Durocher, G.; *J. Photochem. Photobiol. A.,* **56**, 165 (1991).

53. Griffin, R. N.; *Photochem. Photobiol.,* **7**, 175 (1968).

54. Williamson, Helen; MacCallum, James R.; *Eur. Polym. J.*, **29**, 201 (1993).

55. Johnson, G. E.; *J. Chem. Phys.*, **78**, 1512 (1974).

56. Carlier, Eric; Revillon, Andre; Chauvet, Jean Paul; *Eur. Polym. J.*, **29**, 825 (1993).

57. Abbott, David W.; Vo-Dinh, Tuan; *Anal. Chem.,* **57**, 41 (1985).

58. Vo-Dinh, T.; Hooyman, J. R.; *Anal. Chem.,* **51**, 1915 (1979).

59. Morantz, D. J; Bilen, C. S.; Harrison, N.; *Polymer*, **19**, 473 (1978).

60. Femia, Robert A.; Cline Love, L. J.; *Spectrochimica Acta*, **42A**, 1239 (1986).

61. Searle, N. E.; *U.S. Patent 2 444 536*, July 6, 1948.

62. Uno, K.; Makita, M.; Doi, S.; *J. Polym. Sci. A-1*, **6**, 257 (1968).

63. Hart, R.; *Macromol. Chem.*, **47**, 143 (1961).

64. Matsumoto, A.; Kubota, T.; Otsu, T.; *Macromolecules*, **23**, 4508 (1990).

65. Painter, Paul C.; Coleman, Michael M.; *Fundamentals of Polymer Science*; Technomic Publishing Company: Lancaster, PA, 1997.

66. Silverstein, R. M.; Bassler, G. C.; Morrill, T. C.; *Spectrometric Identification of Organic Compounds (5th ed.),* John Wiley & Sons, Inc.: New York, 1991.

67. Sadtler Research Laboratories, Inc.; *Nuclear Magnetic Resonance Spectra,* Philadelphia, 1969.

68. Kawaguchi, T.; Kanaya, T.; Kaji, K.; *Physica B: Condensed Matter*, **213/214**, 510 (1995).

69. Cobler, J. G.; The Dow Chemical Company, unpublished data.

70. Thompson, E. V.; *J. Polym. Sci. A-2*, **4**, 199 (1966).

71. Wittmann, J. C.; Kovacs, A. J.; *J. Polym. Sci. C,* **16**, 4443 (1969).

72. Schnabel, W.; Polymer Degradation: Principlies and Practical Applications, Macmillan Publishing Co., Inc.: New York, 1981.

73. Odian, George G.; *Principles of Polymerization (3rd ed.)*, John Wiley & Sons, Inc.: New York, 1991.

74. Mourey, Thomas H., Eastman Kodak, Co., personal communication, 1999.

75. Camyshan, S. V.; Gritsan, N. P.; Korolev, V. V.; Bazhin, N. M.; *Chem. Phys.*, **142**, 59 (1990).

76. Bicerano, Jozef; *Prediction of Polymer Properties*, Marcel Dekker, Inc.: New York, 1996.

77. Conrow, Paul; personal communication, 1999.

Appendix A: ^{1}H-NMR Spectra of Copolymers

A1

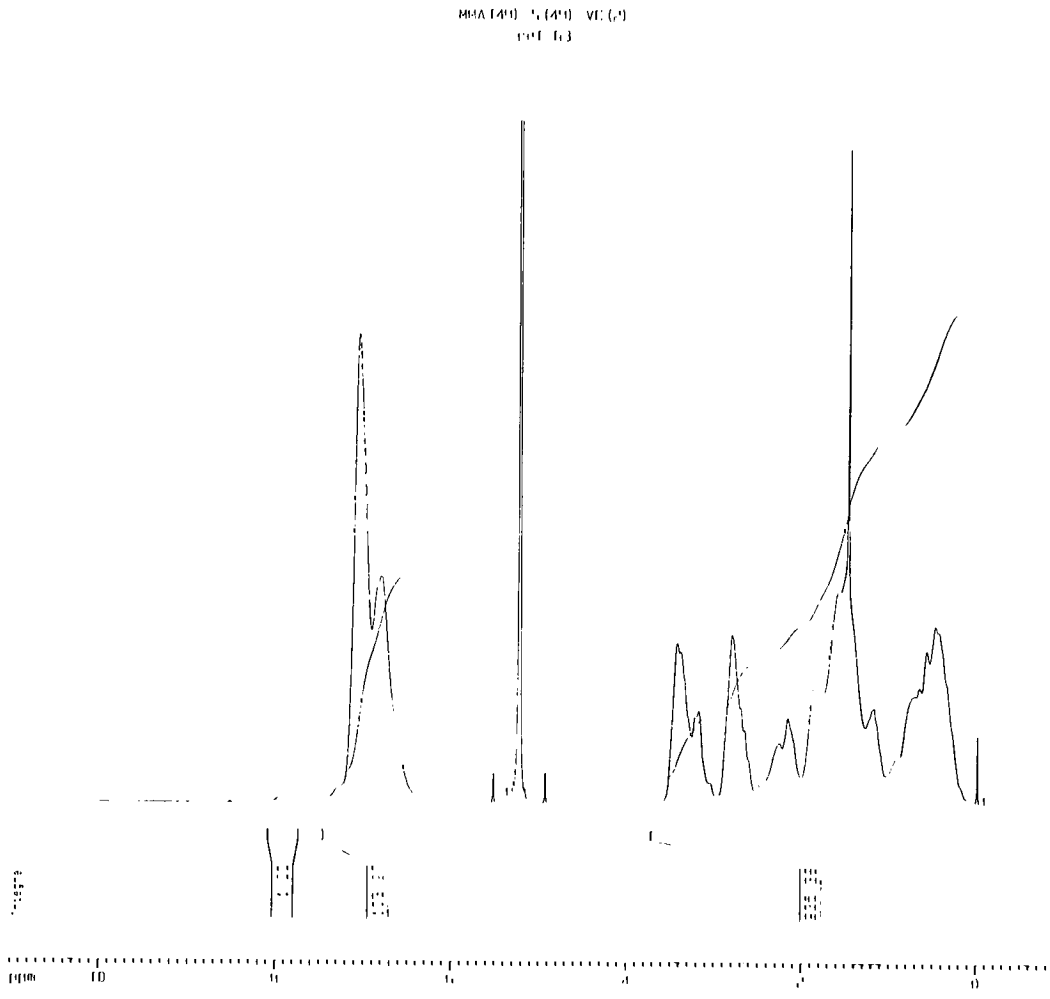

NAME	[illegible]
EXPNO	7
PROCNO	1

F2 - Acquisition Parameters

Date	[illegible]
Time	14.23
INSTRUM	spect
PROBHD	5 mm UNI [illegible]
PULPROG	zg30
TD	32768
SOLVENT	CDCl3
NS	128
DS	0
SWH	6172.8 Hz
FIDRES	0.188 Hz
AQ	2.6542480 sec
RG	114
DW	81.000 usec
DE	6.00 usec
TE	300.0 K
D1	2.00000000 sec
P1	11.00 usec
P2	22.00 usec
SFO1	600.1320 MHz
NUC1	1H
PL1	5.10 dB

F2 - Processing parameters

SI	16384
SF	600.1300 MHz
WDW	EM
SSB	0
LB	0.30 Hz
GB	0
PC	1.00

1H NMR plot parameters

CX	20.00 cm
F1P	11.000 ppm
F1	6601.43 Hz
F2P	1.000 ppm
F2	600.13 Hz
PPMCM	0.500000 ppm/cm
HZCM	300.06500 Hz/cm

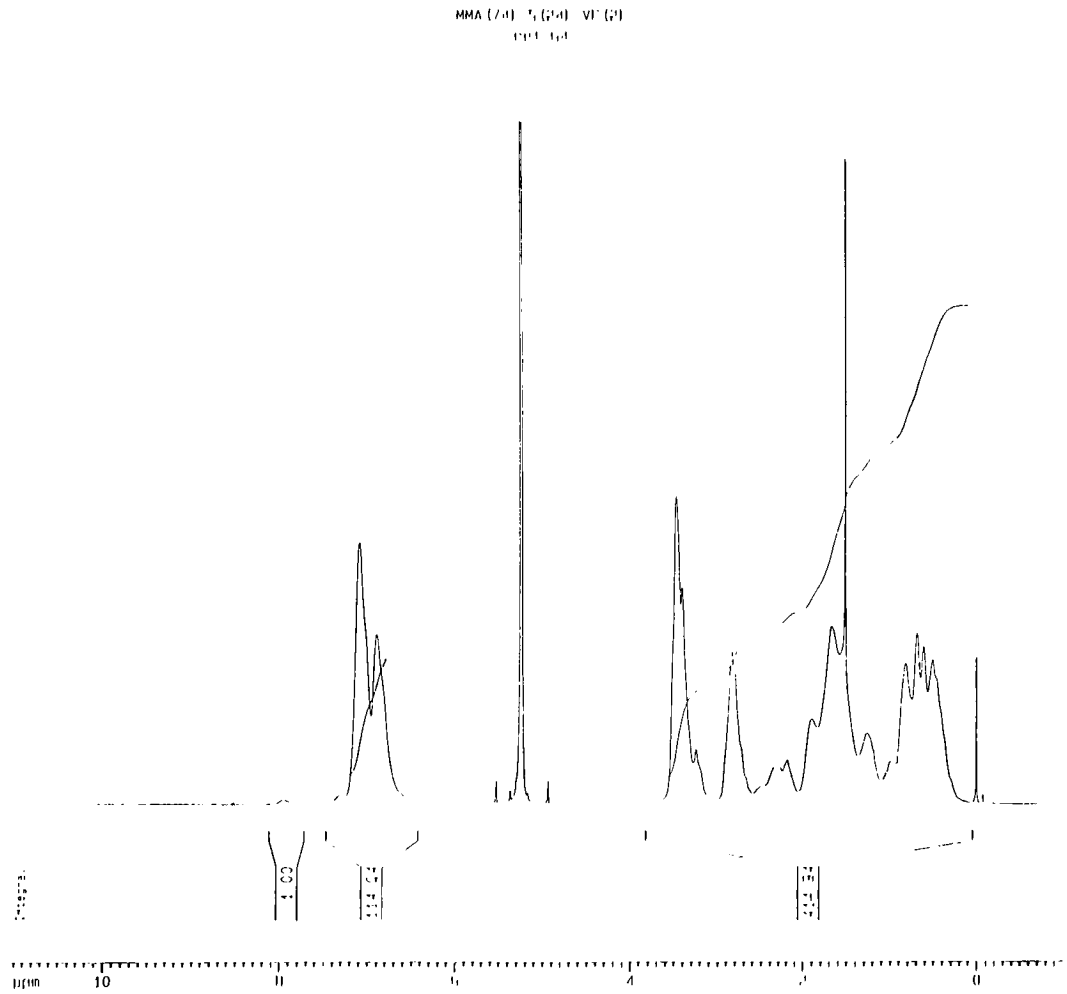

A2

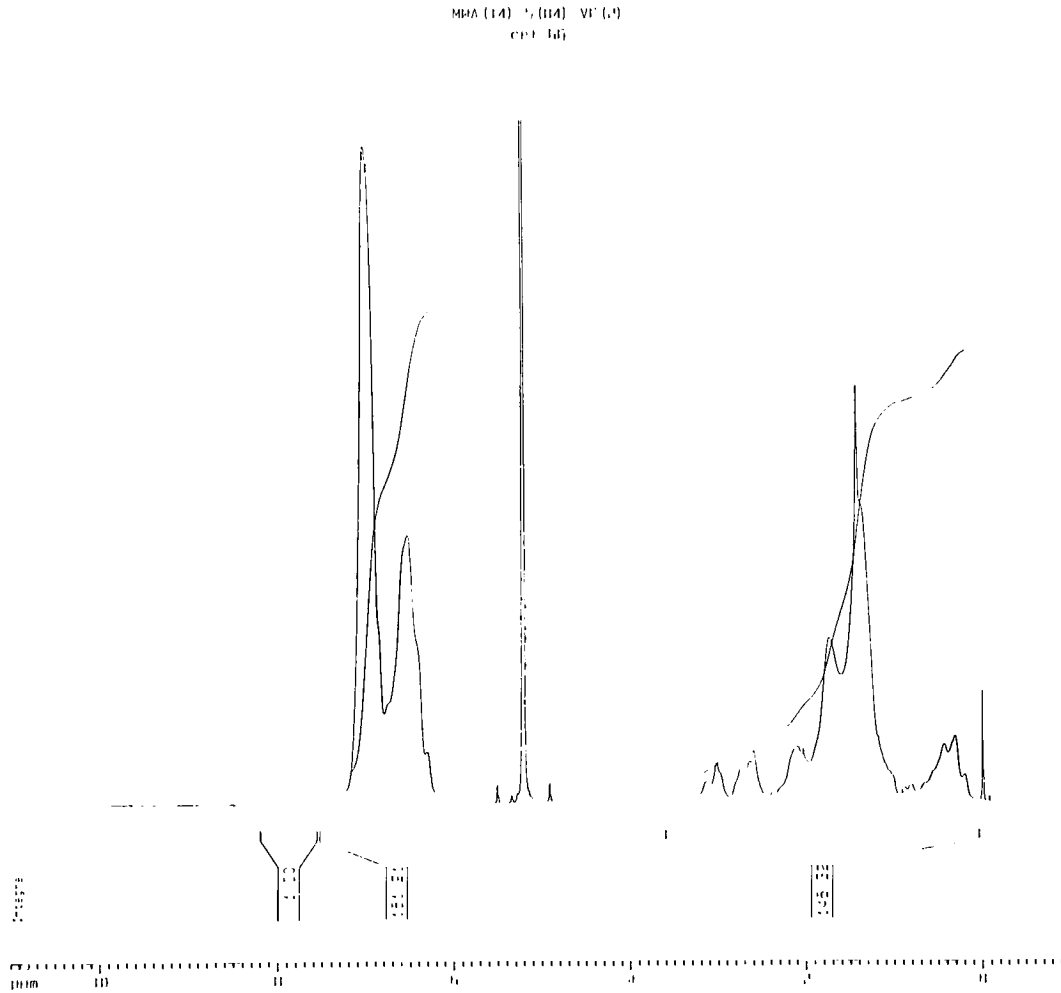

Current Data Parameters
NAME SpinOz 99 toluene
EXPNO 4
PROCNO 1

F2 - Acquisition Parameters
Date_ 990HHz
Time 14 57
INSTRUM spect
PROBHD 5 mm DUL 13
PULPROG zg30
TD 32768
SOLVENT CDCl3
NS 1.00
DS 0
SWH 6172.8 Hz
FIDRES 0.188340 Hz
AQ 2.6544688 sec
RG 114
DW 81.000 usec
DE 6.00 usec
TE 300.0 K
D1 2.00000000 sec
P1 9.00 usec
PL1 6.00 usec
SFO1 300.1300084 MHz
NUC1 1H
PL1 -4.00 dB

F2 - Processing parameters
SI 16384
SF 300.1300086 MHz
WDW EM
SSB 0
LB 0.30 Hz
GB 0
PC 1.00

1H NMR plot parameters
CX 20.00 cm
F1P 11.0000 ppm
F1 3301.43 Hz
F2P 1.0000 ppm
F2 300.13 Hz
PPMCM 0.50000 ppm/cm
HZCM 150.06501 Hz/cm

A3

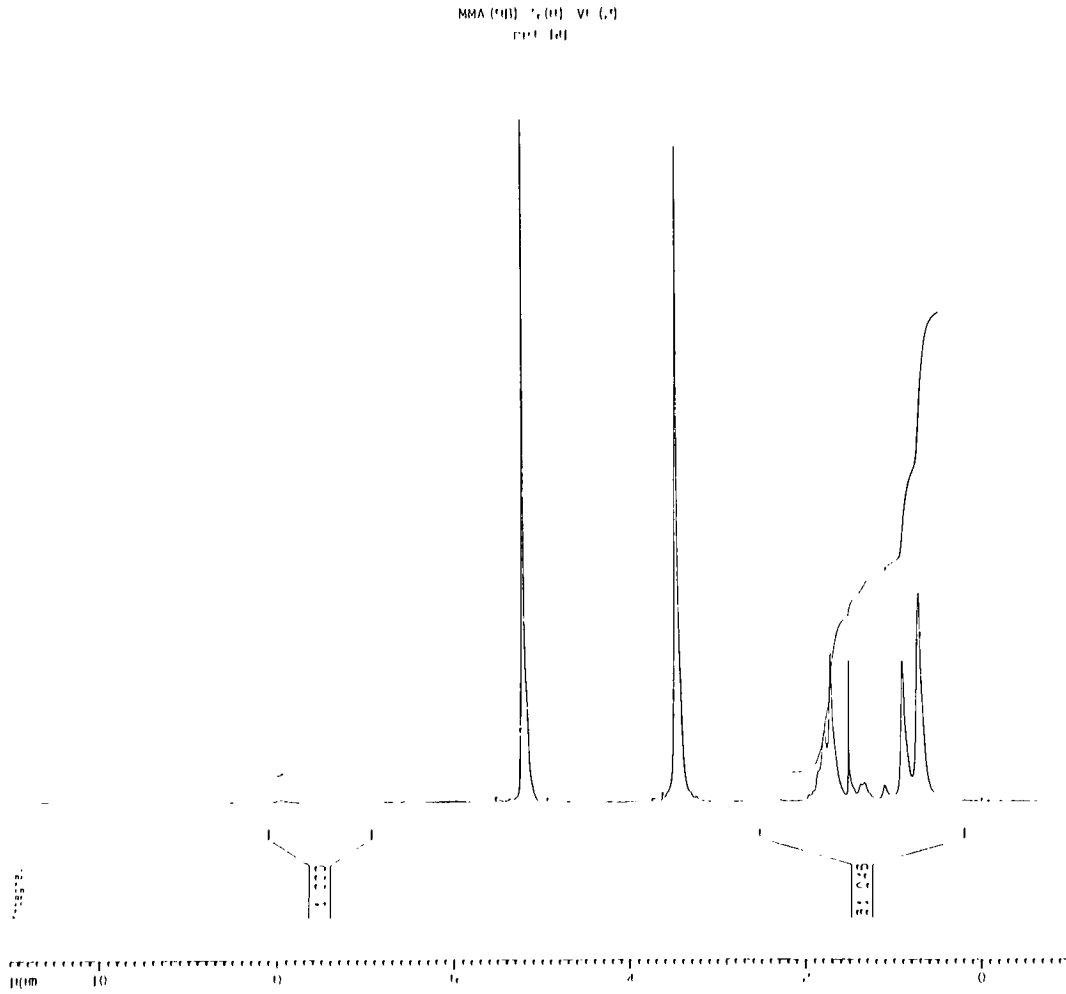

A5

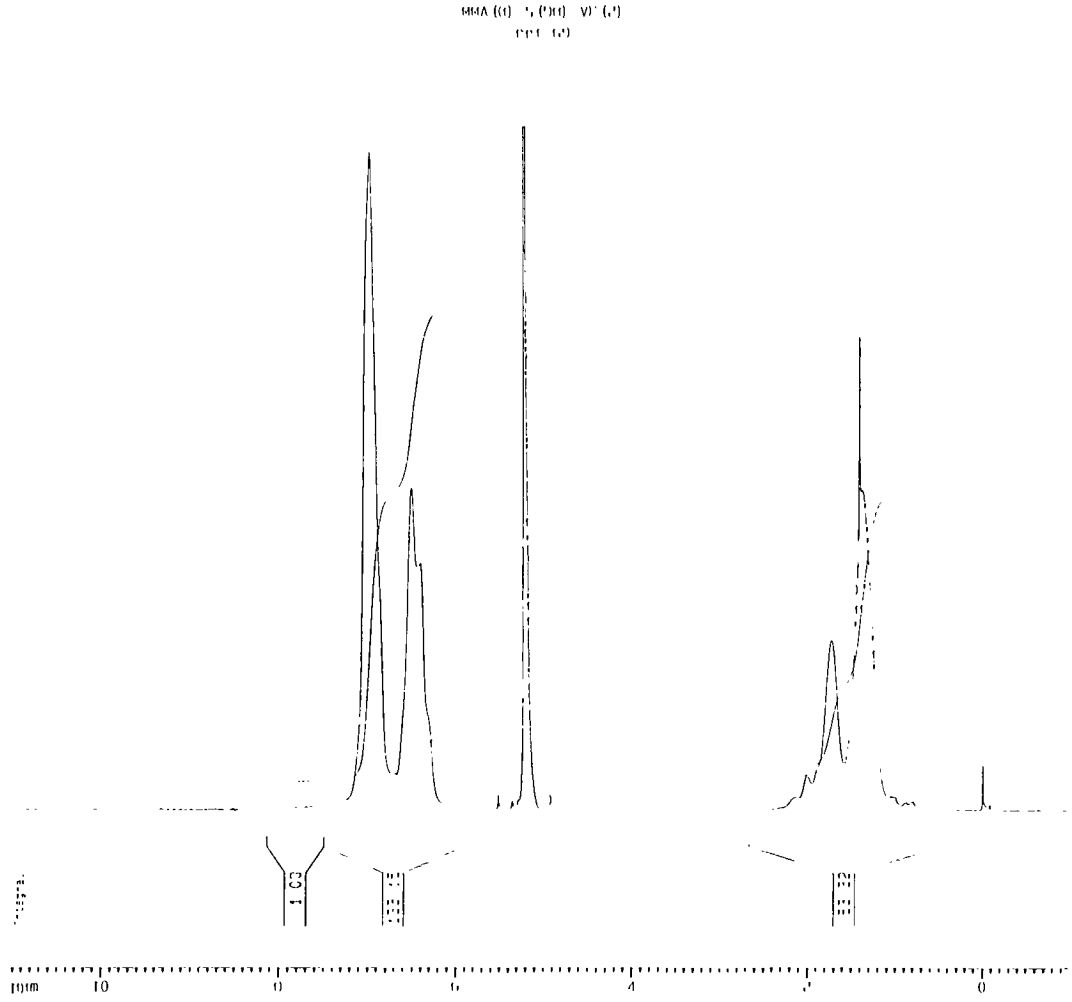

Current Data Parameters
NAME Sept07 PU Compo
EXPNO 7
PROCNO 1

F2 - Acquisition Parameters
Date 20070907
Time 16.24
INSTRUM spect
PROBHD 5 mm BBO BB
PULPROG zg30
TD 32768
SOLVENT CDCl3
NS 64
DS 16
SWH 6172.8 Hz
FIDRES 0.188324 Hz
AQ 2.6542688 sec
RG 228
DW 81.000 usec
DE 6.00 usec
TE 300.0 K
D1 2.00000000 sec
P1 11.00 usec
DB 6.00 usec
SFO1 300.1318014 MHz
NUC1 1H
PL1 -3.00 dB

F2 - Processing parameters
SI 16384
SF 300.1300110 MHz
WDW EM
SSB 0
LB 0.30 Hz
GB 0
PC 1.00

1H NMR plot parameters
CX 20.00 cm
F1P 11.000 ppm
F1 1651.41 Hz
F2P 1.000 ppm
F2 300.13 Hz
PPMCM 0.60000 ppm/cm
HZCM 180.07803 Hz/cm

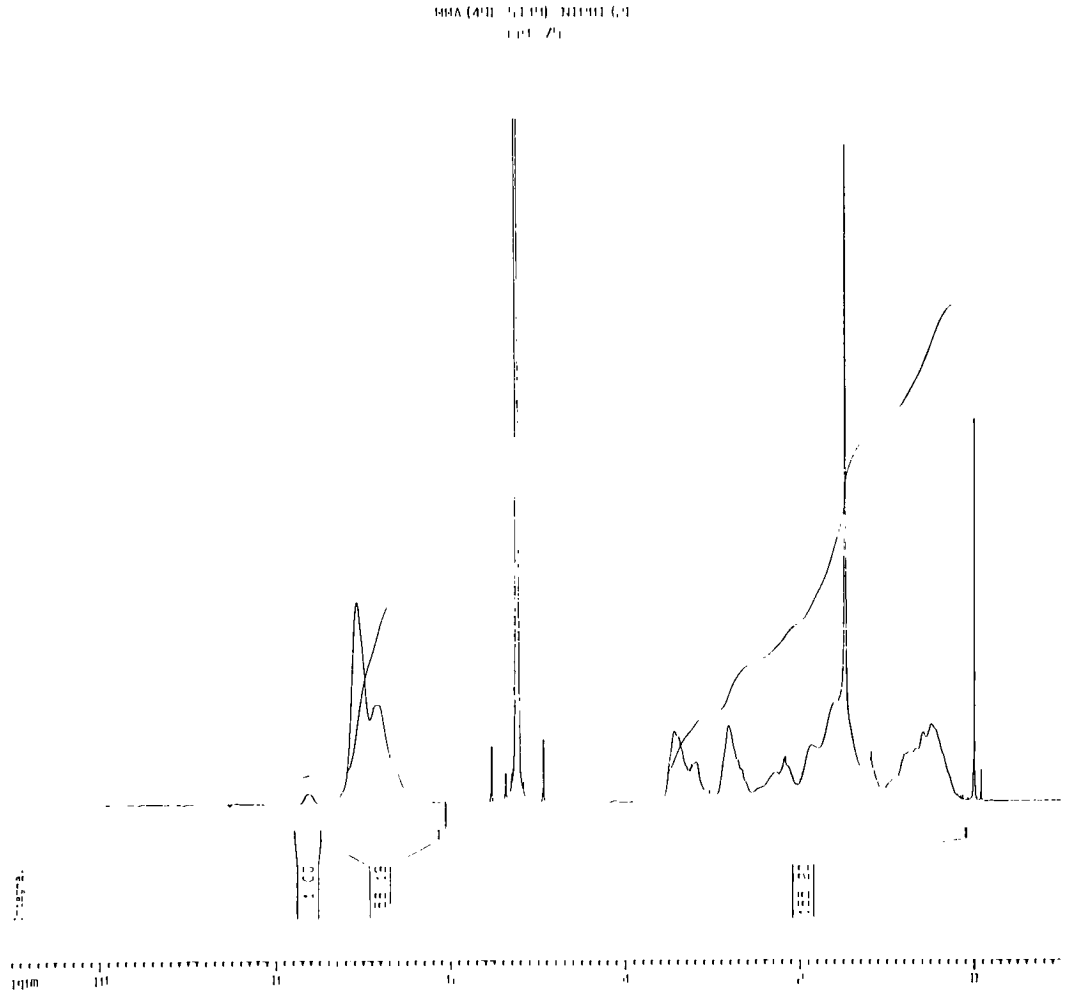

Current Data Parameters
NAME Sept11 PI Group
EXPNO 1
PROCNO 1

F2 - Acquisition Parameters
Date_ 1999111
Time 11 16
INSTRUM spect
PROBHD 5 mm DUAL 13C
PULPROG zg30
TD 65536
SOLVENT CDCl3
NS 1
DS 0
SWH 6172.8 Hz
FIDRES 0.188455 Hz
AQ 5.3084288 sec
RG 1
DW 81.000 usec
DE 6.00 usec
TE 300.0 K
D1 1.00000000 sec
P1 9.00 usec
DC 6.00 usec
SFO1 300.1300014 MHz
NUC1 1H
PL1 -1.00 dB

F2 - Processing parameters
SI 32768
SF 300.1300125 MHz
WDW EM
SSB 0
LB 0.30 Hz
GB 0
PC 1.00

1D NMR plot parameters
CX 20.00 cm
F1P 11.000 ppm
F1 3301.43 Hz
F2P 1.000 ppm
F2 300.13 Hz
PPMCM 0.60000 ppm/cm
HZCM 180.07031 Hz/cm

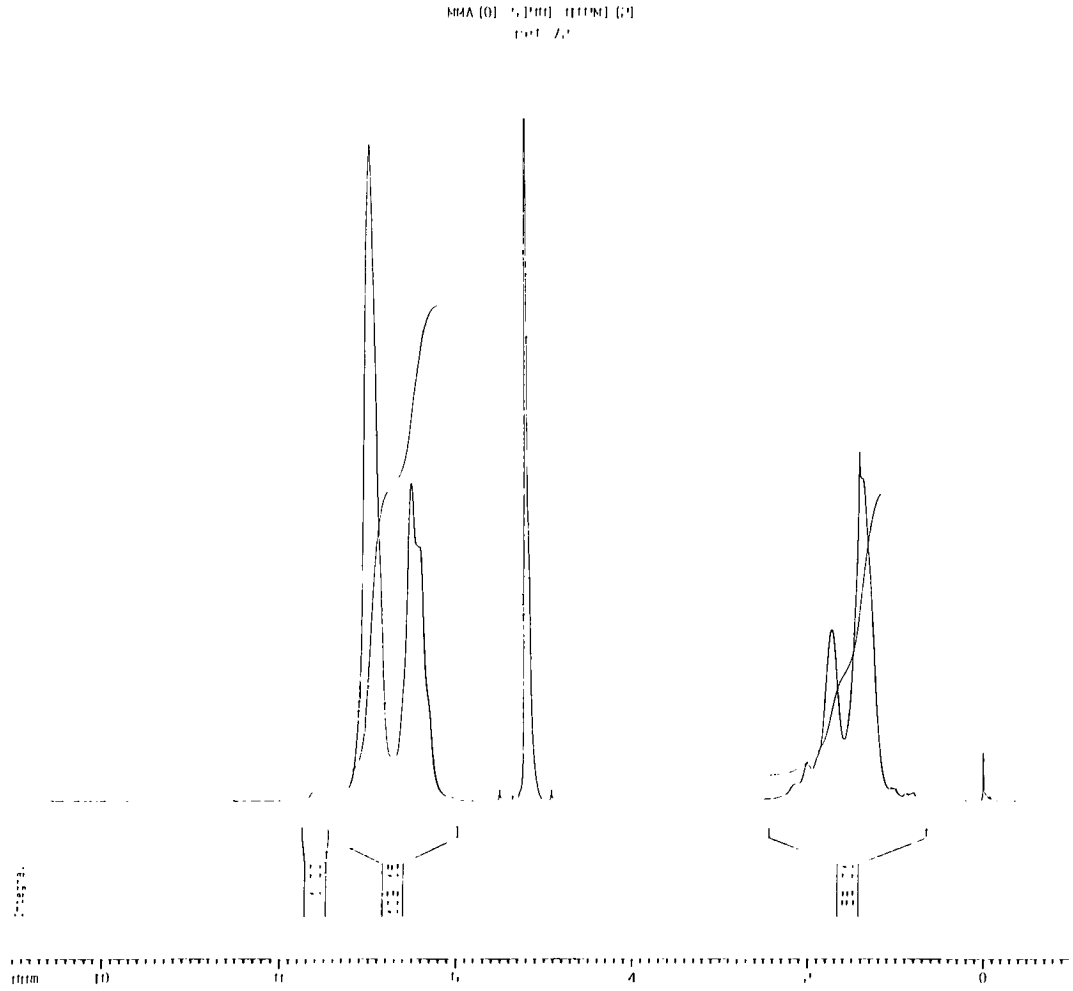
ppm
10
8
6
4
2
0

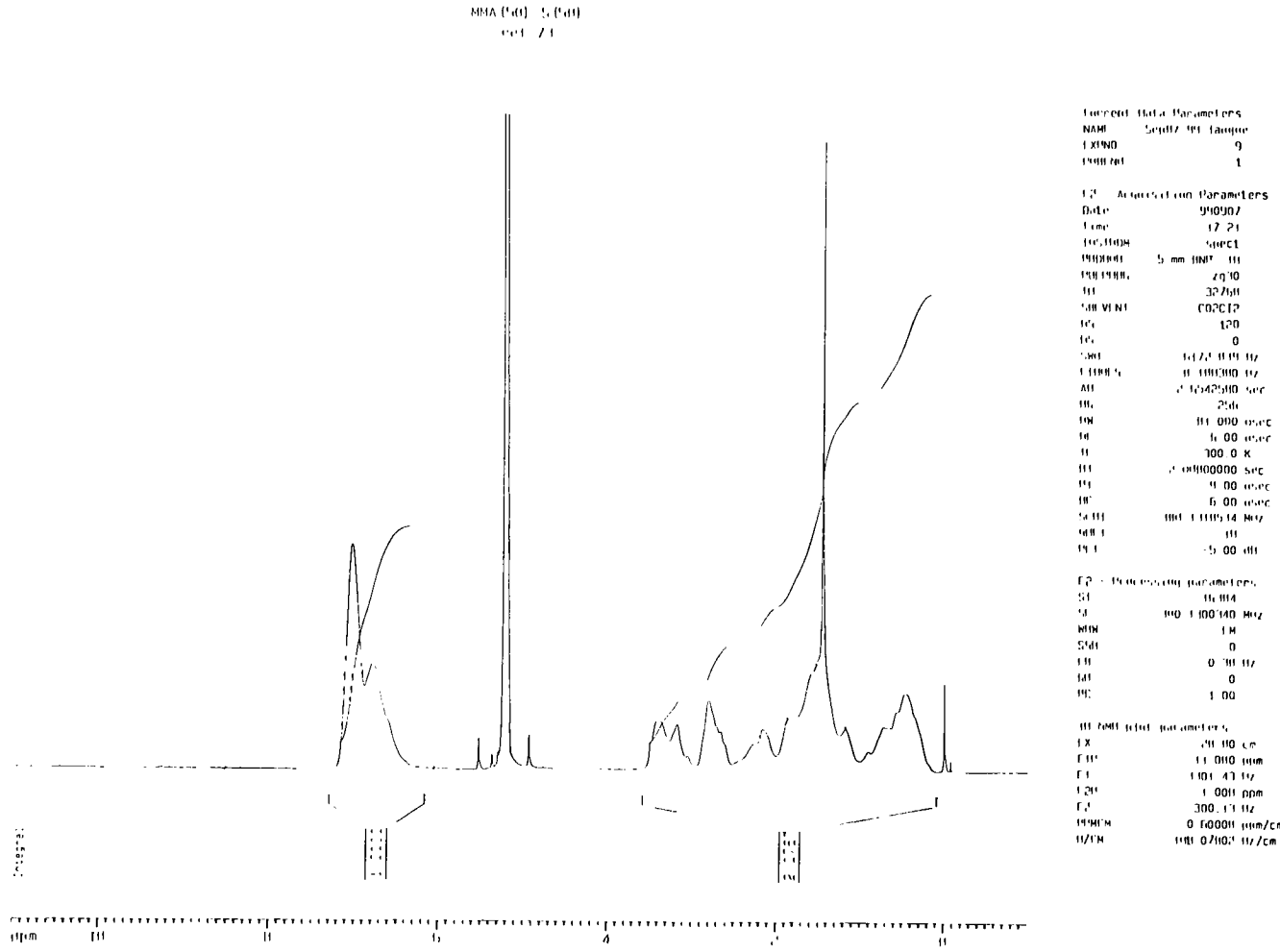

A10

Appendix B: DSC Thermograms of Copolymers

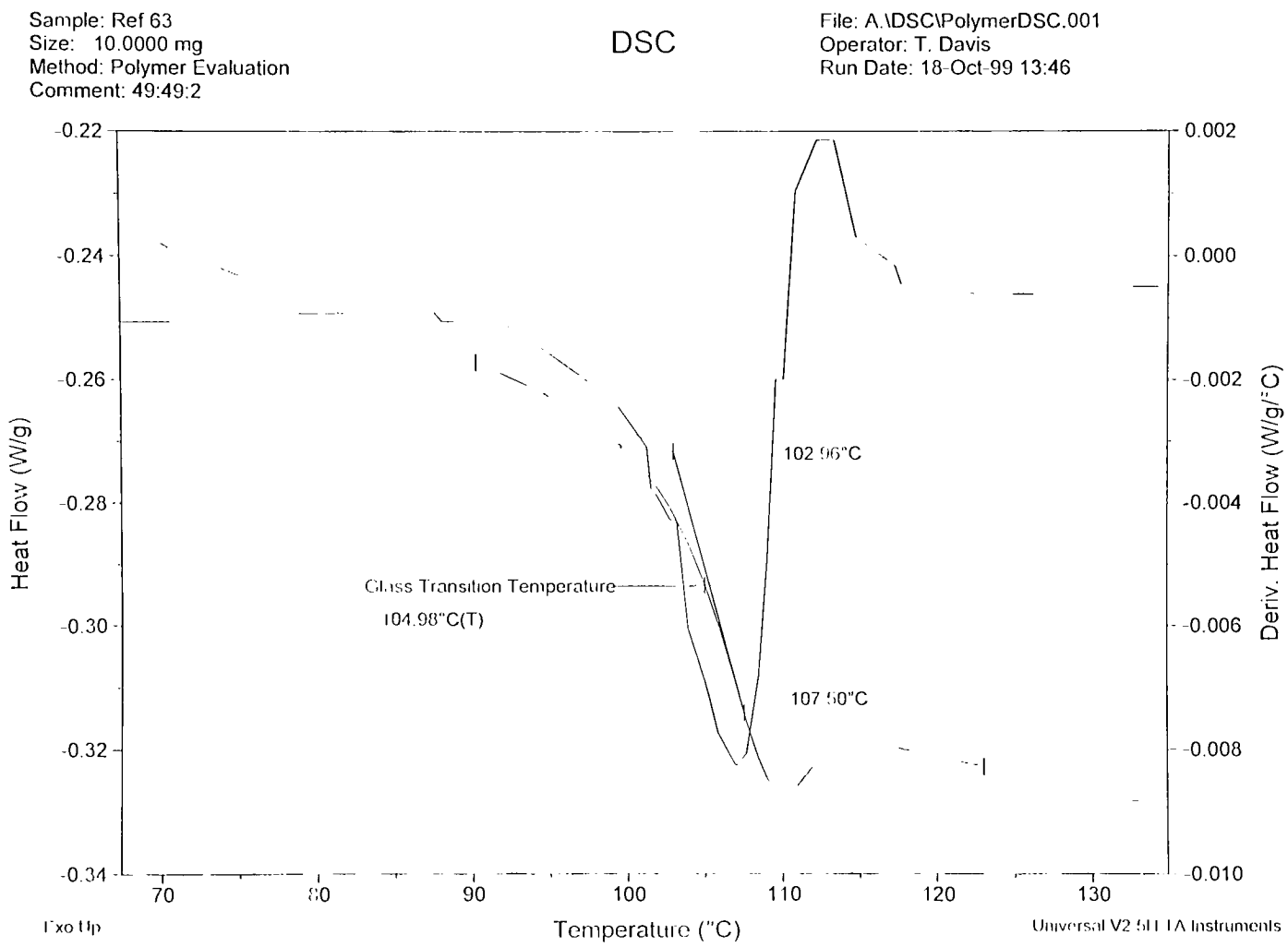
Sample: Ref 63
Size: 10.0000 mg
Method: Polymer Evaluation
Comment: 49:49:2
DSC
File: A:\DSC\PolymerDSC.001
Operator: T. Davis
Run Date: 18-Oct-99 13:46
Heat Flow (W/g)
Deriv. Heat Flow (W/g/°C)
Temperature (°C)
Exo Up
Universal V2.5H TA Instruments
-0.22
-0.24
-0.26
-0.28
-0.30
-0.32
-0.34
0.002
0.000
-0.002
-0.004
-0.006
-0.008
-0.010
70
80
90
100
110
120
130
102.96°C
107.50°C
Glass Transition Temperature
104.98°C(T)

B1

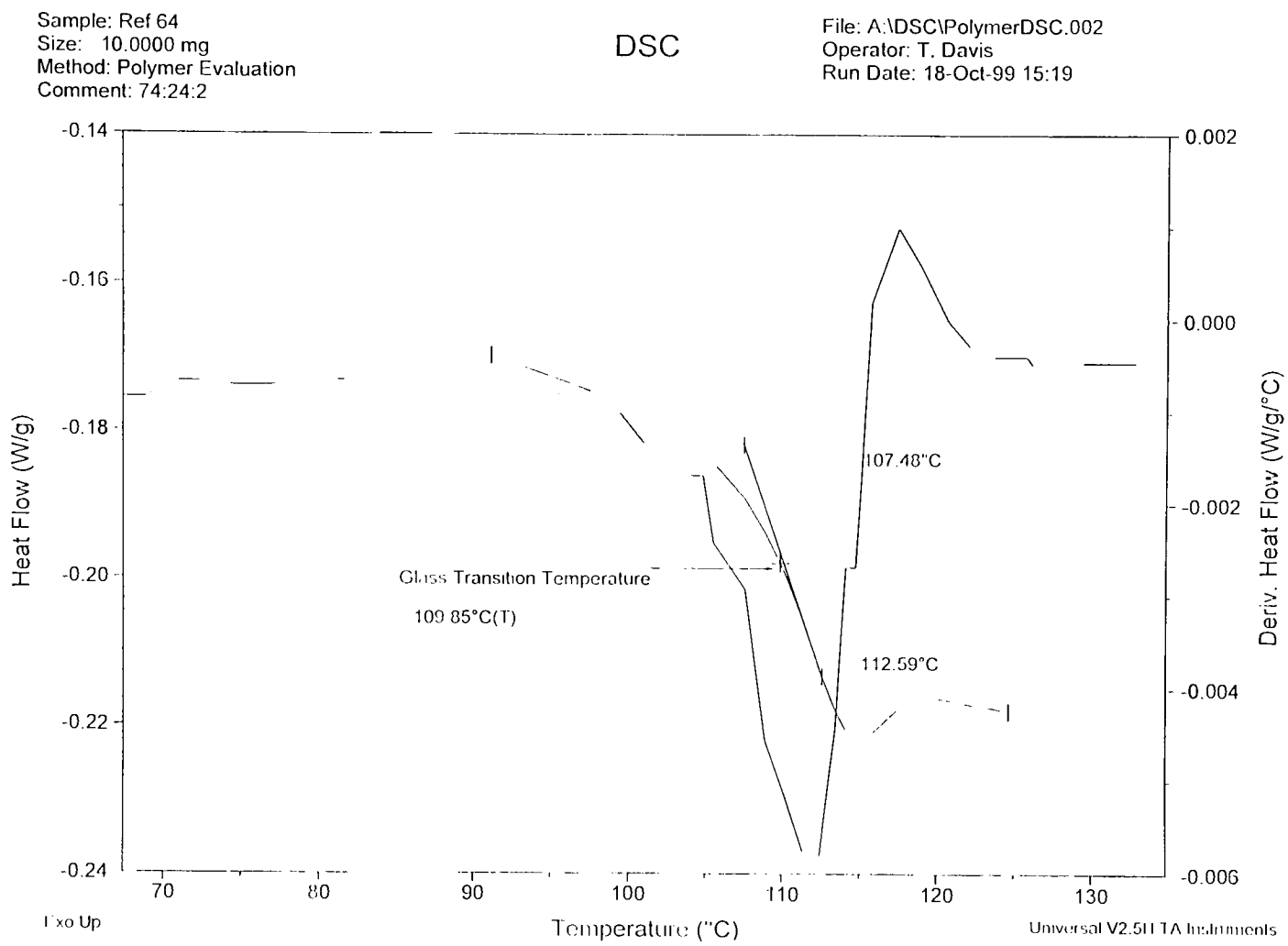
Sample: Ref 64
Size: 10.0000 mg
Method: Polymer Evaluation
Comment: 74:24:2
DSC
File: A:\DSC\PolymerDSC.002
Operator: T. Davis
Run Date: 18-Oct-99 15:19
Heat Flow (W/g)
Deriv. Heat Flow (W/g/°C)
Temperature (°C)
Exo Up
Universal V2.5H TA Instruments
Glass Transition Temperature
109.85°C(T)
107.48°C
112.59°C
-0.14
-0.16
-0.18
-0.20
-0.22
-0.24
0.002
0.000
-0.002
-0.004
-0.006
70
80
90
100
110
120
130

B2

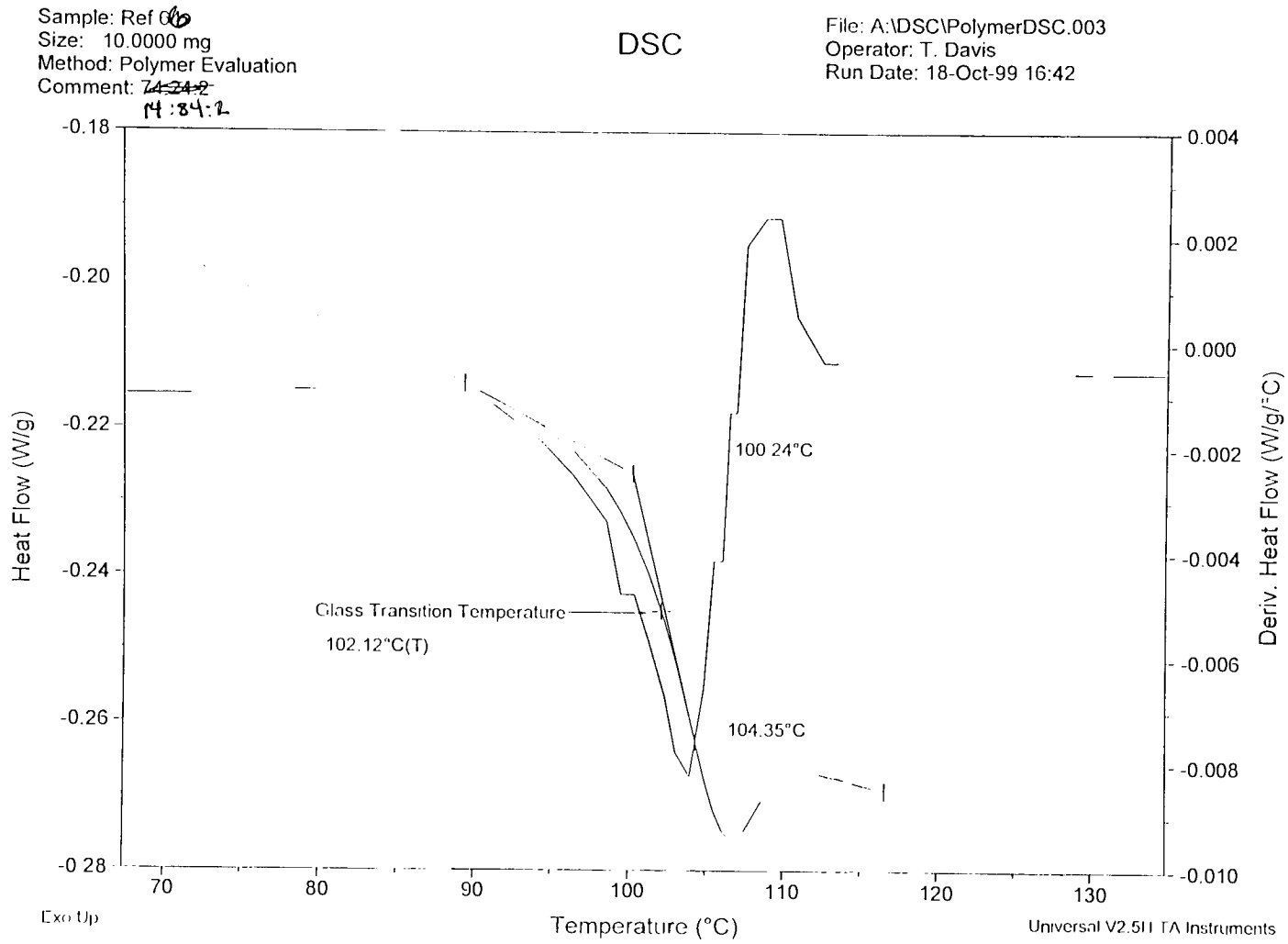
Sample: Ref 0%
Size: 10.0000 mg
Method: Polymer Evaluation
Comment: ~~14:24:2~~ 14:34:2
DSC
File: A:\DSC\PolymerDSC.003
Operator: T. Davis
Run Date: 18-Oct-99 16:42
Heat Flow (W/g)
Deriv. Heat Flow (W/g/°C)
Temperature (°C)
Exo Up
Universal V2.5H TA Instruments
100.24°C
104.35°C
Glass Transition Temperature
102.12°C(T)
-0.18
-0.20
-0.22
-0.24
-0.26
-0.28
0.004
0.002
0.000
-0.002
-0.004
-0.006
-0.008
-0.010
70
80
90
100
110
120
130

B3

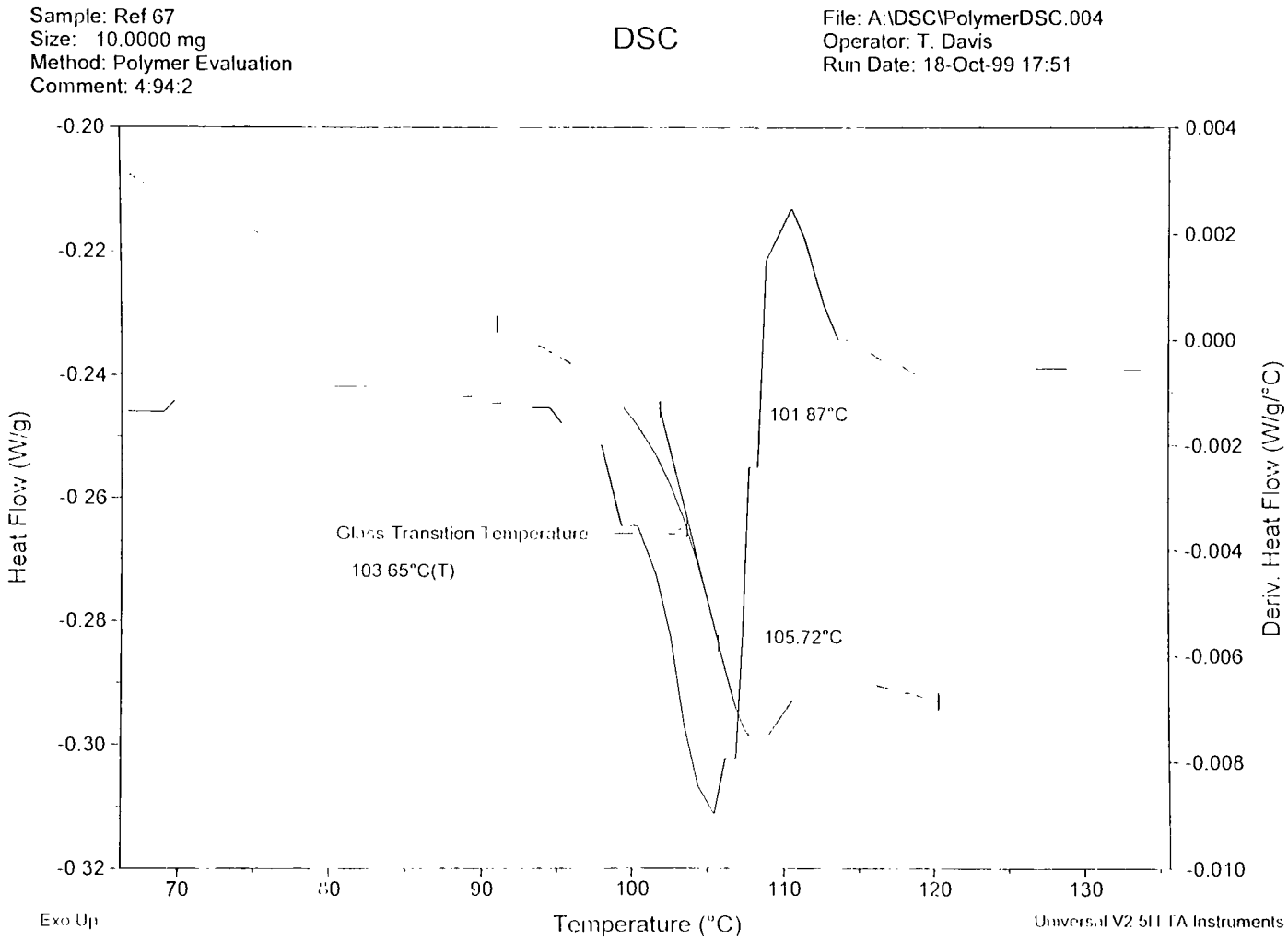
Sample: Ref 67
Size: 10.0000 mg
Method: Polymer Evaluation
Comment: 4:94:2
DSC
File: A:\DSC\PolymerDSC.004
Operator: T. Davis
Run Date: 18-Oct-99 17:51
Heat Flow (W/g)
Deriv. Heat Flow (W/g/°C)
Temperature (°C)
Exo Up
Universal V2.5H TA Instruments
Glass Transition Temperature
103.65°C(T)
101.87°C
105.72°C
-0.20
-0.22
-0.24
-0.26
-0.28
-0.30
-0.32
0.004
0.002
0.000
-0.002
-0.004
-0.006
-0.008
-0.010
70
80
90
100
110
120
130

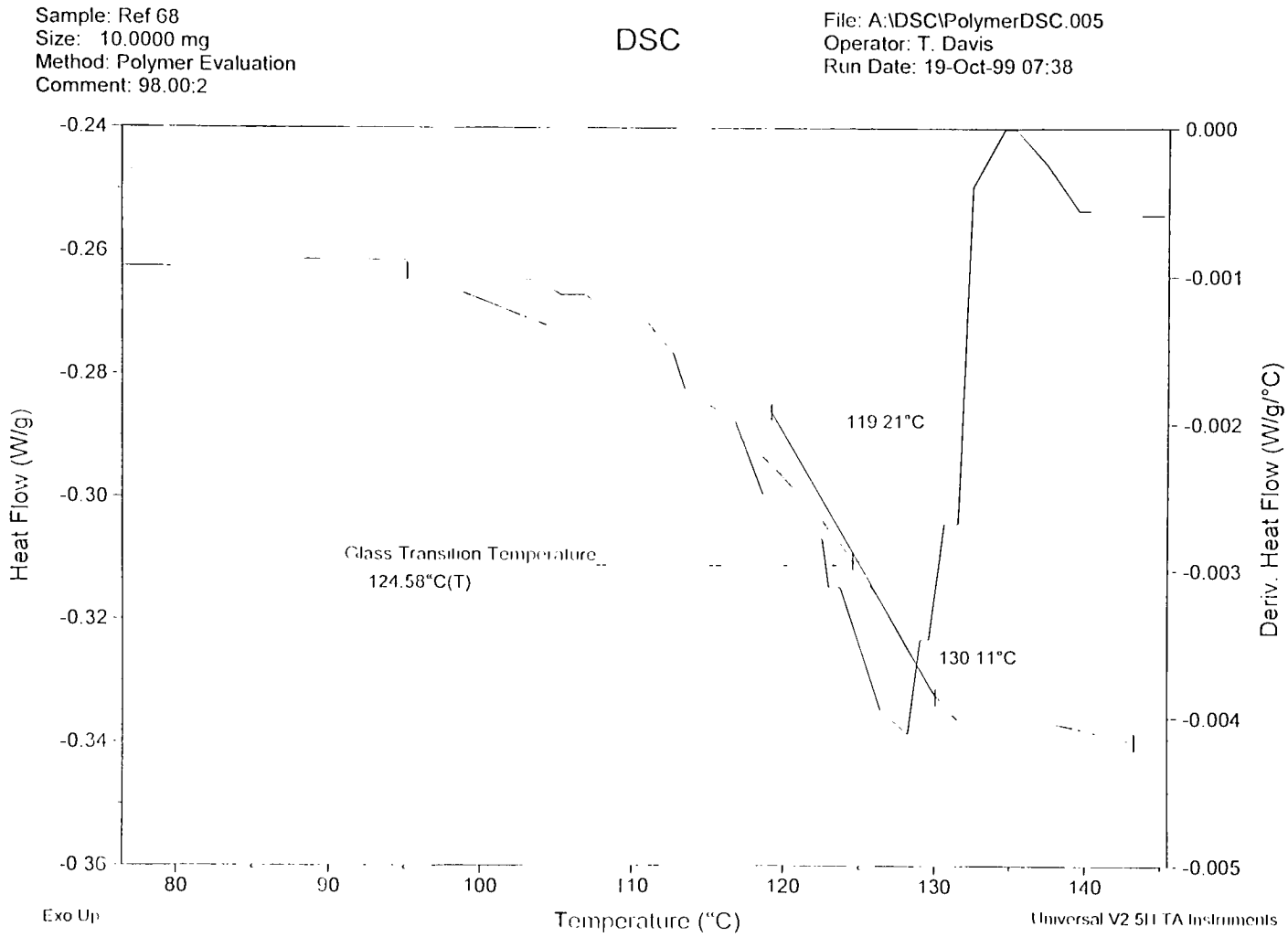
Sample: Ref 68
Size: 10.0000 mg
Method: Polymer Evaluation
Comment: 98.00:2
DSC
File: A:\DSC\PolymerDSC.005
Operator: T. Davis
Run Date: 19-Oct-99 07:38
-0.24
-0.26
-0.28
-0.30
-0.32
-0.34
-0 36
Heat Flow (W/g)
0.000
-0.001
-0.002
-0.003
-0.004
-0.005
Deriv. Heat Flow (W/g/°C)
119 21°C
Glass Transition Temperature
124.58°C(T)
130 11°C
80
90
100
110
120
130
140
Exo Up
Temperature (°C)
Universal V2 5H TA Instruments

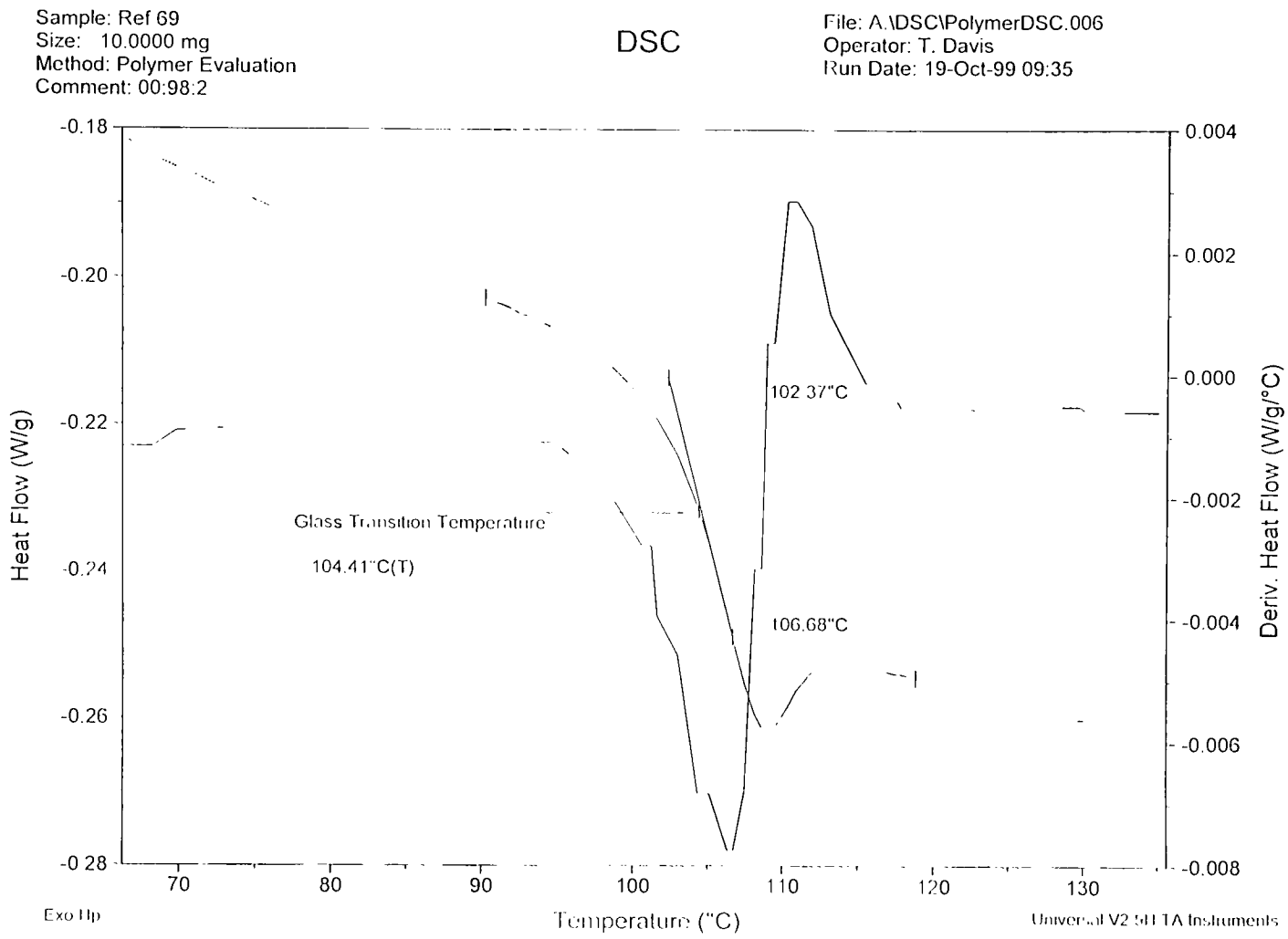
Sample: Ref 69
Size: 10.0000 mg
Method: Polymer Evaluation
Comment: 00:98:2
DSC
File: A:\DSC\PolymerDSC.006
Operator: T. Davis
Run Date: 19-Oct-99 09:35
Heat Flow (W/g)
Deriv. Heat Flow (W/g/°C)
Temperature (°C)
Glass Transition Temperature
104.41°C(T)
102.37°C
106.68°C
Exo Up
Universal V2.5H TA Instruments

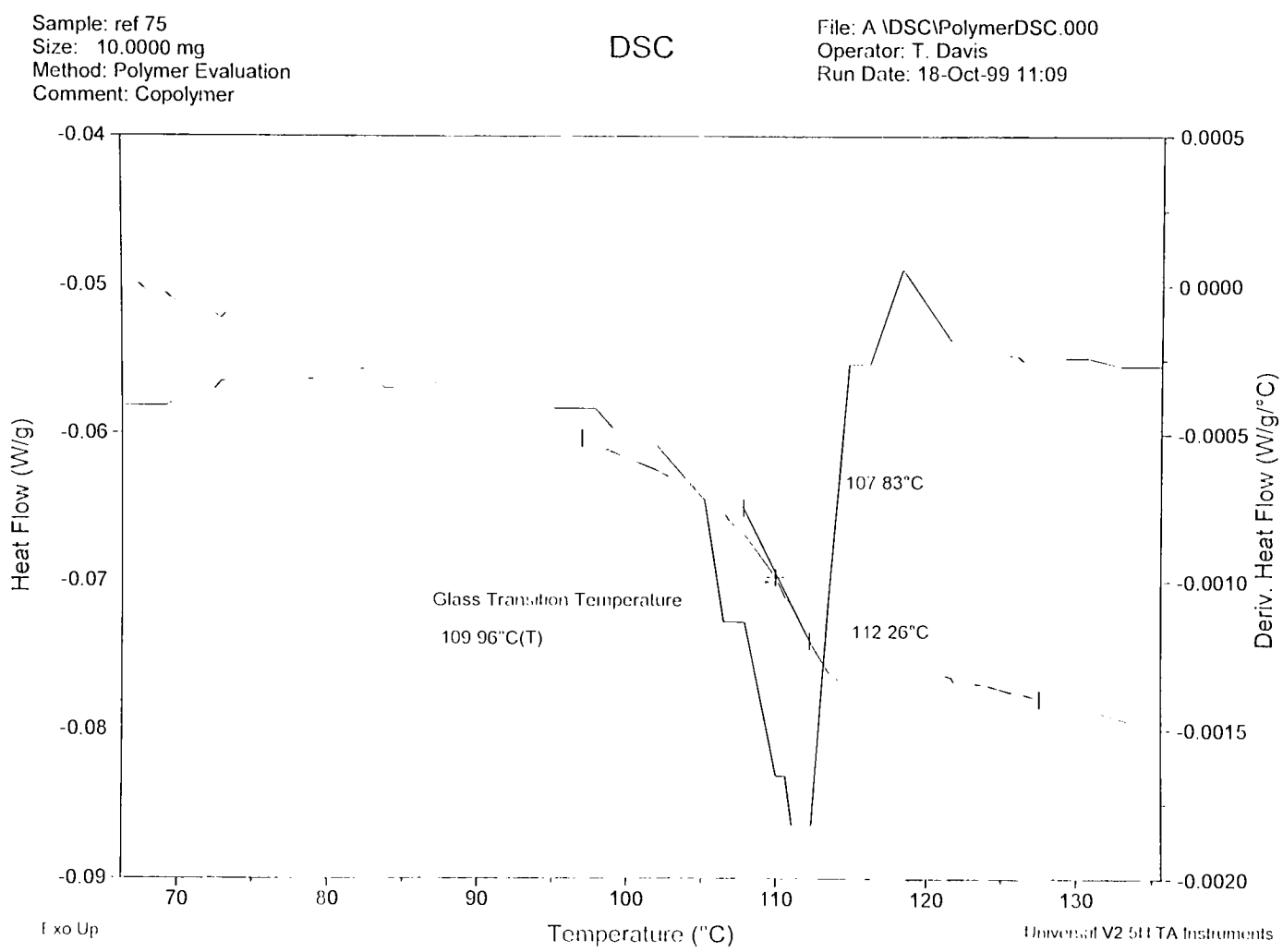
Sample: ref 75
Size: 10.0000 mg
Method: Polymer Evaluation
Comment: Copolymer
DSC
File: A \DSC\PolymerDSC.000
Operator: T. Davis
Run Date: 18-Oct-99 11:09
-0.04
-0.05
-0.06
-0.07
-0.08
-0.09
Heat Flow (W/g)
0.0005
0 0000
-0.0005
-0.0010
-0.0015
-0.0020
Deriv. Heat Flow (W/g/°C)
107 83°C
Glass Transition Temperature
109 96°C(T)
112 26°C
70
80
90
100
110
120
130
Exo Up
Temperature (°C)
Universal V2 5H TA Instruments

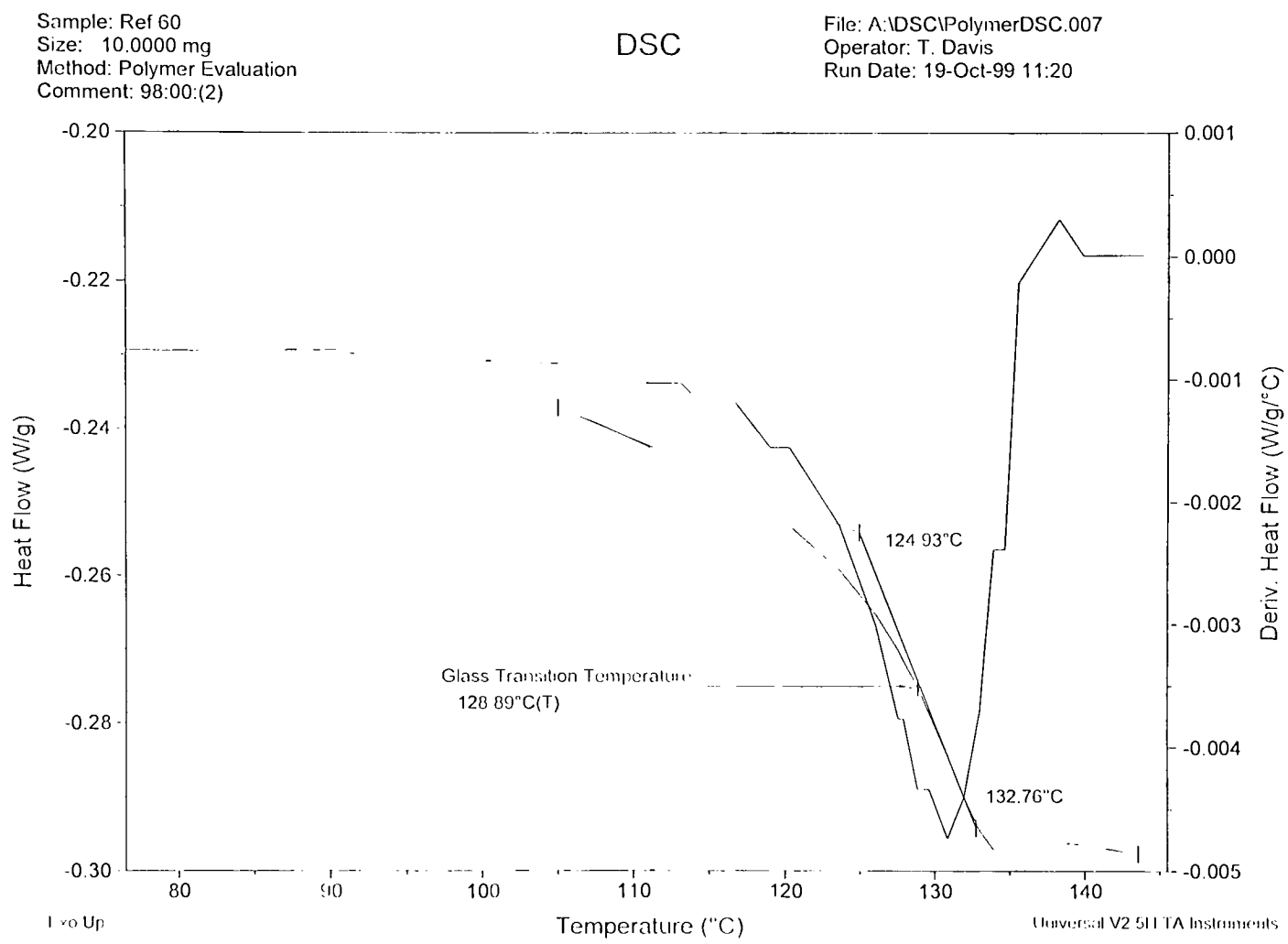
Sample: Ref 60
Size: 10.0000 mg
Method: Polymer Evaluation
Comment: 98:00:(2)
DSC
File: A:\DSC\PolymerDSC.007
Operator: T. Davis
Run Date: 19-Oct-99 11:20
Heat Flow (W/g)
Deriv. Heat Flow (W/g/°C)
Temperature (°C)
Exo Up
Universal V2.5H TA Instruments
124.93°C
Glass Transition Temperature
128.89°C(T)
132.76°C
-0.20
-0.22
-0.24
-0.26
-0.28
-0.30
0.001
0.000
-0.001
-0.002
-0.003
-0.004
-0.005
80
90
100
110
120
130
140

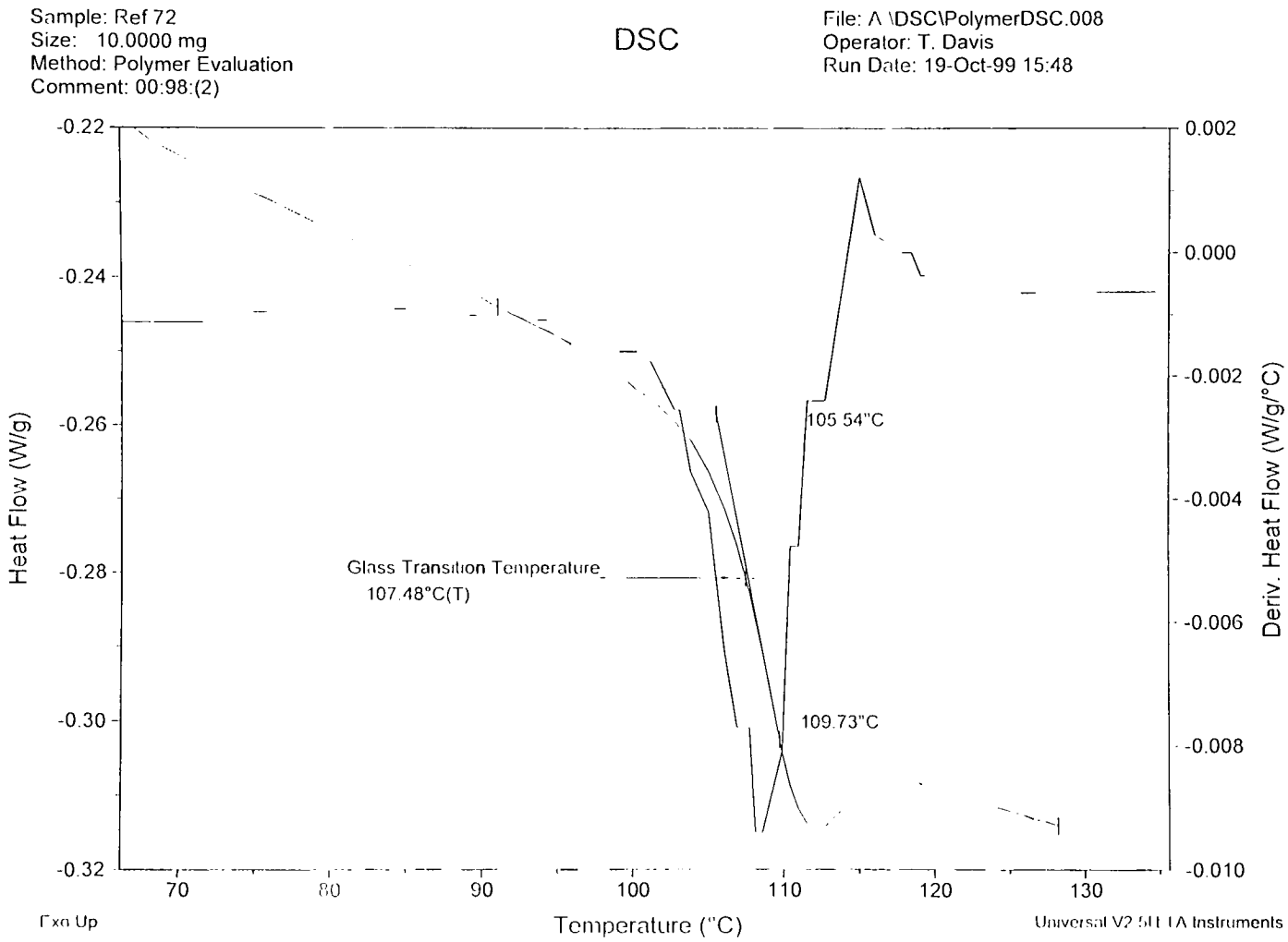
Sample: Ref 72
Size: 10.0000 mg
Method: Polymer Evaluation
Comment: 00:98:(2)
DSC
File: A \DSC\PolymerDSC.008
Operator: T. Davis
Run Date: 19-Oct-99 15:48
-0.22
-0.24
-0.26
-0.28
-0.30
-0.32
Heat Flow (W/g)
0.002
0.000
-0.002
-0.004
-0.006
-0.008
-0.010
Deriv. Heat Flow (W/g/°C)
105.54°C
Glass Transition Temperature
107.48°C(T)
109.73°C
70
80
90
100
110
120
130
Exo Up
Temperature (°C)
Universal V2.5H TA Instruments

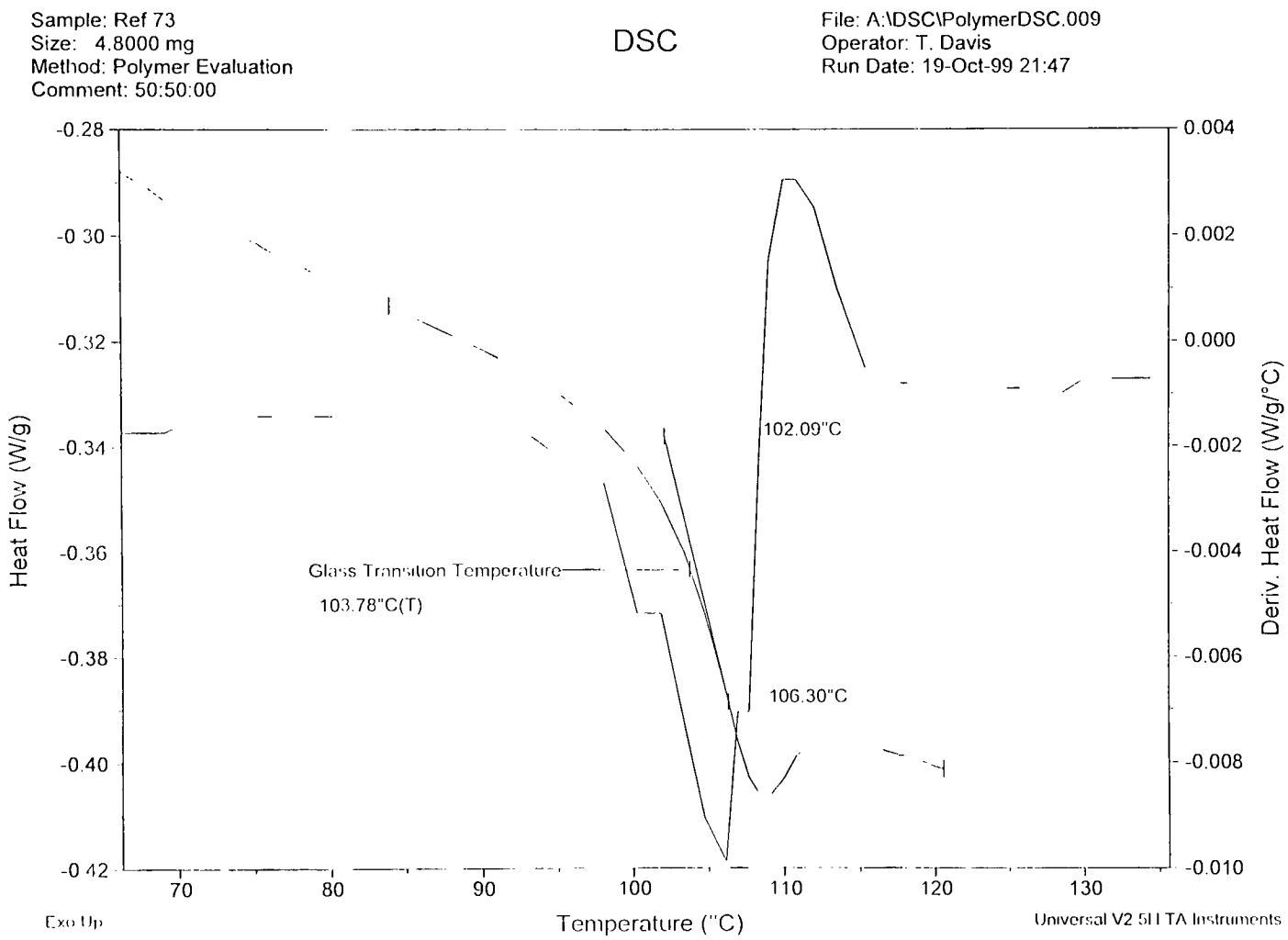
Sample: Ref 73
Size: 4.8000 mg
Method: Polymer Evaluation
Comment: 50:50:00
DSC
File: A:\DSC\PolymerDSC.009
Operator: T. Davis
Run Date: 19-Oct-99 21:47
Heat Flow (W/g)
Deriv. Heat Flow (W/g/°C)
Temperature (°C)
Glass Transition Temperature
103.78°C(T)
102.09°C
106.30°C
Exo Up
Universal V2.5H TA Instruments

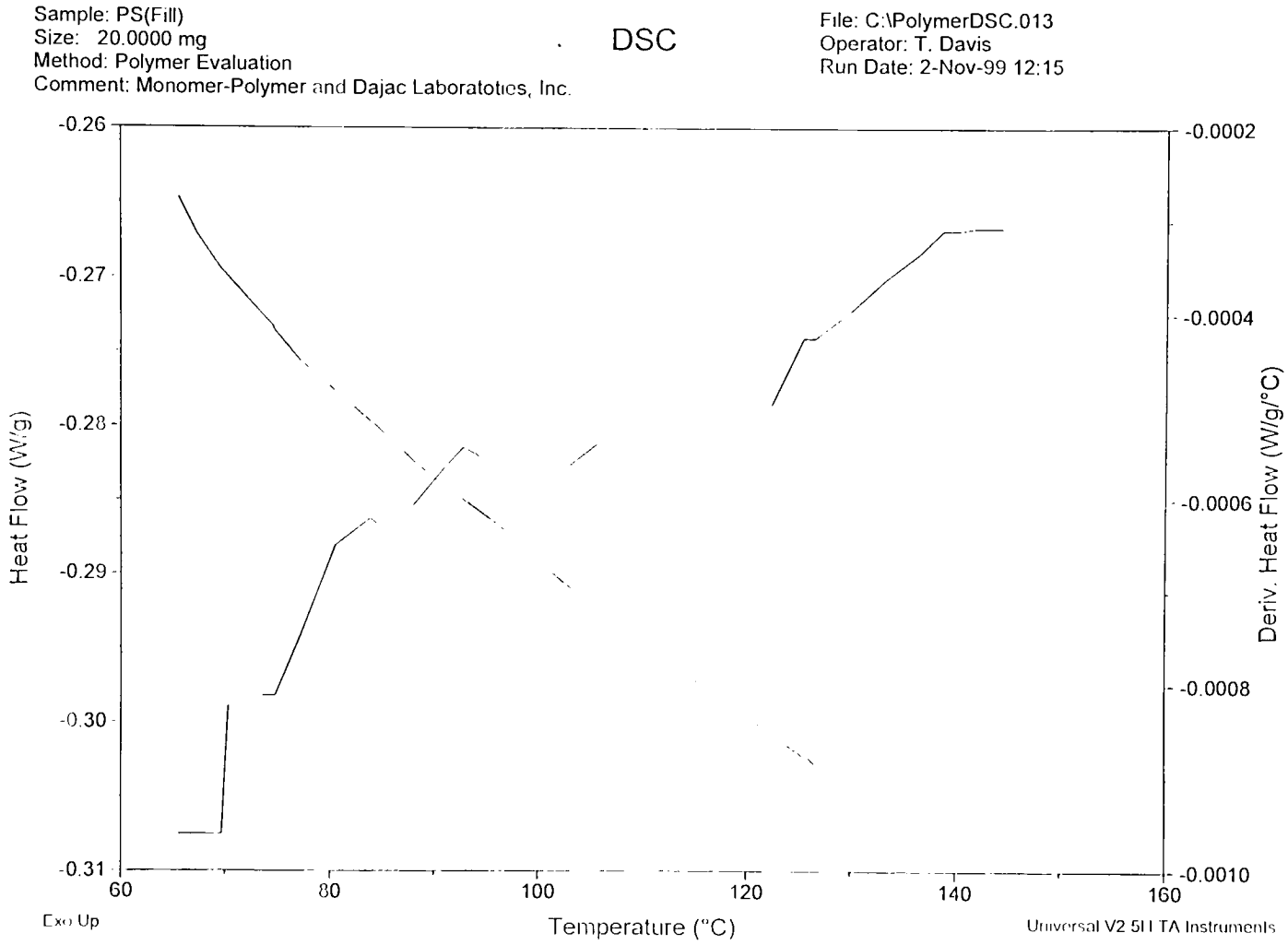
Sample: PS(Fill)
Size: 20.0000 mg
Method: Polymer Evaluation
Comment: Monomer-Polymer and Dajac Laboratories, Inc.
DSC
File: C:\PolymerDSC.013
Operator: T. Davis
Run Date: 2-Nov-99 12:15
-0.26
-0.27
-0.28
-0.29
-0.30
-0.31
Heat Flow (W/g)
-0.0002
-0.0004
-0.0006
-0.0008
-0.0010
Deriv. Heat Flow (W/g/°C)
60
80
100
120
140
160
Temperature (°C)
Exo Up
Universal V2.5H TA Instruments

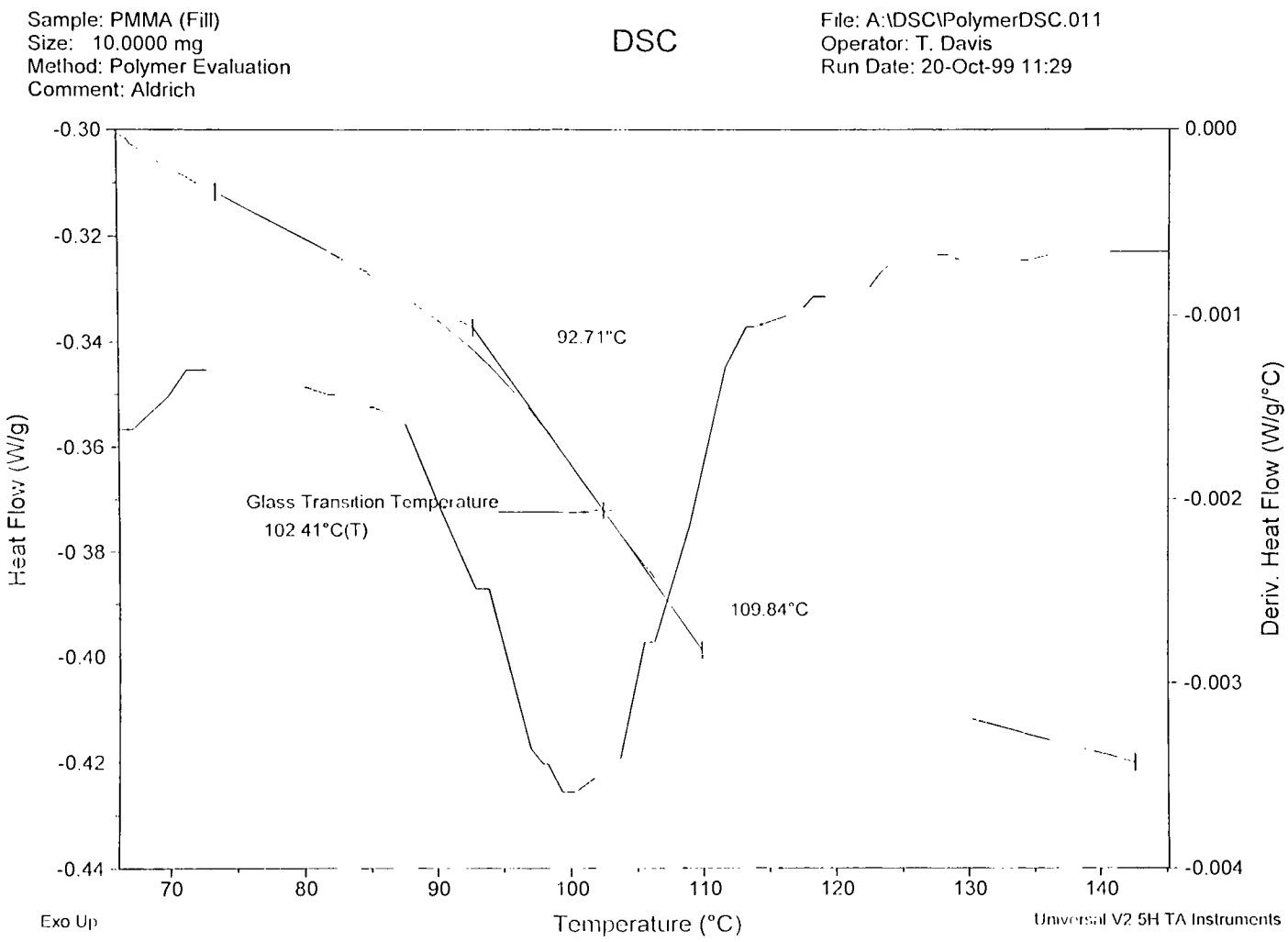
Sample: PMMA (Fill)
Size: 10.0000 mg
Method: Polymer Evaluation
Comment: Aldrich
DSC
File: A:\DSC\PolymerDSC.011
Operator: T. Davis
Run Date: 20-Oct-99 11:29
-0.30
-0.32
-0.34
-0.36
-0.38
-0.40
-0.42
-0.44
Heat Flow (W/g)
0.000
-0.001
-0.002
-0.003
-0.004
Deriv. Heat Flow (W/g/°C)
92.71°C
Glass Transition Temperature
102.41°C(T)
109.84°C
70
80
90
100
110
120
130
140
Exo Up
Temperature (°C)
Universal V2.5H TA Instruments

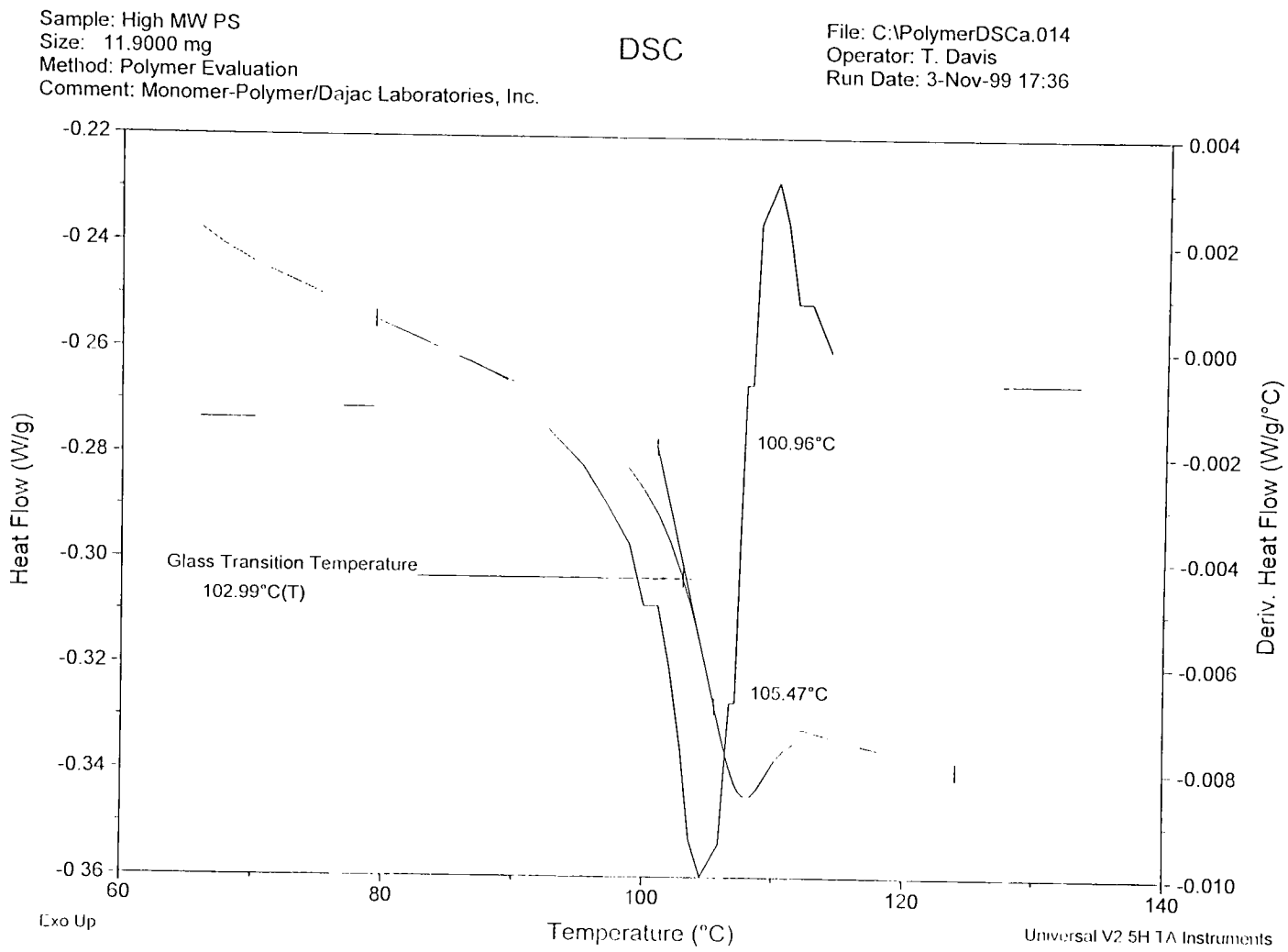
Sample: High MW PS
Size: 11.9000 mg
Method: Polymer Evaluation
Comment: Monomer-Polymer/Dajac Laboratories, Inc.
DSC
File: C:\PolymerDSCa.014
Operator: T. Davis
Run Date: 3-Nov-99 17:36
Heat Flow (W/g)
Deriv. Heat Flow (W/g/°C)
Temperature (°C)
Exo Up
Universal V2.5H TA Instruments
Glass Transition Temperature
102.99°C(T)
100.96°C
105.47°C
-0.22
-0.24
-0.26
-0.28
-0.30
-0.32
-0.34
-0.36
0.004
0.002
0.000
-0.002
-0.004
-0.006
-0.008
-0.010
60
80
100
120
140

Appendix C: TGA Thermograms of Copolymers

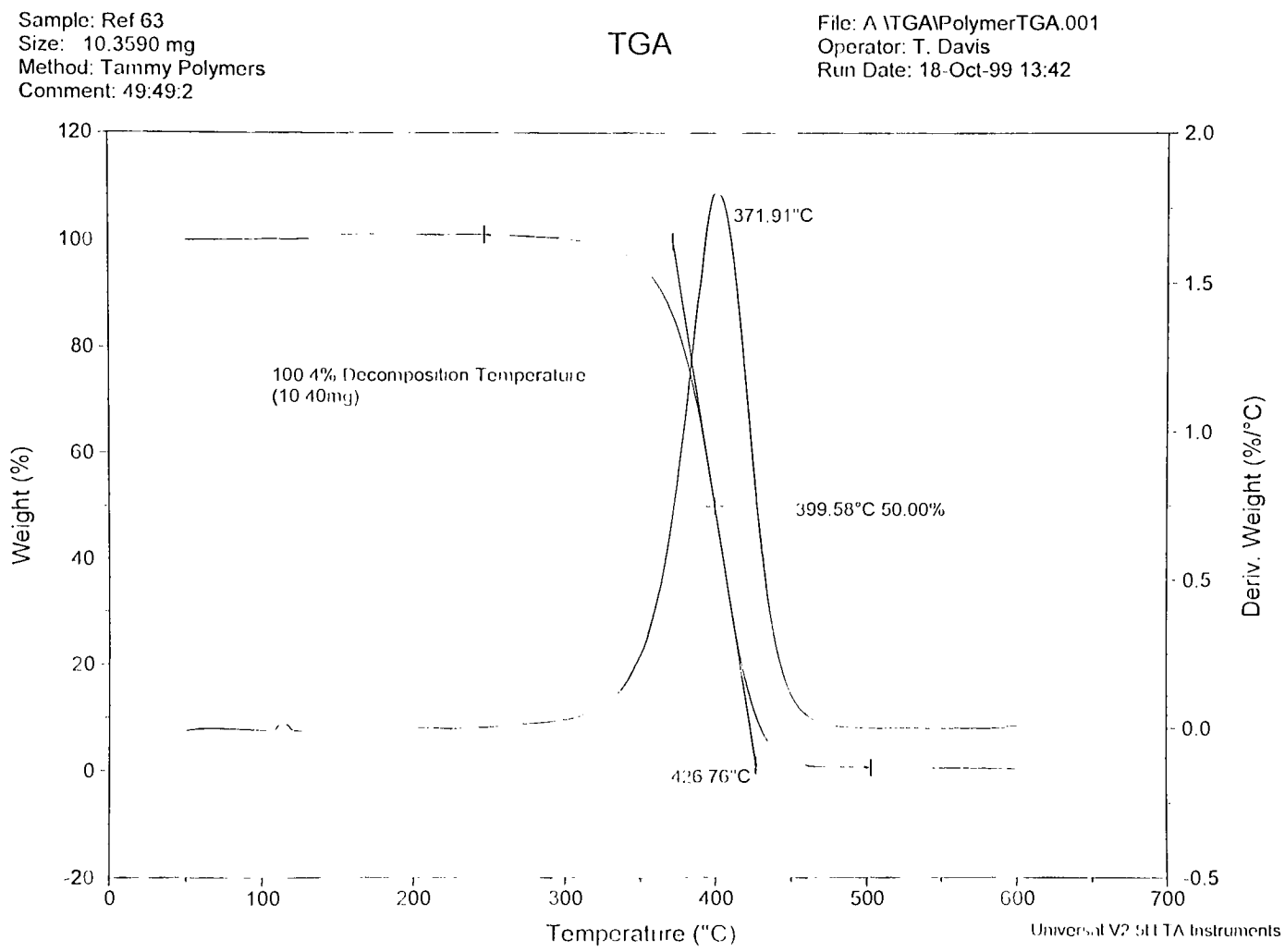
Sample: Ref 63
Size: 10.3590 mg
Method: Tammy Polymers
Comment: 49:49:2
TGA
File: A \TGA\PolymerTGA.001
Operator: T. Davis
Run Date: 18-Oct-99 13:42
371.91°C
100.4% Decomposition Temperature
(10.40mg)
399.58°C 50.00%
426.76°C
Weight (%)
Deriv. Weight (%/°C)
Temperature (°C)
Universal V2.5H TA Instruments

C1

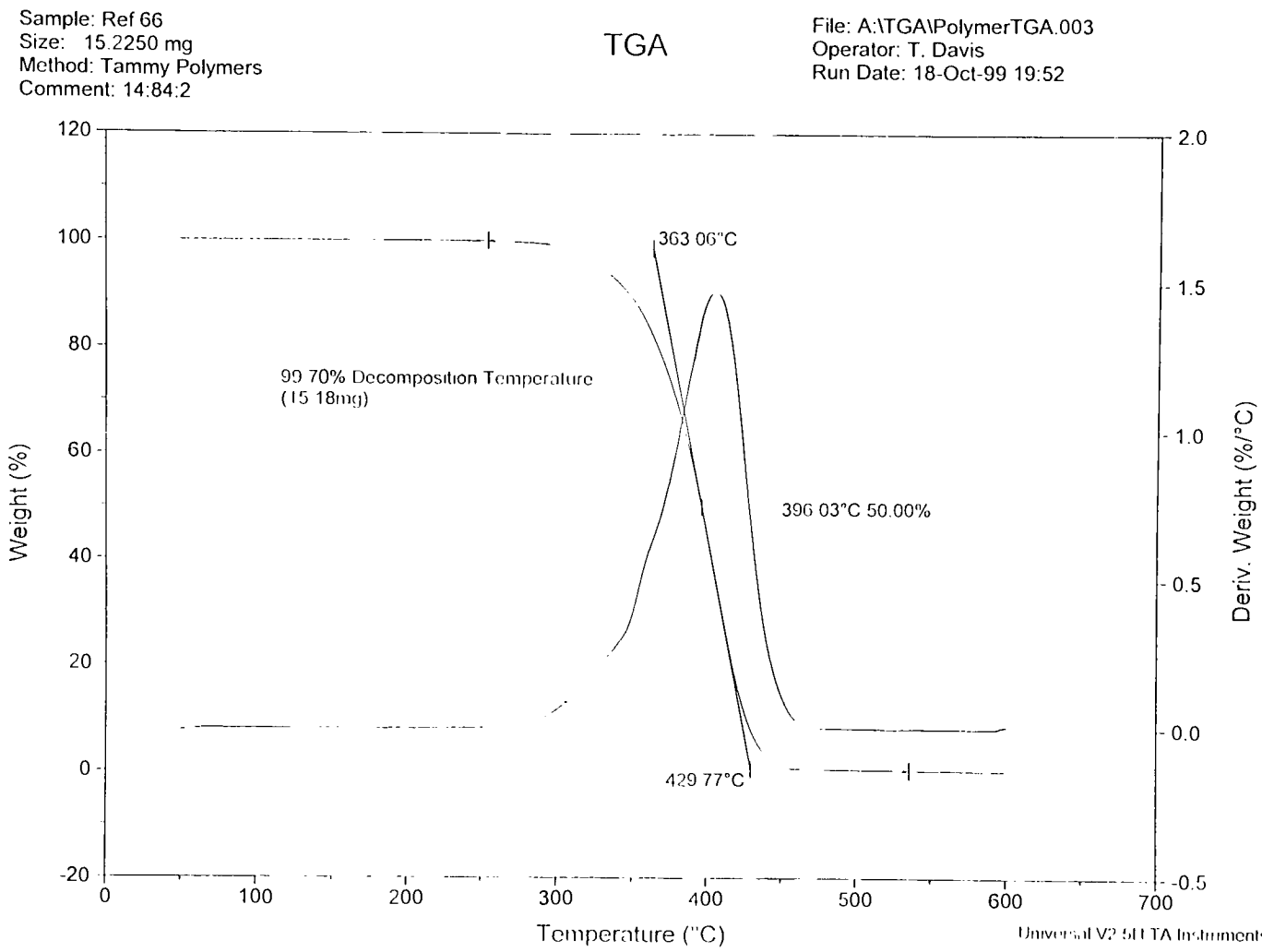
Sample: Ref 66
Size: 15.2250 mg
Method: Tammy Polymers
Comment: 14:84:2
TGA
File: A:\TGA\PolymerTGA.003
Operator: T. Davis
Run Date: 18-Oct-99 19:52
363.06°C
99.70% Decomposition Temperature
(15.18mg)
396.03°C 50.00%
429.77°C
Weight (%)
Deriv. Weight (%/°C)
Temperature (°C)
Universal V2.5H TA Instruments

C2

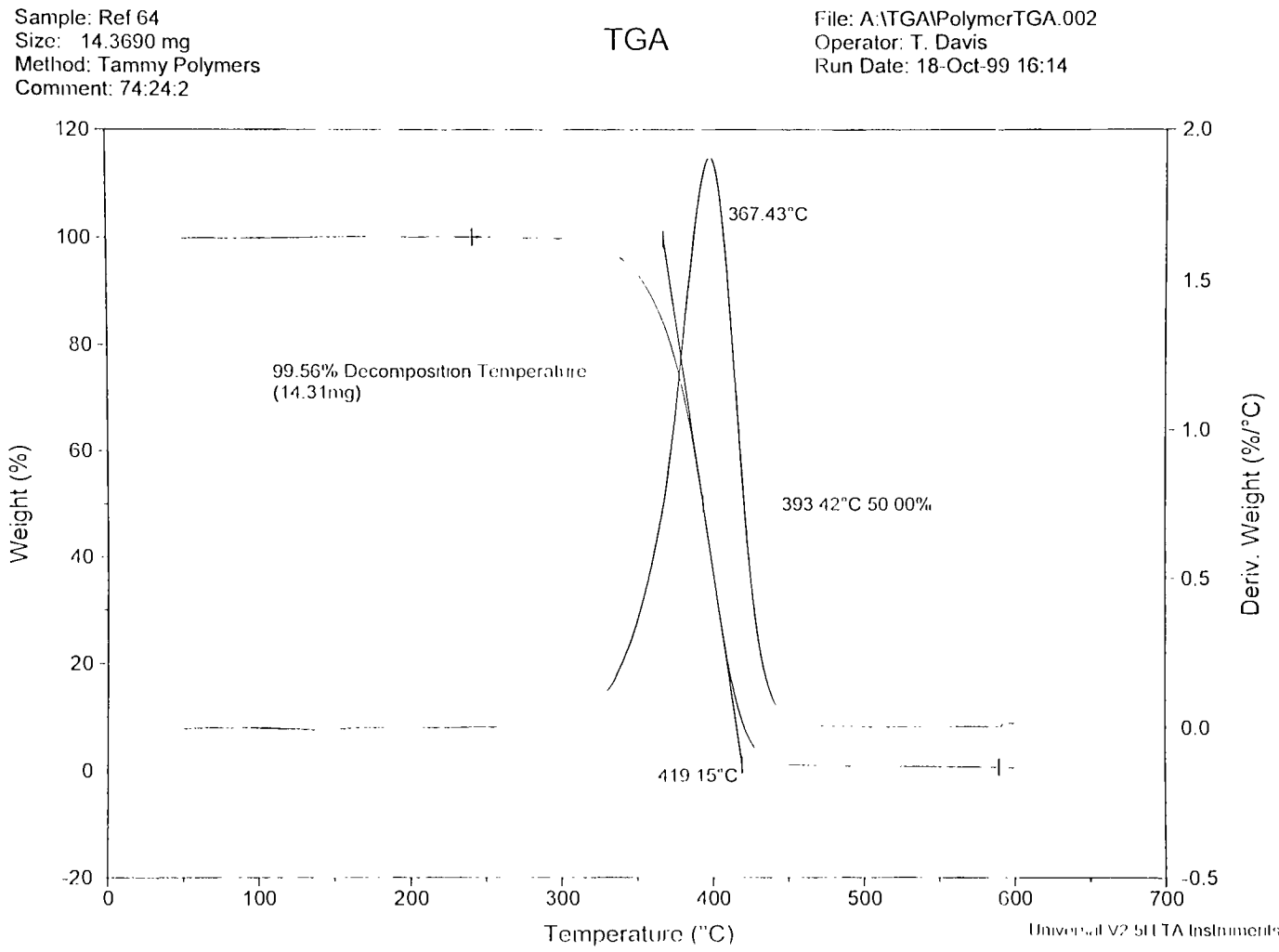
Sample: Ref 64
Size: 14.3690 mg
Method: Tammy Polymers
Comment: 74:24:2
TGA
File: A:\TGA\PolymerTGA.002
Operator: T. Davis
Run Date: 18-Oct-99 16:14
367.43°C
99.56% Decomposition Temperature
(14.31mg)
393.42°C 50.00%
419.15°C
Weight (%)
Deriv. Weight (%/°C)
Temperature (°C)
120
100
80
60
40
20
0
-20
2.0
1.5
1.0
0.5
0.0
-0.5
0
100
200
300
400
500
600
700

C3

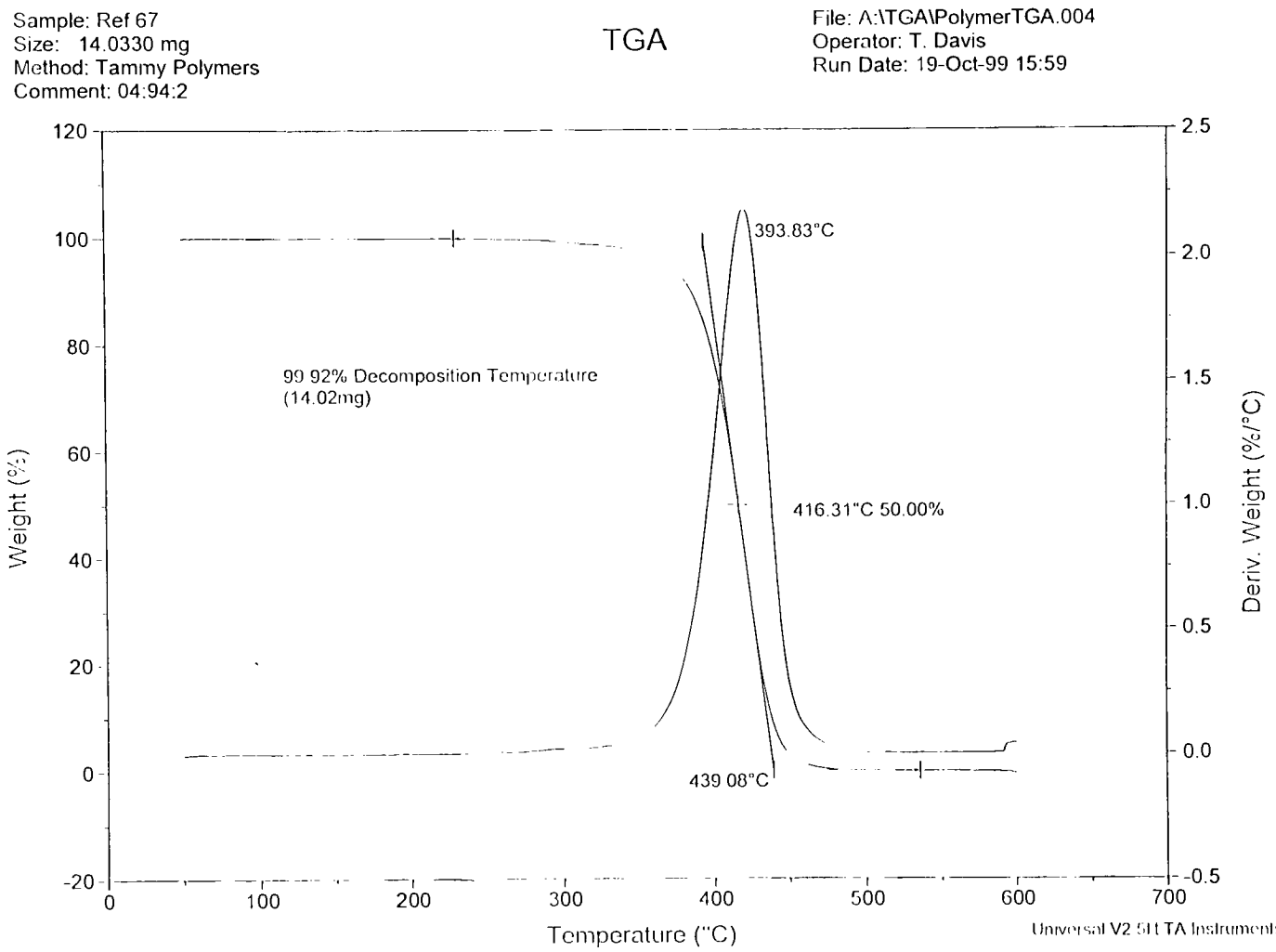
Sample: Ref 67
Size: 14.0330 mg
Method: Tammy Polymers
Comment: 04:94:2
TGA
File: A:\TGA\PolymerTGA.004
Operator: T. Davis
Run Date: 19-Oct-99 15:59
393.83°C
99 92% Decomposition Temperature
(14.02mg)
416.31°C 50.00%
439 08°C
Weight (%)
Deriv. Weight (%/°C)
Temperature (°C)
Universal V2 5H TA Instruments

C4

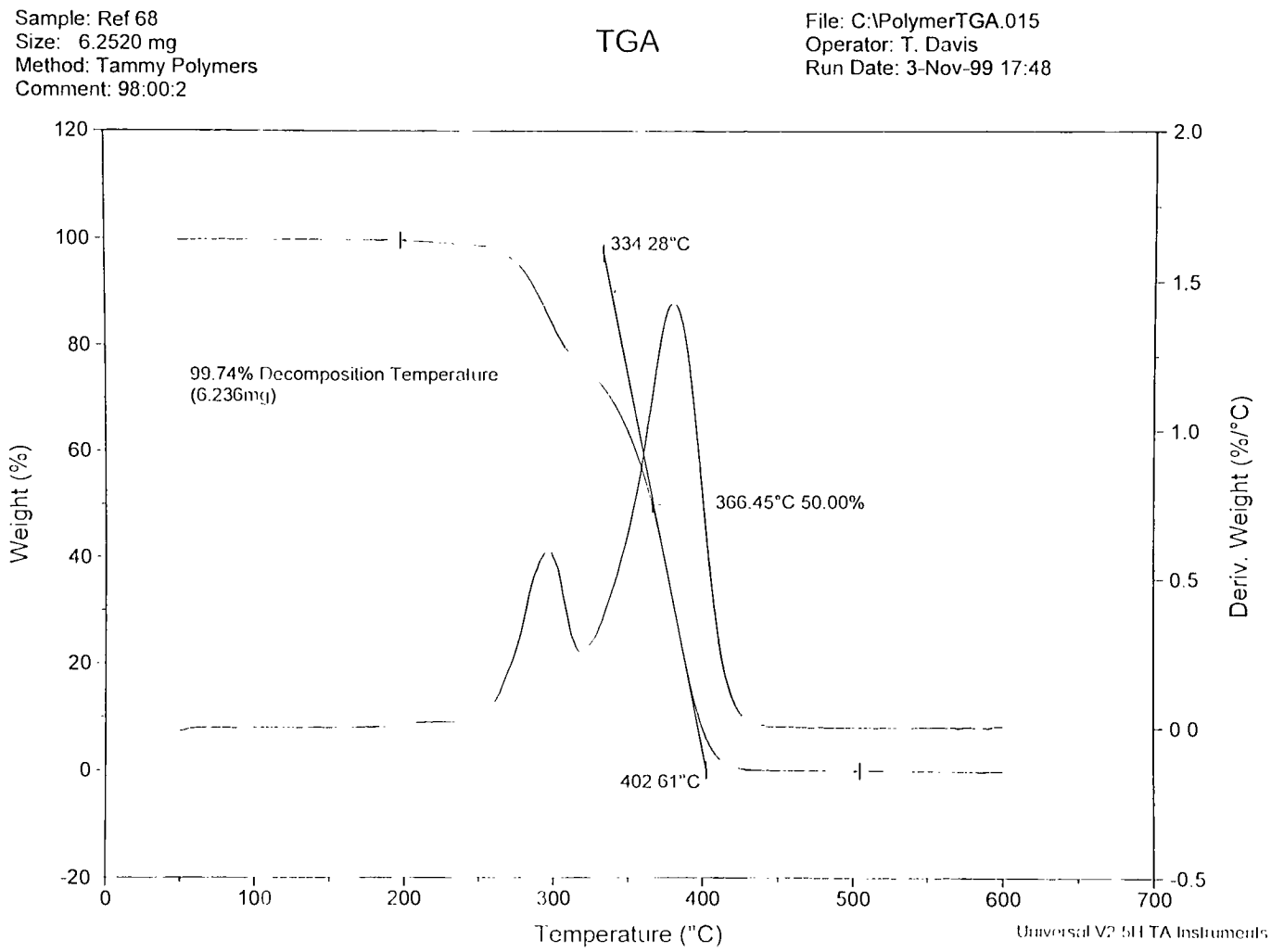
Sample: Ref 68
Size: 6.2520 mg
Method: Tammy Polymers
Comment: 98:00:2
TGA
File: C:\PolymerTGA.015
Operator: T. Davis
Run Date: 3-Nov-99 17:48
334.28°C
99.74% Decomposition Temperature
(6.236mg)
366.45°C 50.00%
402.61°C
Weight (%)
Deriv. Weight (%/°C)
Temperature (°C)
120
100
80
60
40
20
0
-20
2.0
1.5
1.0
0.5
0.0
-0.5
0
100
200
300
400
500
600
700
Universal V2.5H TA Instruments

C5

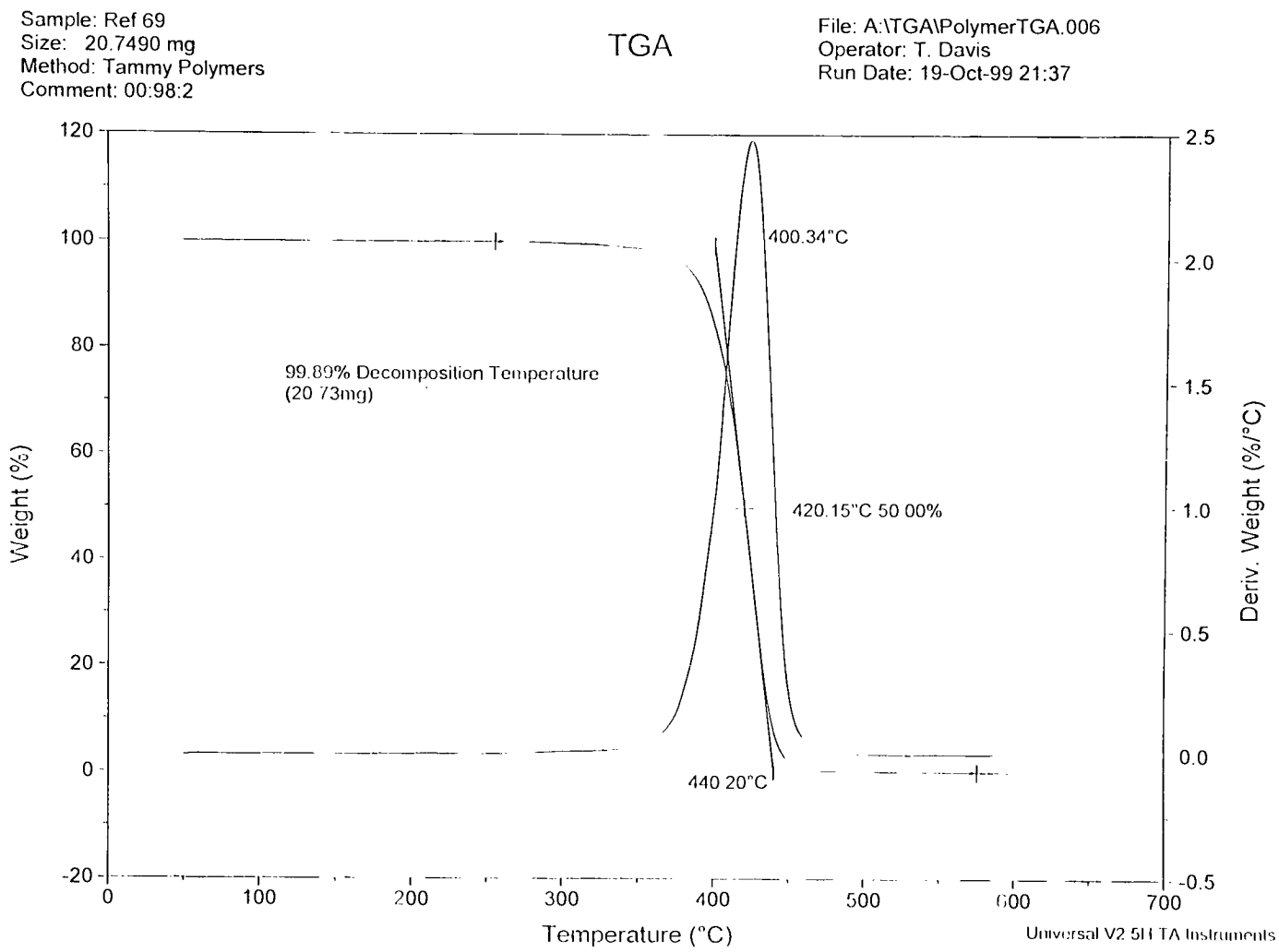
Sample: Ref 69
Size: 20.7490 mg
Method: Tammy Polymers
Comment: 00:98:2
TGA
File: A:\TGA\PolymerTGA.006
Operator: T. Davis
Run Date: 19-Oct-99 21:37
400.34°C
99.89% Decomposition Temperature
(20.73mg)
420.15°C 50.00%
440.20°C
Weight (%)
Deriv. Weight (%/°C)
Temperature (°C)
Universal V2.5H TA Instruments

C6

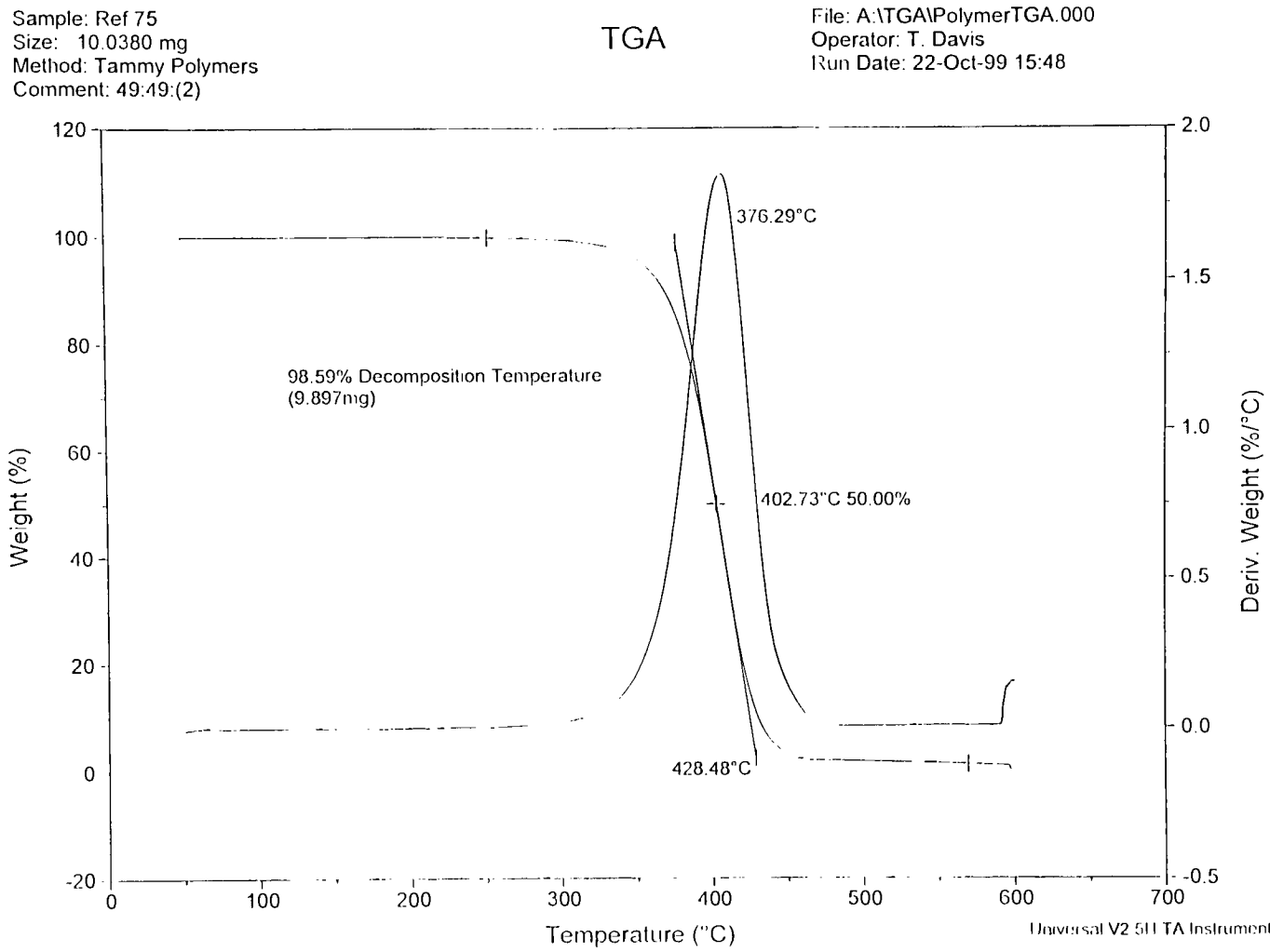
Sample: Ref 75
Size: 10.0380 mg
Method: Tammy Polymers
Comment: 49:49:(2)
TGA
File: A:\TGA\PolymerTGA.000
Operator: T. Davis
Run Date: 22-Oct-99 15:48
376.29°C
98.59% Decomposition Temperature
(9.897mg)
402.73°C 50.00%
428.48°C
Weight (%)
Deriv. Weight (%/°C)
Temperature (°C)
Universal V2.5H TA Instruments

Missing Page

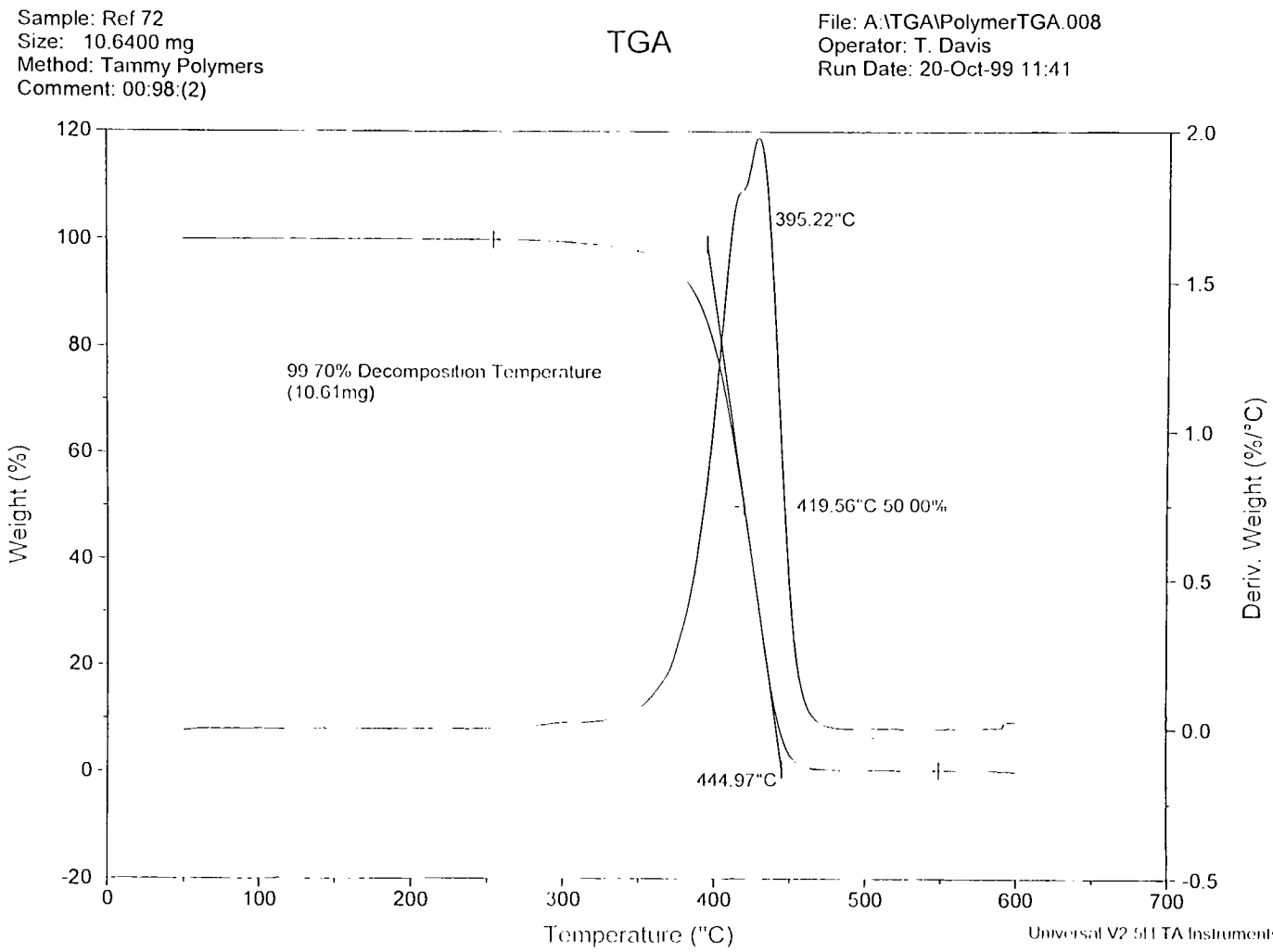
Sample: Ref 72
Size: 10.6400 mg
Method: Tammy Polymers
Comment: 00:98:(2)
TGA
File: A:\TGA\PolymerTGA.008
Operator: T. Davis
Run Date: 20-Oct-99 11:41
99.70% Decomposition Temperature
(10.61mg)
395.22°C
419.56°C 50.00%
444.97°C
Weight (%)
Deriv. Weight (%/°C)
Temperature (°C)
Universal V2.5H TA Instruments

C9

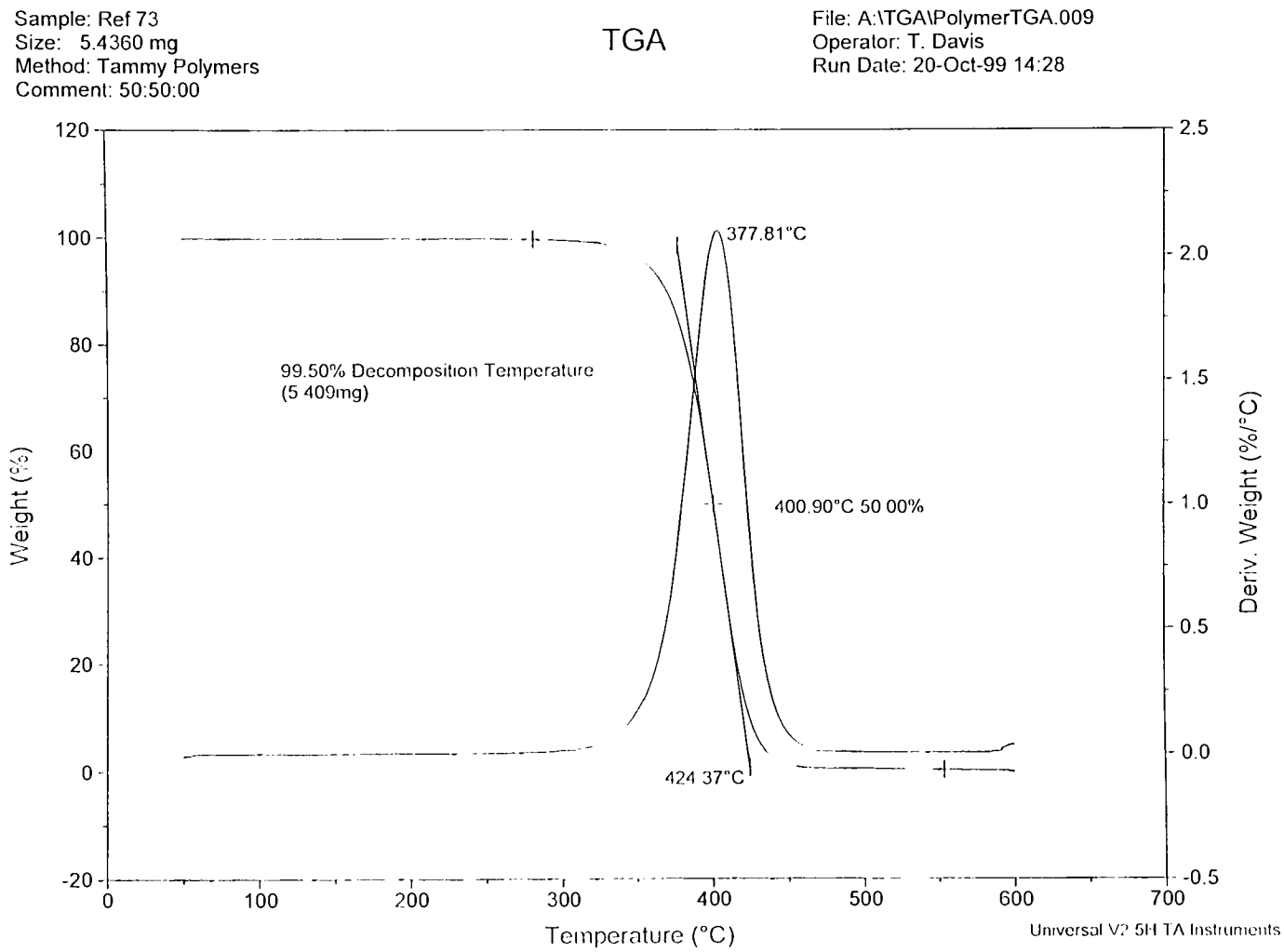
Sample: Ref 73
Size: 5.4360 mg
Method: Tammy Polymers
Comment: 50:50:00
TGA
File: A:\TGA\PolymerTGA.009
Operator: T. Davis
Run Date: 20-Oct-99 14:28
377.81°C
99.50% Decomposition Temperature
(5 409mg)
400.90°C 50 00%
424 37°C
Weight (%)
Deriv. Weight (%/°C)
Temperature (°C)
Universal V2 5H TA Instruments

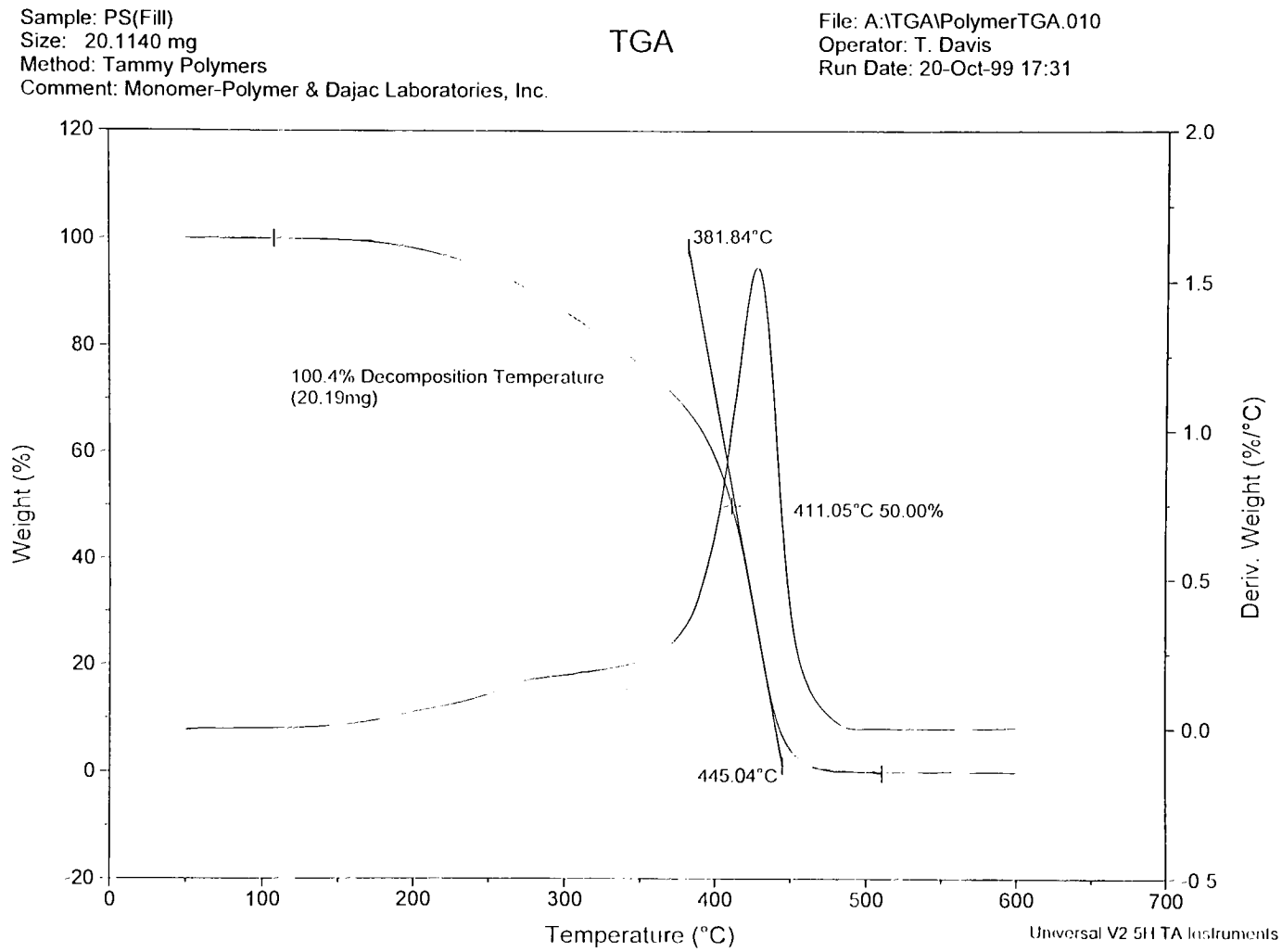
Sample: PS(Fill)
Size: 20.1140 mg
Method: Tammy Polymers
Comment: Monomer-Polymer & Dajac Laboratories, Inc.
TGA
File: A:\TGA\PolymerTGA.010
Operator: T. Davis
Run Date: 20-Oct-99 17:31
381.84°C
100.4% Decomposition Temperature
(20.19mg)
411.05°C 50.00%
445.04°C
Weight (%)
Deriv. Weight (%/°C)
Temperature (°C)
Universal V2.5H TA Instruments

C11

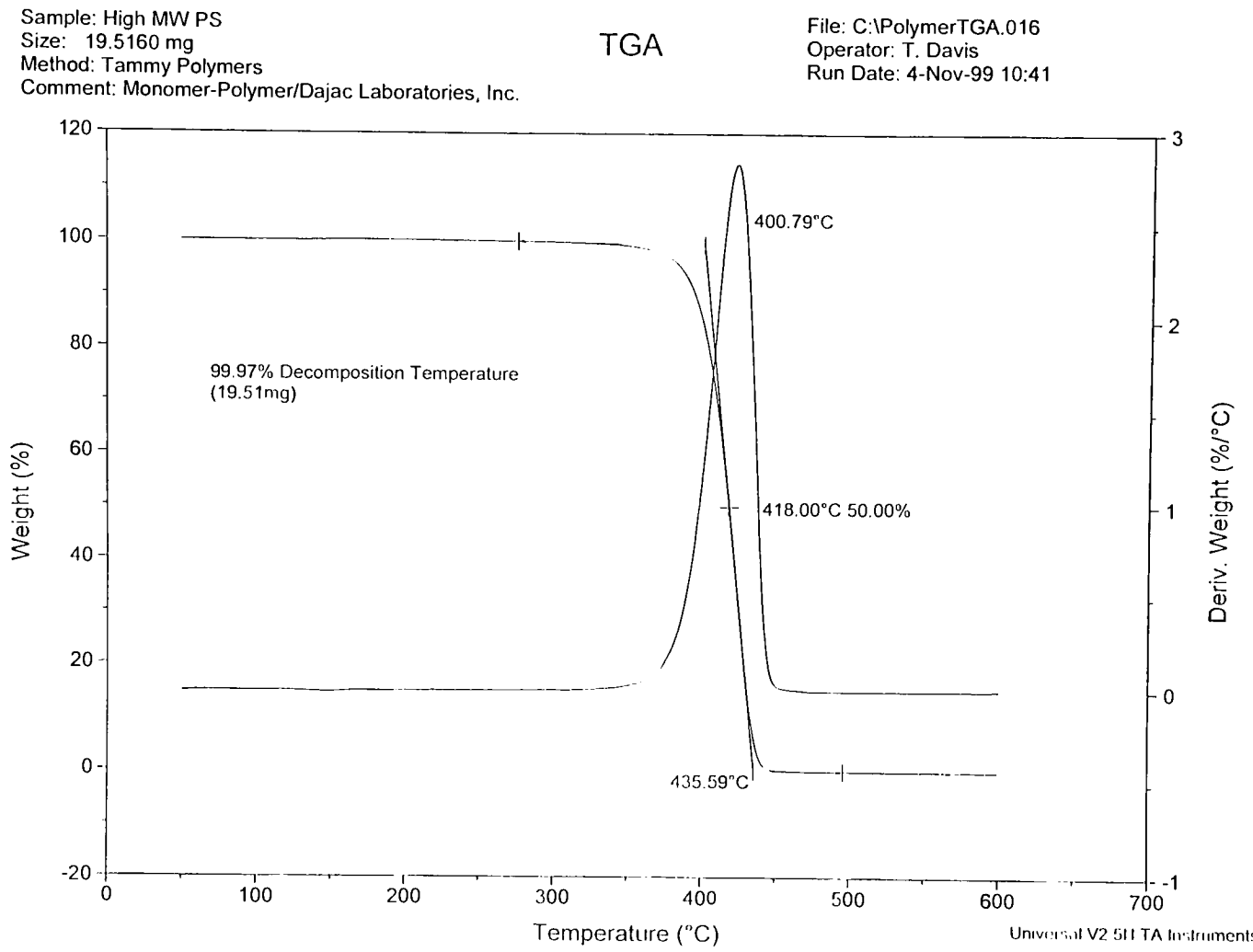
Sample: High MW PS
Size: 19.5160 mg
Method: Tammy Polymers
Comment: Monomer-Polymer/Dajac Laboratories, Inc.
TGA
File: C:\PolymerTGA.016
Operator: T. Davis
Run Date: 4-Nov-99 10:41
400.79°C
99.97% Decomposition Temperature
(19.51mg)
418.00°C 50.00%
435.59°C
Weight (%)
Deriv. Weight (%/°C)
Temperature (°C)
Universal V2.5H TA Instruments

C12

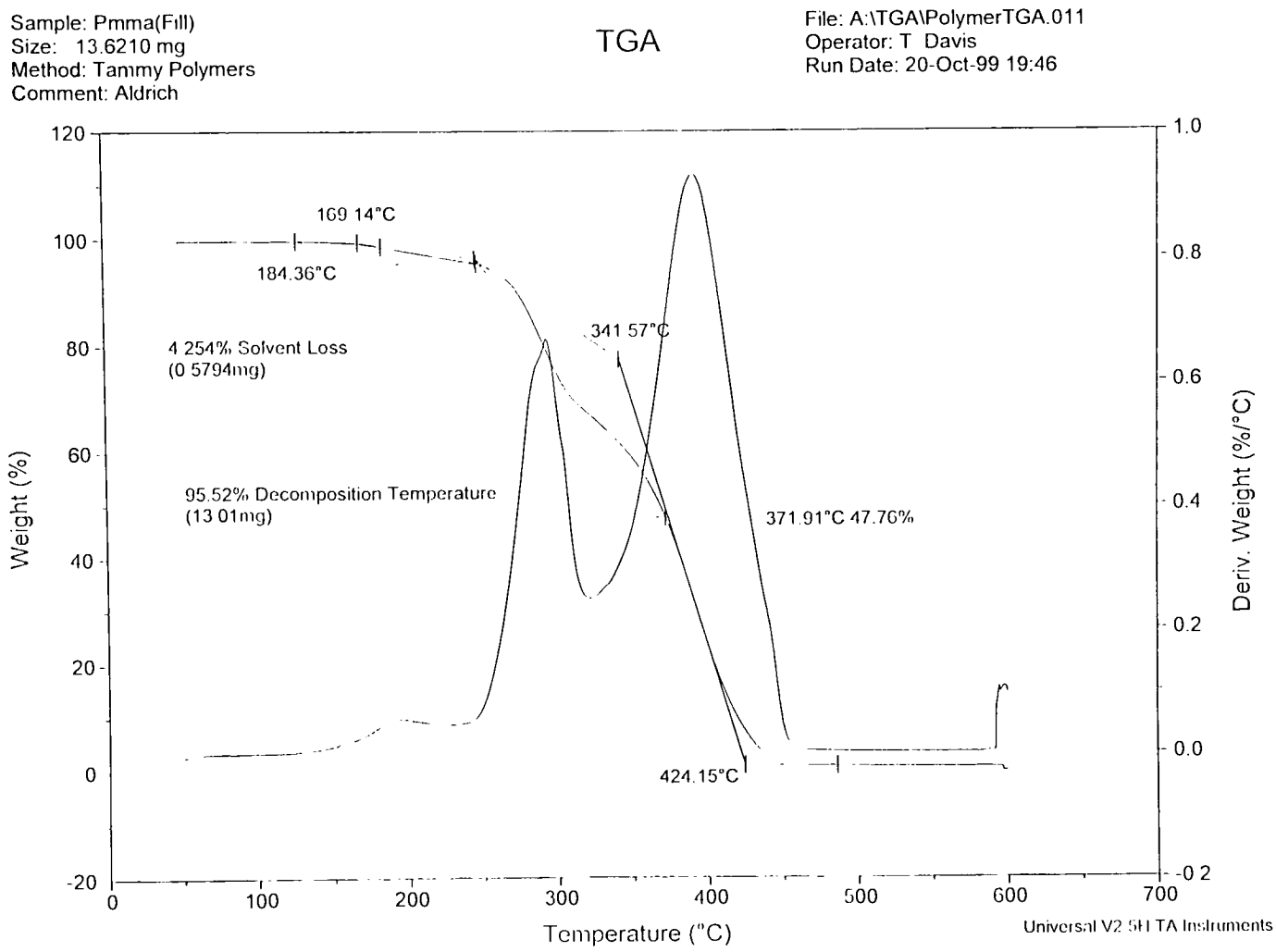
Sample: Pmma(Fill)
Size: 13.6210 mg
Method: Tammy Polymers
Comment: Aldrich
TGA
File: A:\TGA\PolymerTGA.011
Operator: T Davis
Run Date: 20-Oct-99 19:46
169.14°C
184.36°C
4.254% Solvent Loss
(0.5794mg)
341.57°C
95.52% Decomposition Temperature
(13.01mg)
371.91°C 47.76%
424.15°C
Weight (%)
Deriv. Weight (%/°C)
Temperature (°C)
Universal V2.5H TA Instruments

Appendix D: SEC Chromatograms of Copolymers

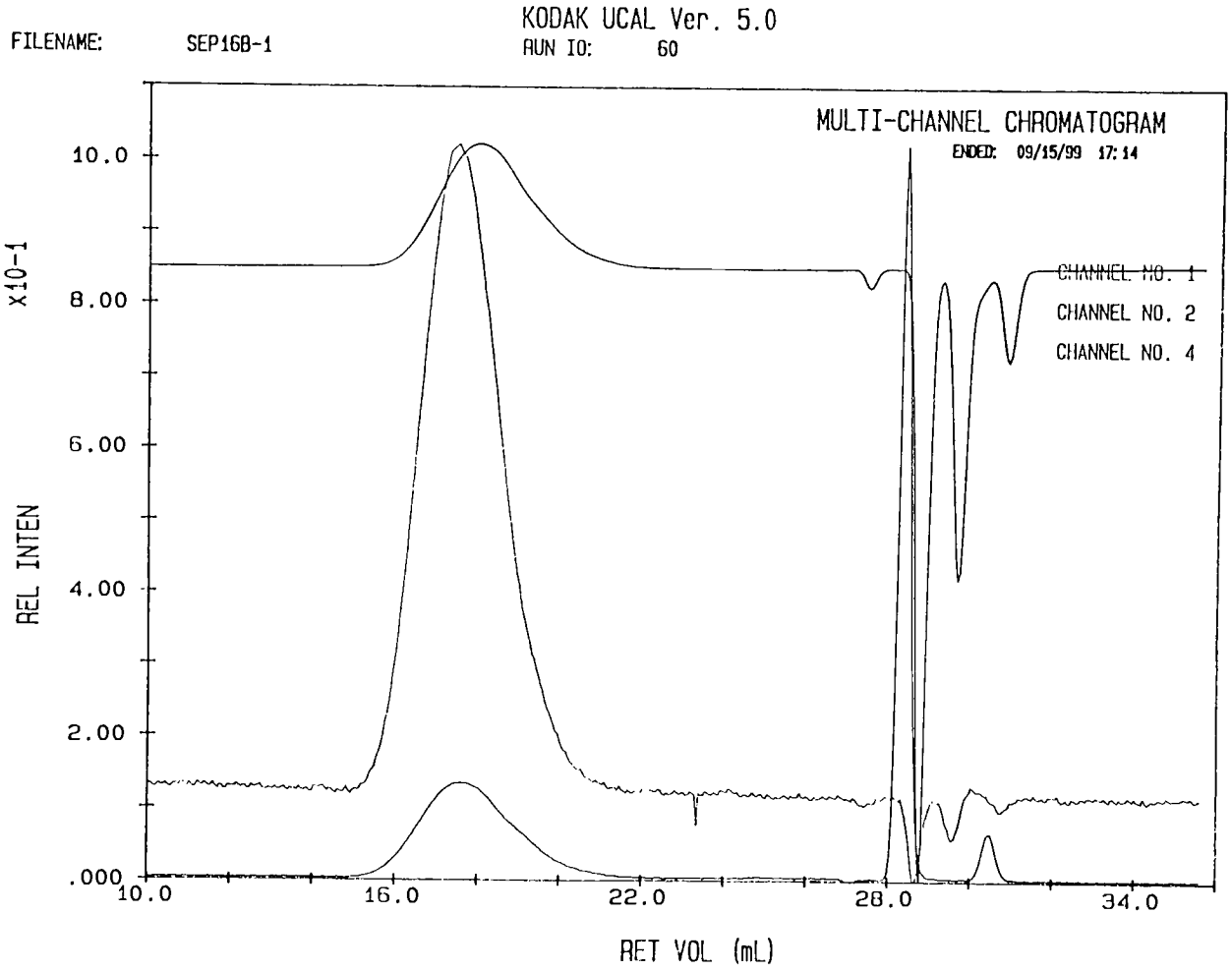
KODAK UCAL Ver. 5.0
FILENAME: SEP16B-1
RUN IO: 60
MULTI-CHANNEL CHROMATOGRAM
ENDED: 09/15/99 17:14
CHANNEL NO. 1
CHANNEL NO. 2
CHANNEL NO. 4
X10-1
REL INTEN
10.0
8.00
6.00
4.00
2.00
.000
10.0
16.0
22.0
28.0
34.0
RET VOL (mL)

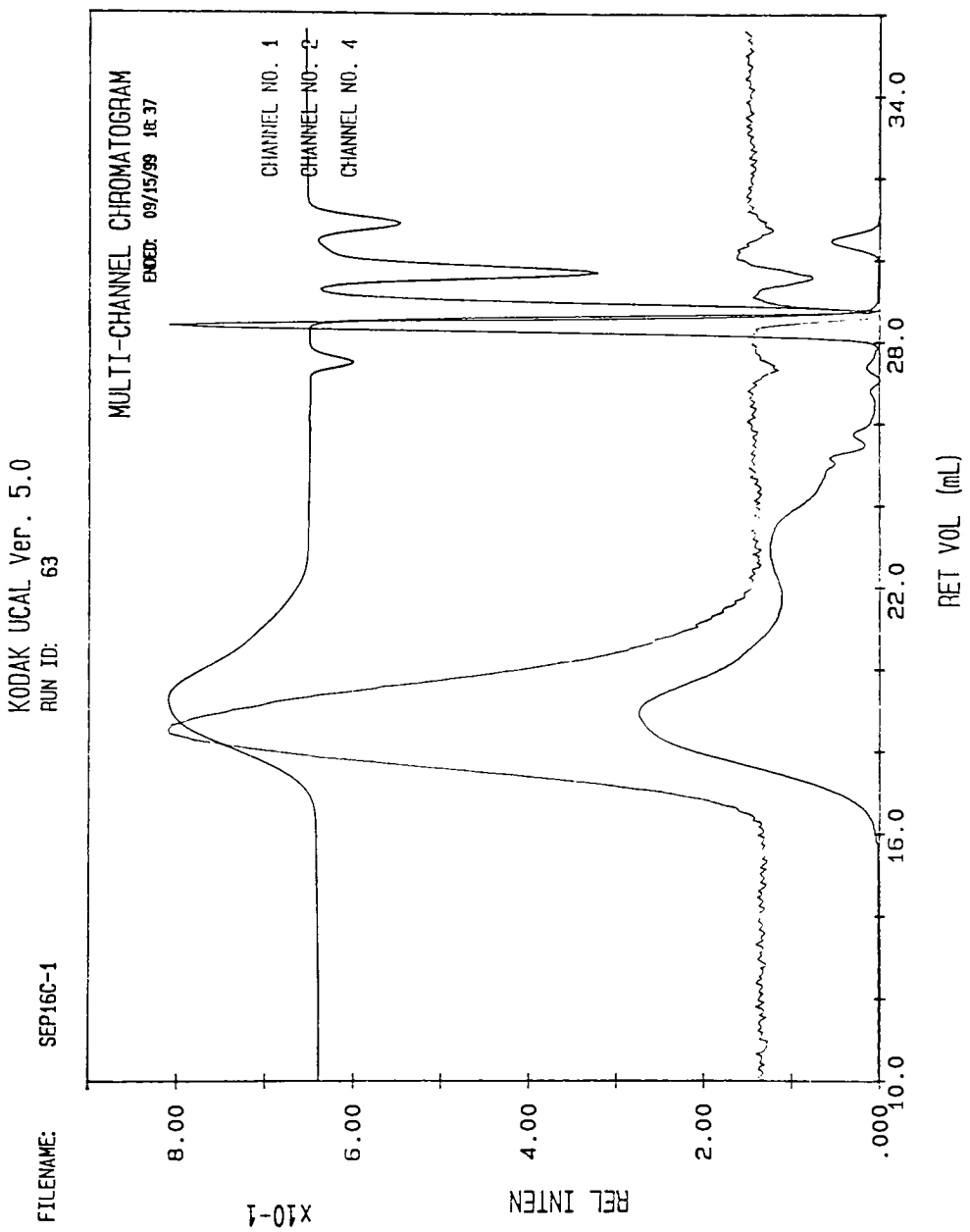
KODAK UCAL Ver. 5.0
FILENAME: SEP16C-1
RUN ID: 63
MULTI-CHANNEL CHROMATOGRAM
ENDED: 09/15/99 18:37
CHANNEL NO. 1
CHANNEL NO. 2
CHANNEL NO. 4
REL INTEN
X10-1
8.00
6.00
4.00
2.00
.000
10.0
16.0
22.0
28.0
34.0
RET VOL (mL)

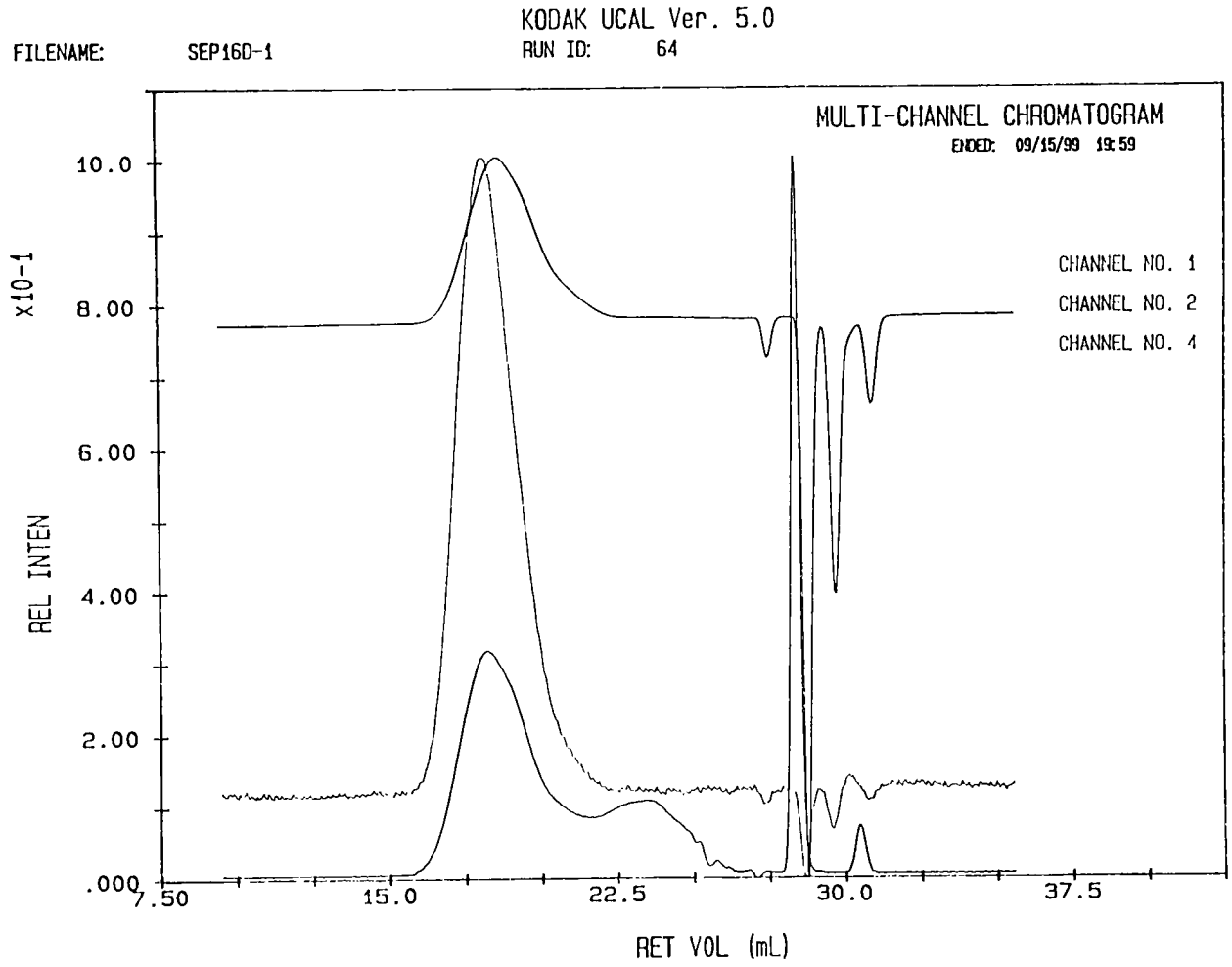
KODAK UCAL Ver. 5.0
FILENAME: SEP16D-1
RUN ID: 64
MULTI-CHANNEL CHROMATOGRAM
ENDED: 09/15/99 19:59
CHANNEL NO. 1
CHANNEL NO. 2
CHANNEL NO. 4
x10-1
REL INTEN
10.0
8.00
6.00
4.00
2.00
.000
7.50
15.0
22.5
30.0
37.5
RET VOL (mL)

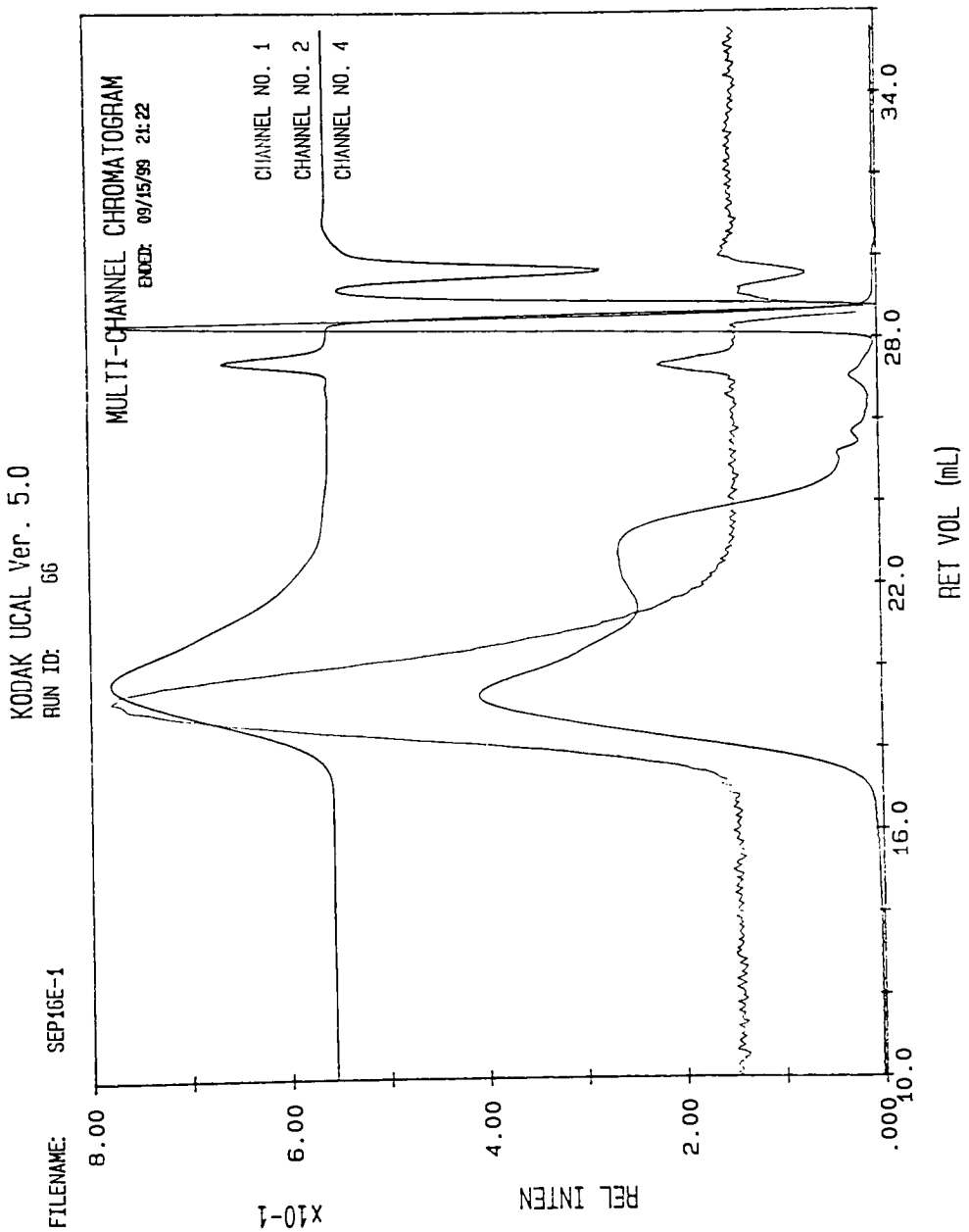
KODAK UCAL Ver. 5.0
RUN ID: 66
FILENAME: SEP16E-1
MULTI-CHANNEL CHROMATOGRAM
09/15/99 21:22
CHANNEL NO. 1
CHANNEL NO. 2
CHANNEL NO. 4
8.00
6.00
4.00
2.00
.000
x10-1
REL INTEN
10.0
16.0
22.0
28.0
34.0
RET VOL (mL)

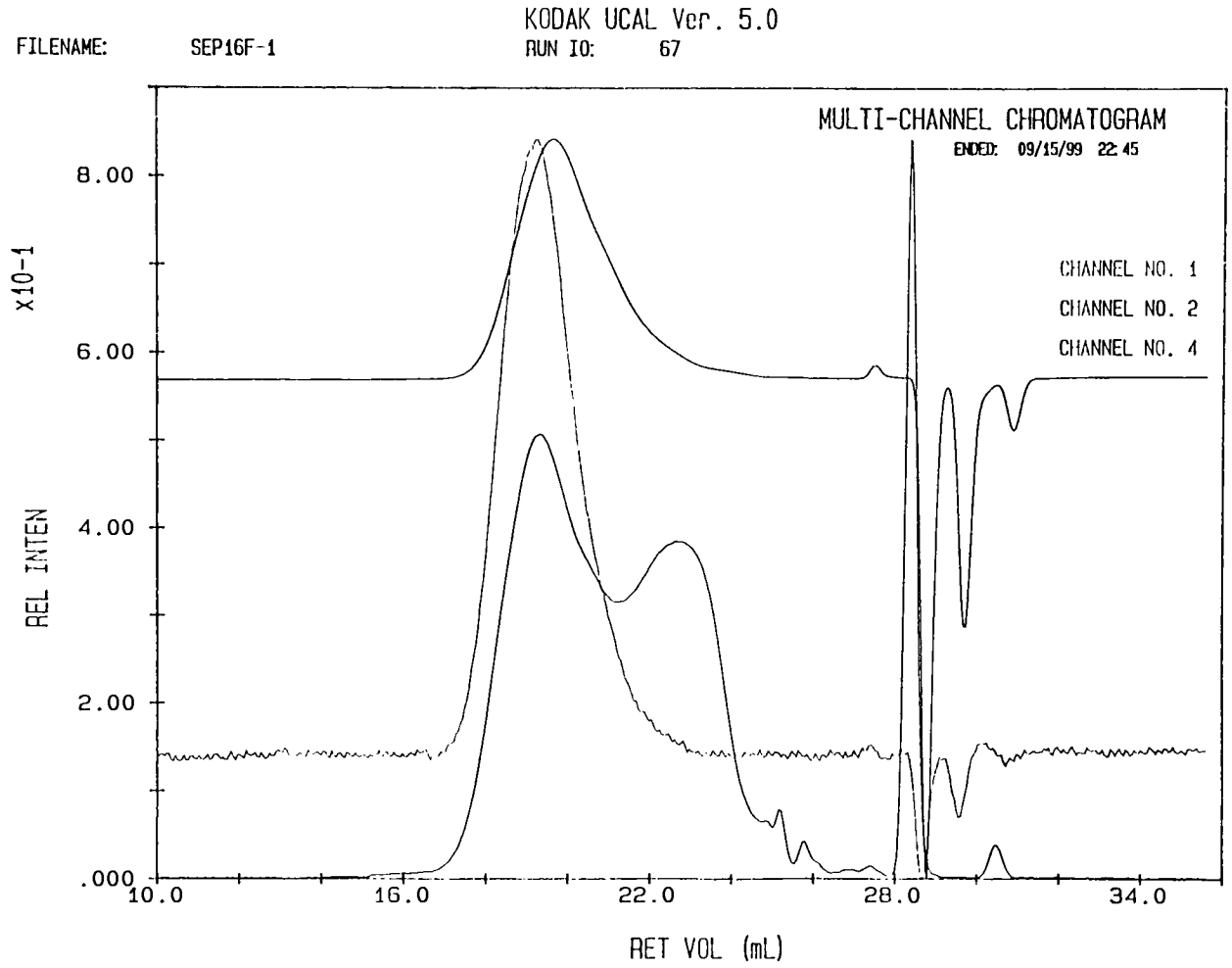
KODAK UCAL Ver. 5.0
FILENAME: SEP16F-1
RUN IO: 67
MULTI-CHANNEL CHROMATOGRAM
ENDED: 09/15/99 22:45
CHANNEL NO. 1
CHANNEL NO. 2
CHANNEL NO. 4
X10-1
REL INTEN
8.00
6.00
4.00
2.00
.000
10.0
16.0
22.0
28.0
34.0
RET VOL (mL)

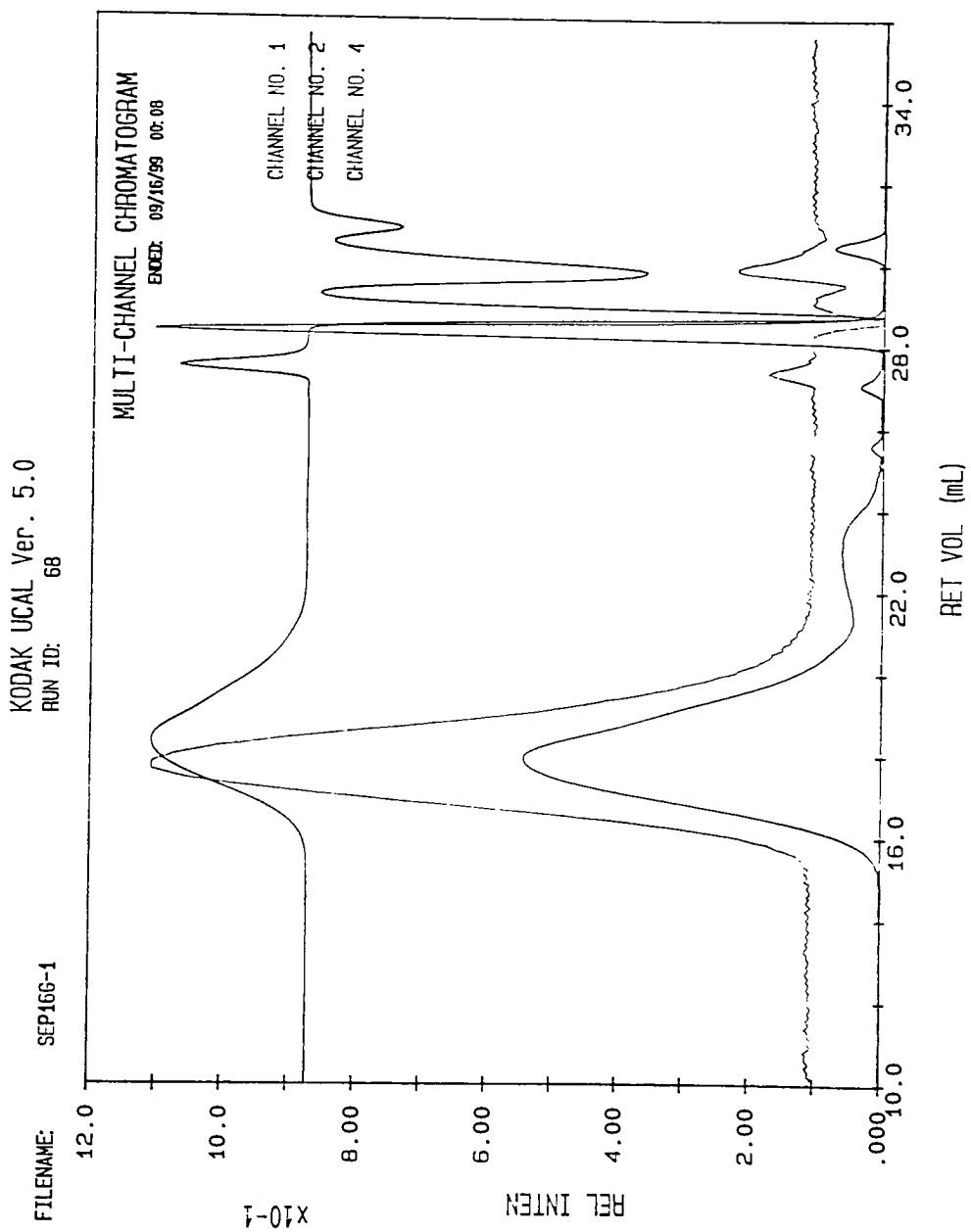
KODAK UCAL Ver. 5.0
FILENAME: SEP16G-1
RUN ID: 68
MULTI-CHANNEL CHROMATOGRAM
ENDED: 09/16/99 00:08
CHANNEL NO. 1
CHANNEL NO. 2
CHANNEL NO. 4
X10-4
REL INTEN
12.0
10.0
8.00
6.00
4.00
2.00
.000
10.0
16.0
22.0
28.0
34.0
RET VOL (mL)

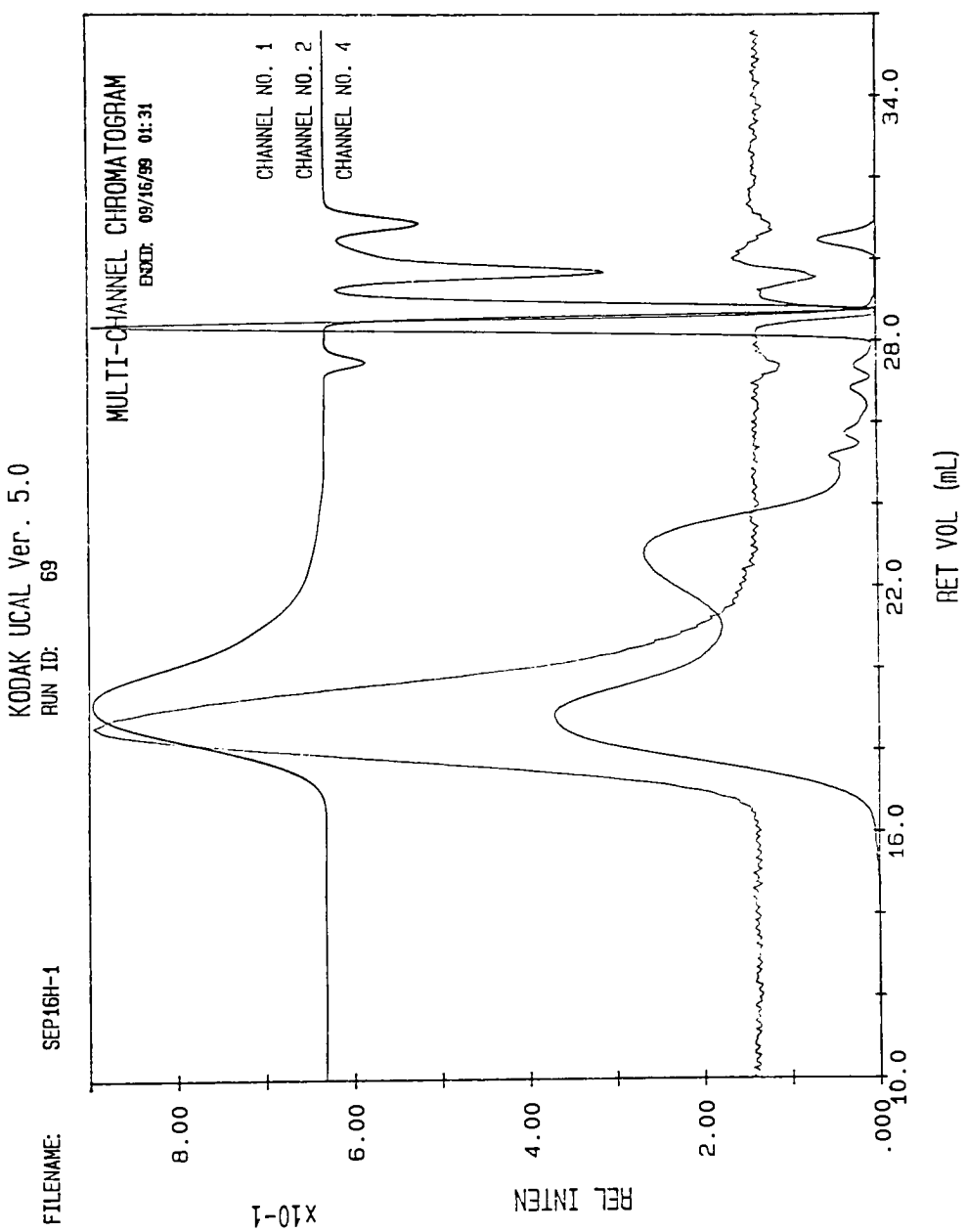
KODAK UCAL Ver. 5.0
FILENAME: SEP16H-1
RUN ID: 69
MULTI-CHANNEL CHROMATOGRAM
ENDED: 09/16/99 01:31
CHANNEL NO. 1
CHANNEL NO. 2
CHANNEL NO. 4
x10-1
8.00
6.00
4.00
2.00
.000
REL INTEN
10.0
16.0
22.0
28.0
34.0
RET VOL (mL)

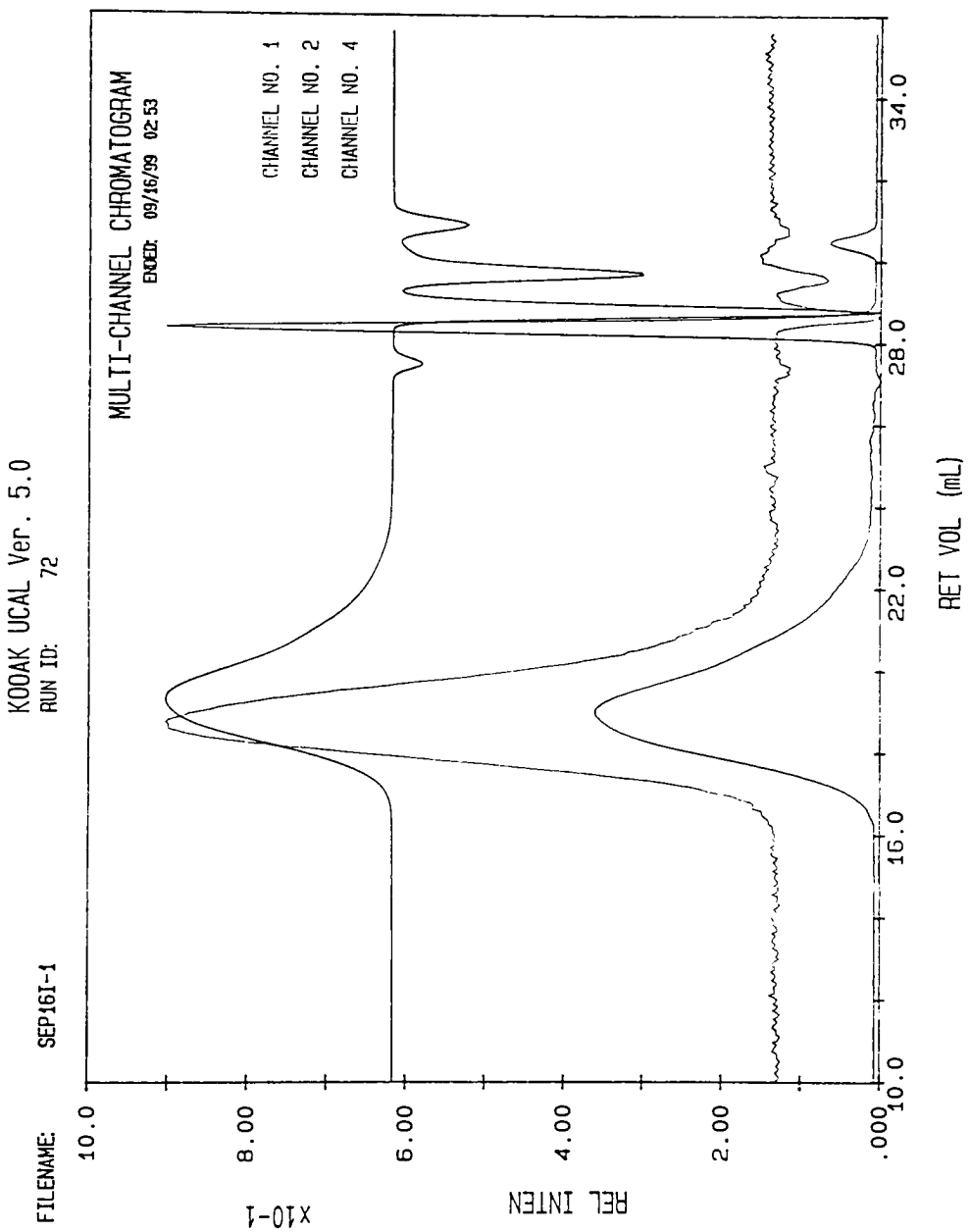
KODAK UCAL Ver. 5.0
FILENAME: SEP16I-1
RUN ID: 72
MULTI-CHANNEL CHROMATOGRAM
ENDED: 09/16/99 02:53
CHANNEL NO. 1
CHANNEL NO. 2
CHANNEL NO. 4
REL INTEN
X10-1
10.0
8.00
6.00
4.00
2.00
.000
10.0
16.0
22.0
28.0
34.0
RET VOL (mL)

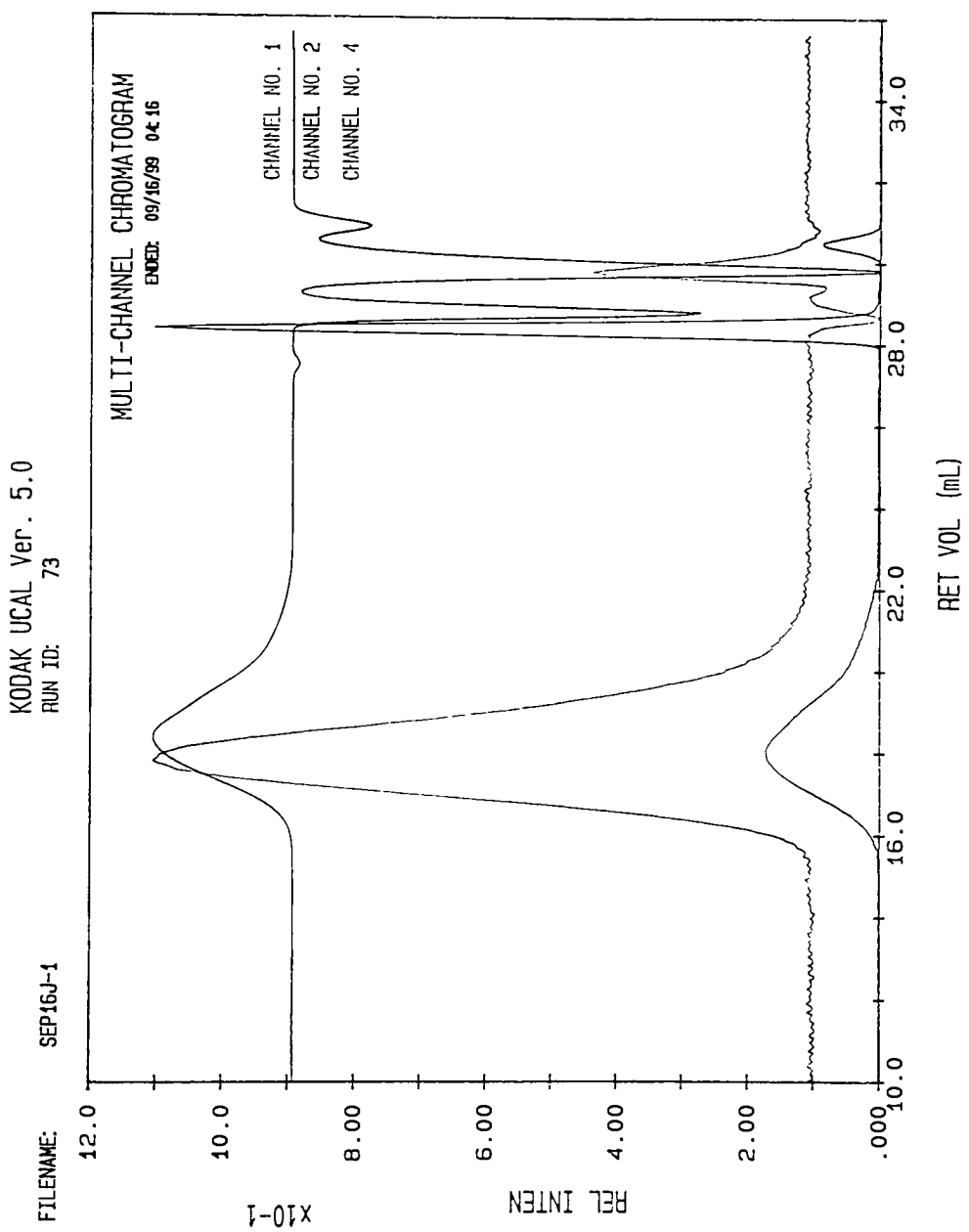
KODAK UCAL Ver. 5.0
FILENAME: SEP16J-1
RUN ID: 73
MULTI-CHANNEL CHROMATOGRAM
ENDED: 09/16/99 04:16
CHANNEL NO. 1
CHANNEL NO. 2
CHANNEL NO. 4
x10-1
REL INTEN
RET VOL (mL)
12.0
10.0
8.00
6.00
4.00
2.00
.000
10.0
16.0
22.0
28.0
34.0

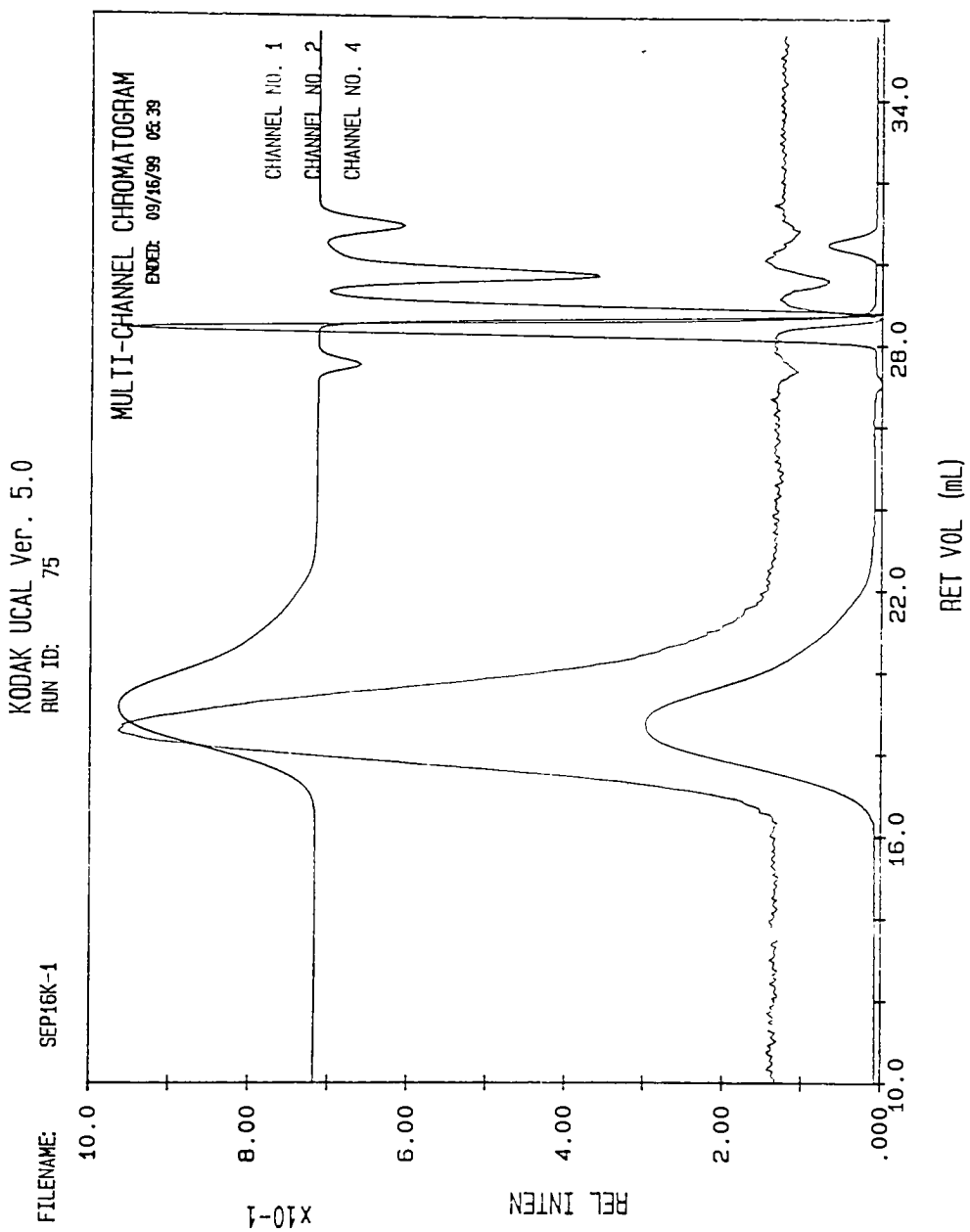
KODAK UCAL Ver. 5.0
FILENAME: SEP16K-1
RUN ID: 75
MULTI-CHANNEL CHROMATOGRAM
ENDED: 09/16/99 05:39
CHANNEL NO. 1
CHANNEL NO. 2
CHANNEL NO. 4
REL INTEN
x10-1
10.0
8.00
6.00
4.00
2.00
.000
10.0
16.0
22.0
28.0
34.0
RET VOL (mL)

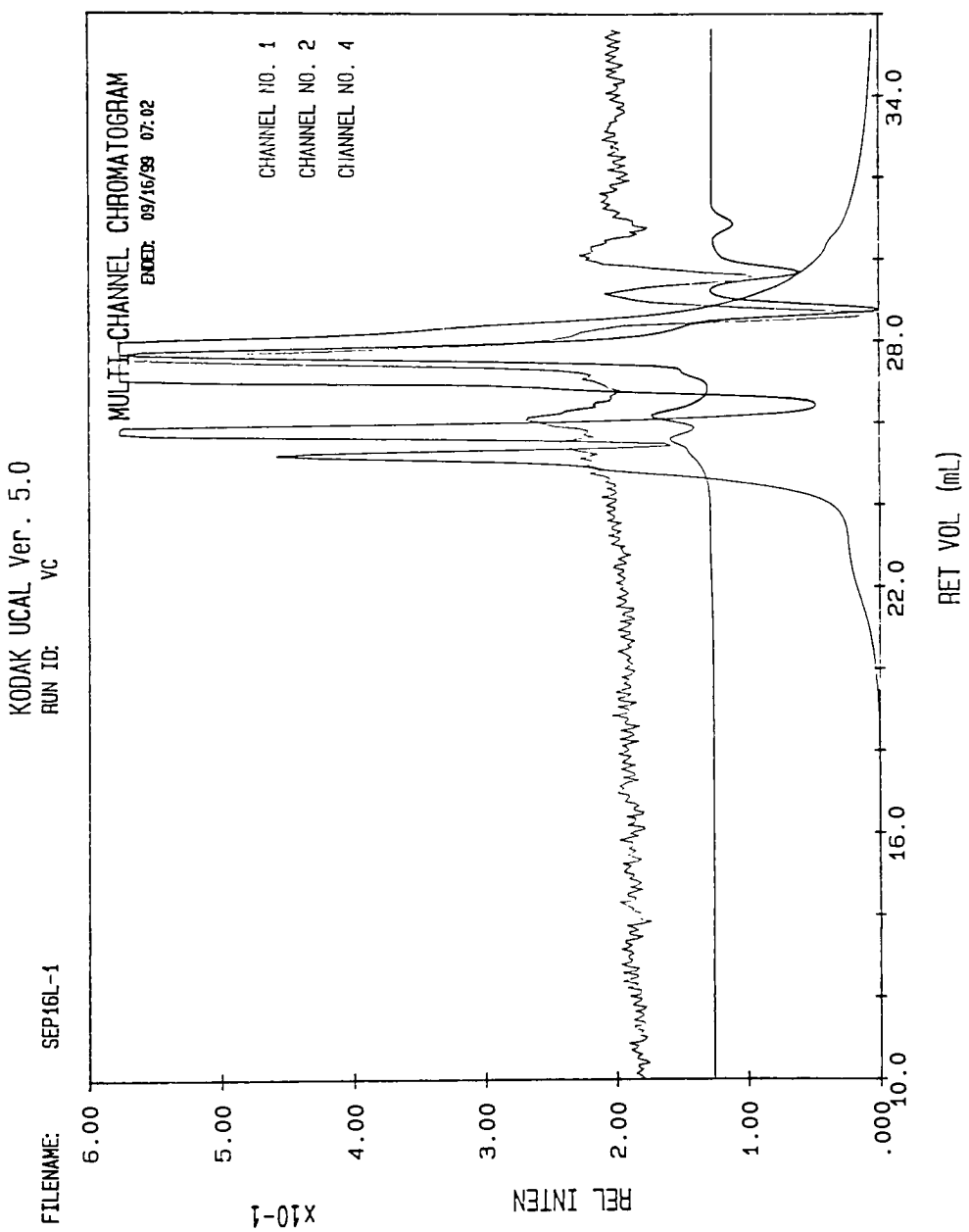
KODAK UCAL Ver. 5.0
FILENAME: SEP16L-1
RUN ID: VC
MULTI CHANNEL CHROMATOGRAM
09/16/99 07:02
CHANNEL NO. 1
CHANNEL NO. 2
CHANNEL NO. 4
x10-1
REL INTEN
6.00
5.00
4.00
3.00
2.00
1.00
.000
10.0
16.0
22.0
28.0
34.0
RET VOL (mL)

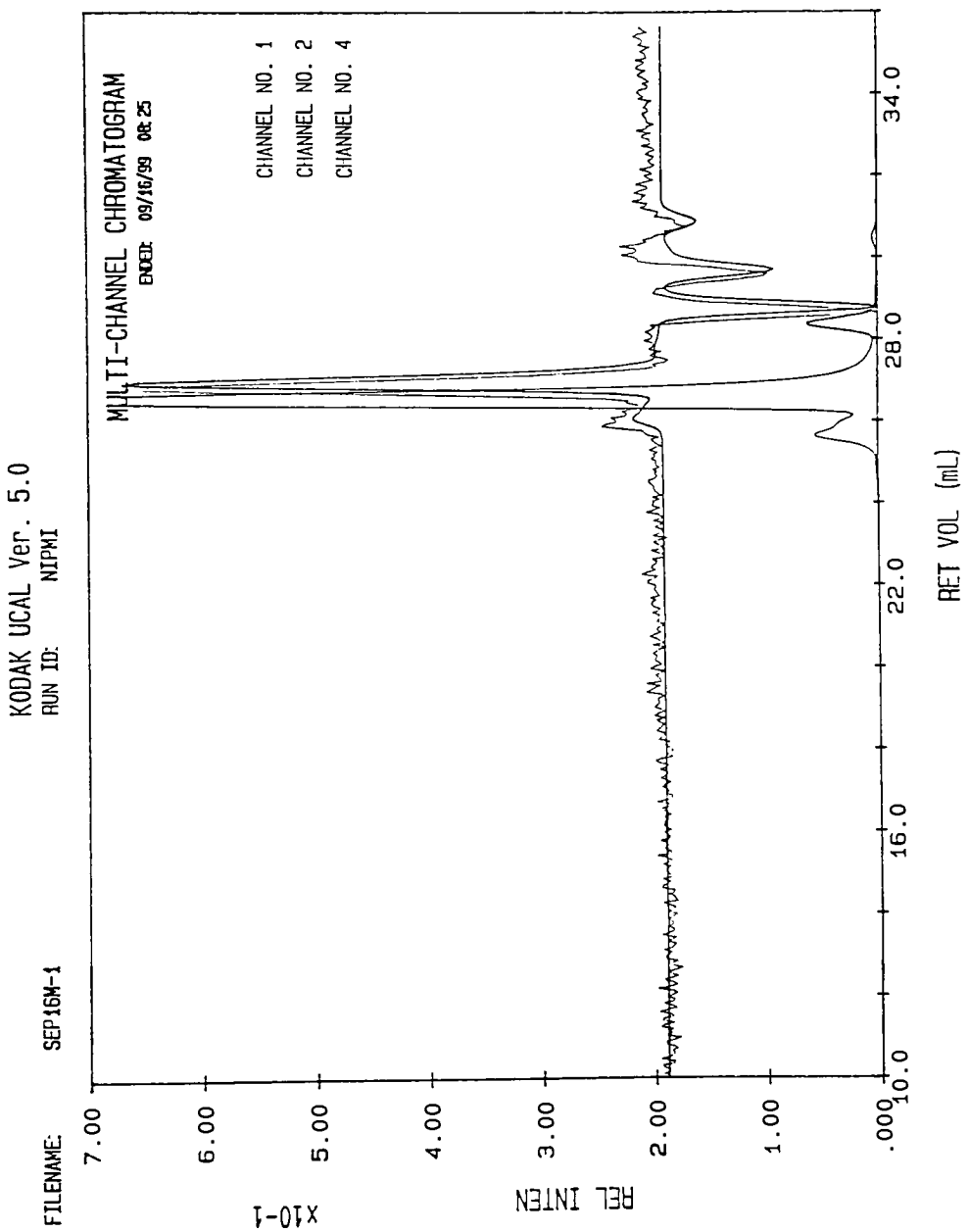
KODAK UCAL Ver. 5.0
FILENAME: SEP16M-1
RUN ID: NIPMI
MULTI-CHANNEL CHROMATOGRAM
ENDED: 09/16/99 08:25
CHANNEL NO. 1
CHANNEL NO. 2
CHANNEL NO. 4
7.00
6.00
5.00
4.00
3.00
2.00
1.00
.000
X10-1
REL INTEN
10.0
16.0
22.0
28.0
34.0
RET VOL (mL)

Appendix E: SEC Molecular Weight Distributions of Copolymers

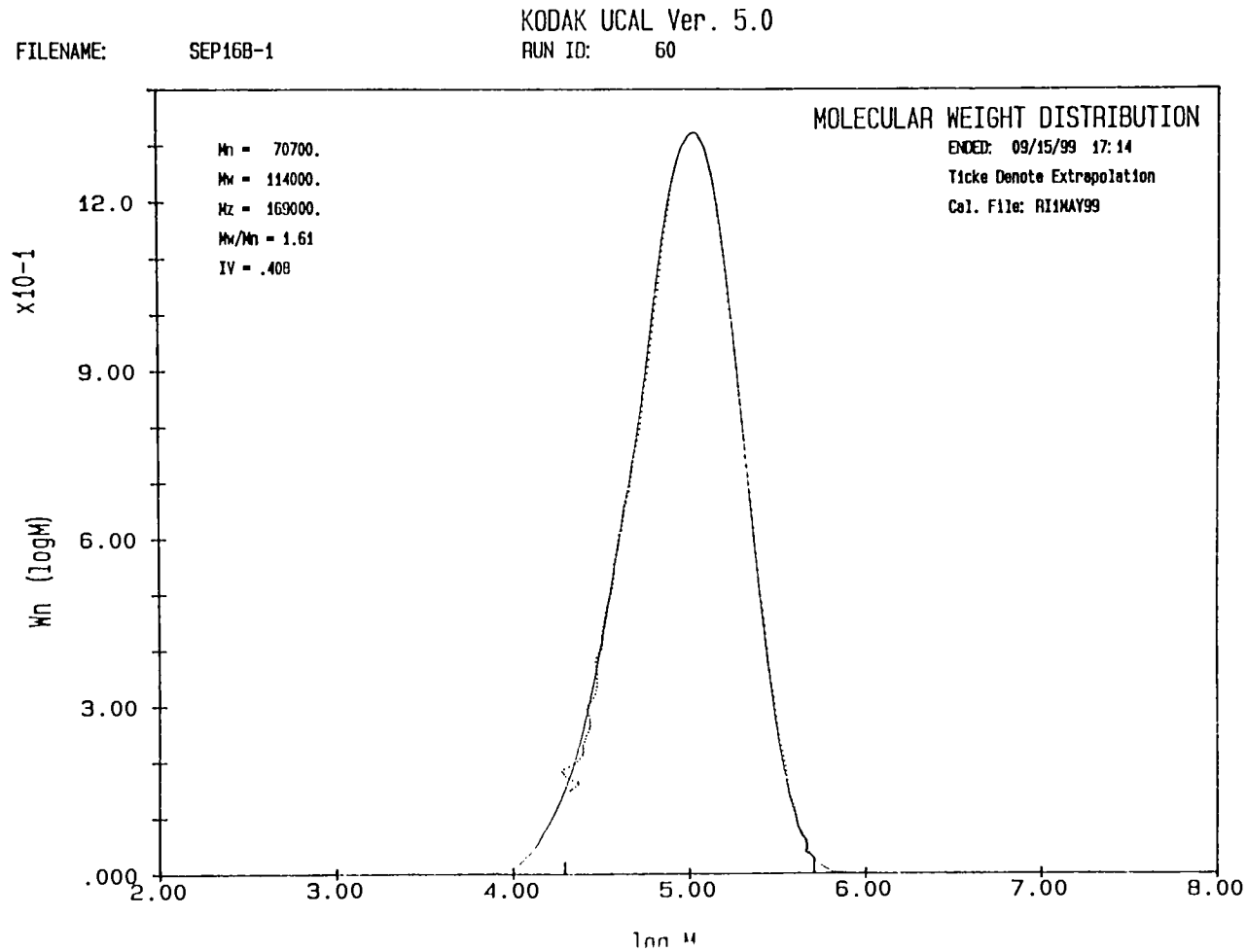
KODAK UCAL Ver. 5.0
FILENAME: SEP16B-1
RUN ID: 60
MOLECULAR WEIGHT DISTRIBUTION
ENDED: 09/15/99 17:14
Ticke Denote Extrapolation
Cal. File: RI1MAY99
Mn = 70700.
Mw = 114000.
Mz = 169000.
Mw/Mn = 1.61
IV = .408
x10-1
Wn (logM)
12.0
9.00
6.00
3.00
.000
2.00
3.00
4.00
5.00
6.00
7.00
8.00
log M

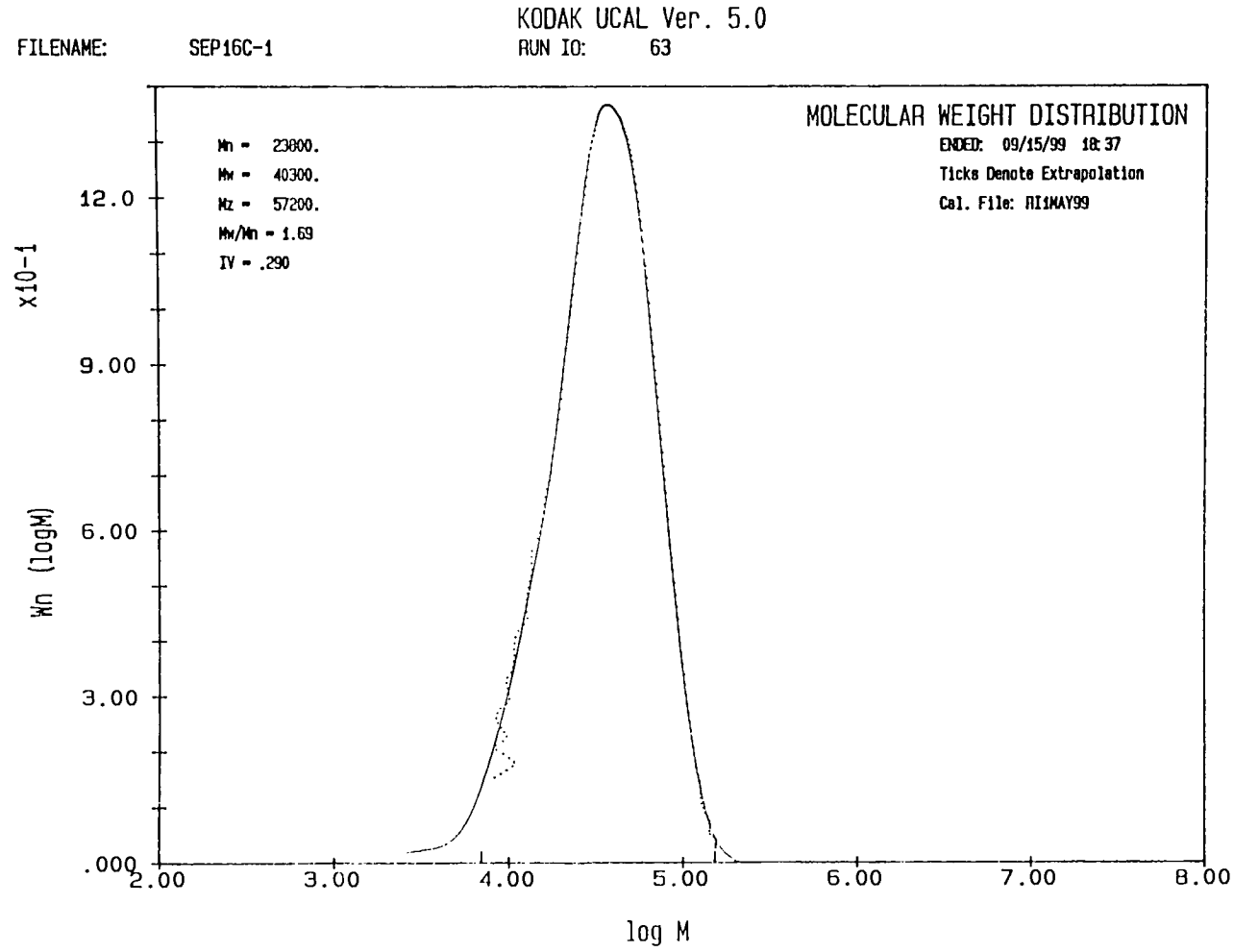
KODAK UCAL Ver. 5.0
FILENAME: SEP16C-1
RUN IO: 63
MOLECULAR WEIGHT DISTRIBUTION
ENDED: 09/15/99 18:37
Ticks Denote Extrapolation
Cal. File: M11MAY99
Mn = 23800.
Mw = 40300.
Mz = 57200.
Mw/Mn = 1.69
IV = .290
X10-1
Wn (logM)
12.0
9.00
6.00
3.00
.000
2.00
3.00
4.00
5.00
6.00
7.00
8.00
log M

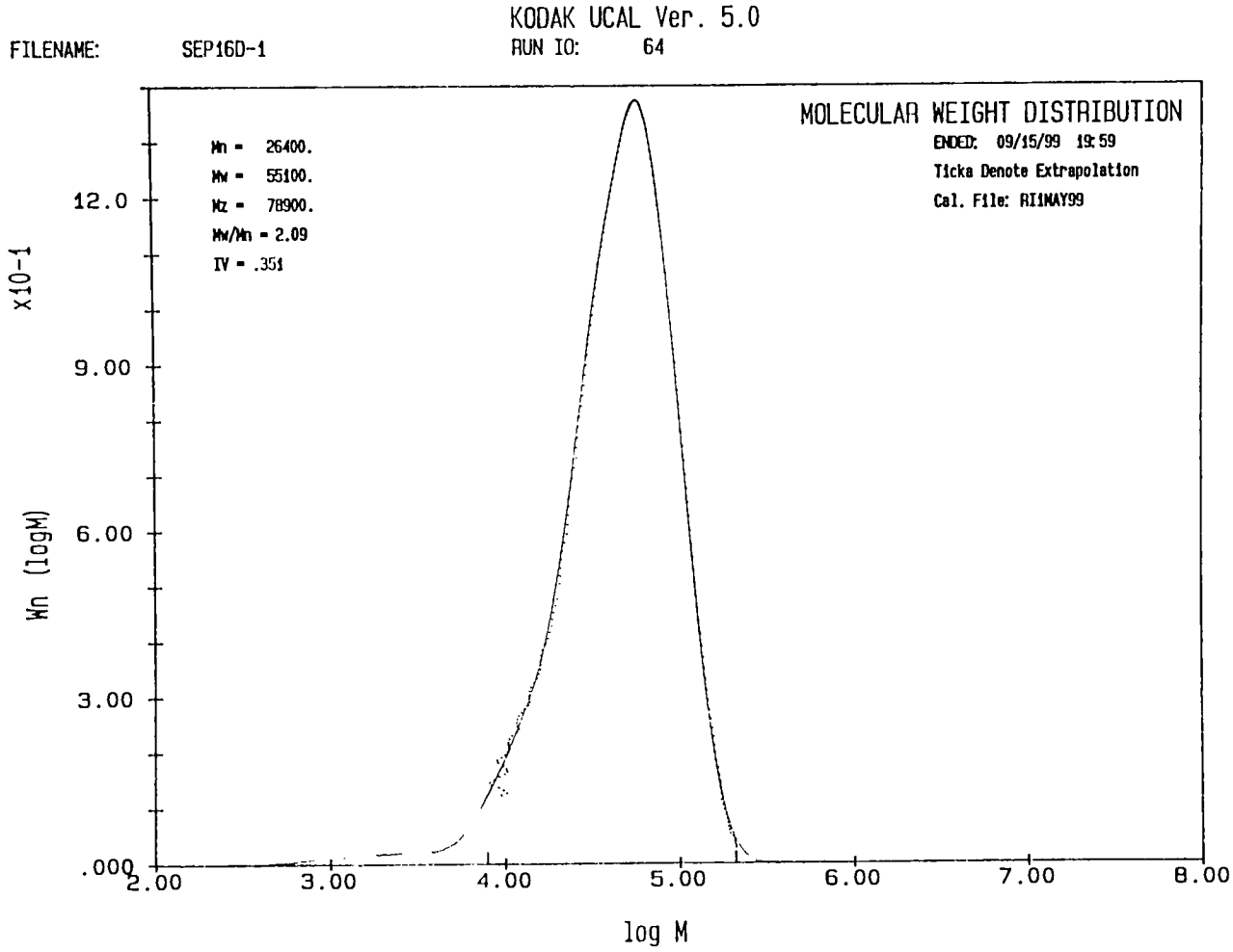
KODAK UCAL Ver. 5.0
FILENAME: SEP16D-1
RUN IO: 64
MOLECULAR WEIGHT DISTRIBUTION
ENDED: 09/15/99 19:59
Ticks Denote Extrapolation
Cal. File: RI1MAY99
Mn = 26400.
Mw = 55100.
Mz = 78900.
Mw/Mn = 2.09
IV = .351
x10-1
Wn (logM)
12.0
9.00
6.00
3.00
.000
2.00
3.00
4.00
5.00
6.00
7.00
8.00
log M

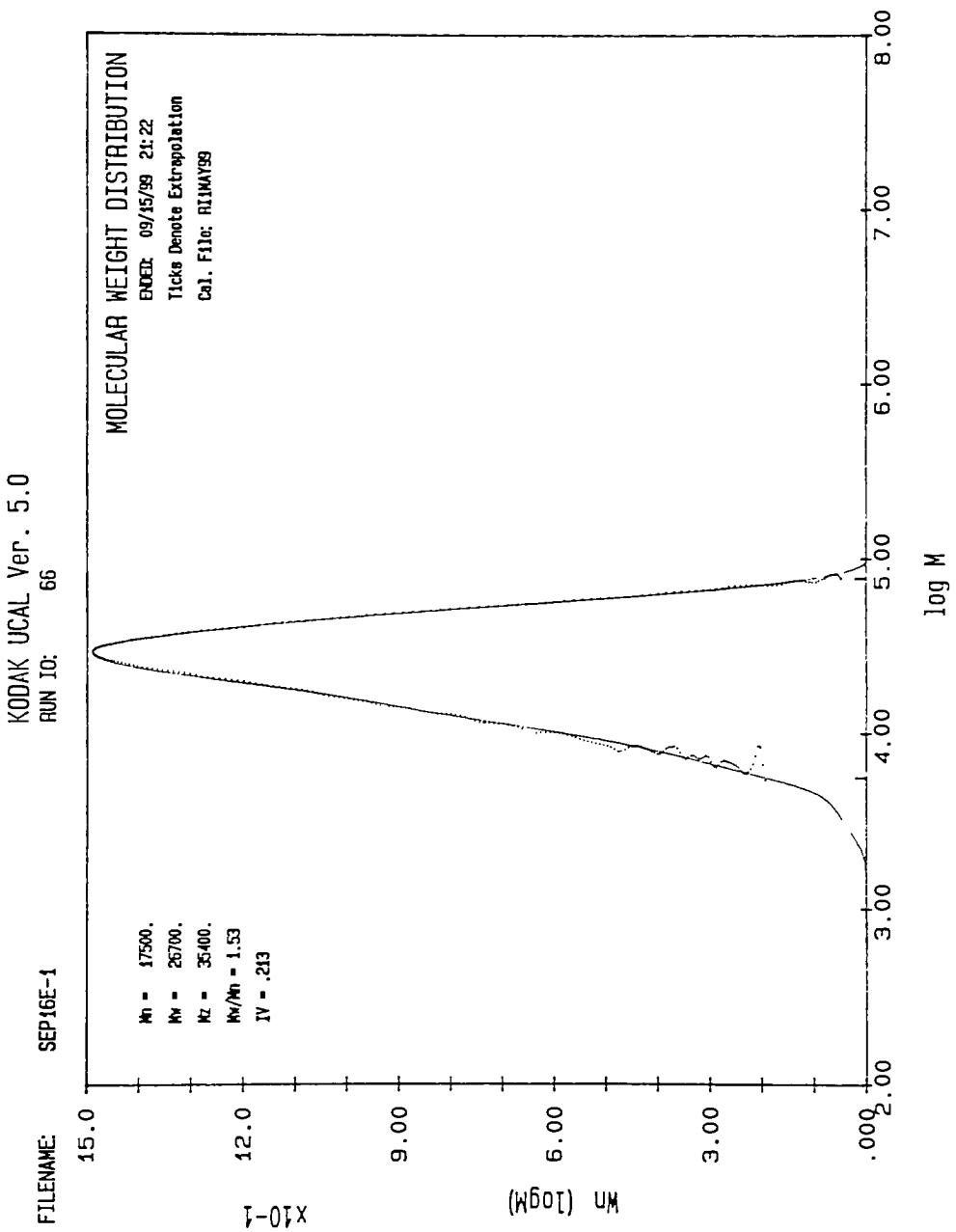
KODAK UCAL Ver. 5.0
RUN IO: 66
FILENAME: SEP16E-1
MOLECULAR WEIGHT DISTRIBUTION
ENDED: 09/15/99 21:22
Ticks Denote Extrapolation
Cal. File: A11MAY99
Mn = 17500.
Mw = 26700.
Mz = 35400.
Mw/Mn = 1.53
IV = .213
x10-1
Wn (logM)
log M
15.0
12.0
9.00
6.00
3.00
.000
2.00
3.00
4.00
5.00
6.00
7.00
8.00

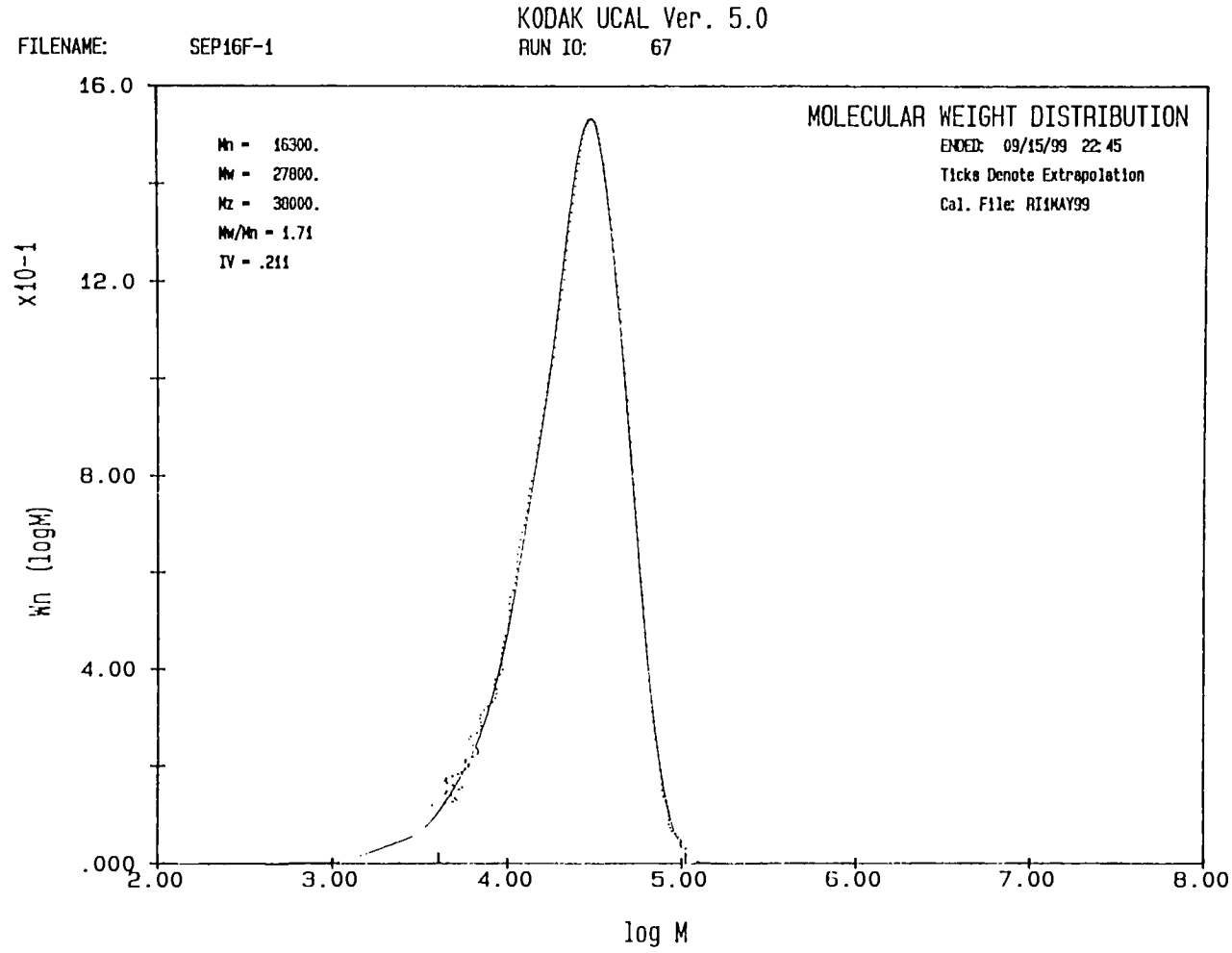
KODAK UCAL Ver. 5.0
FILENAME: SEP16F-1
RUN IO: 67
MOLECULAR WEIGHT DISTRIBUTION
Mn = 16300.
Mw = 27800.
Mz = 38000.
Mw/Mn = 1.71
IV = .211
ENDED: 09/15/99 22:45
Ticks Denote Extrapolation
Cal. File: RI1MAY99
X10-1
Wn (logM)
16.0
12.0
8.00
4.00
.000
2.00
3.00
4.00
5.00
6.00
7.00
8.00
log M

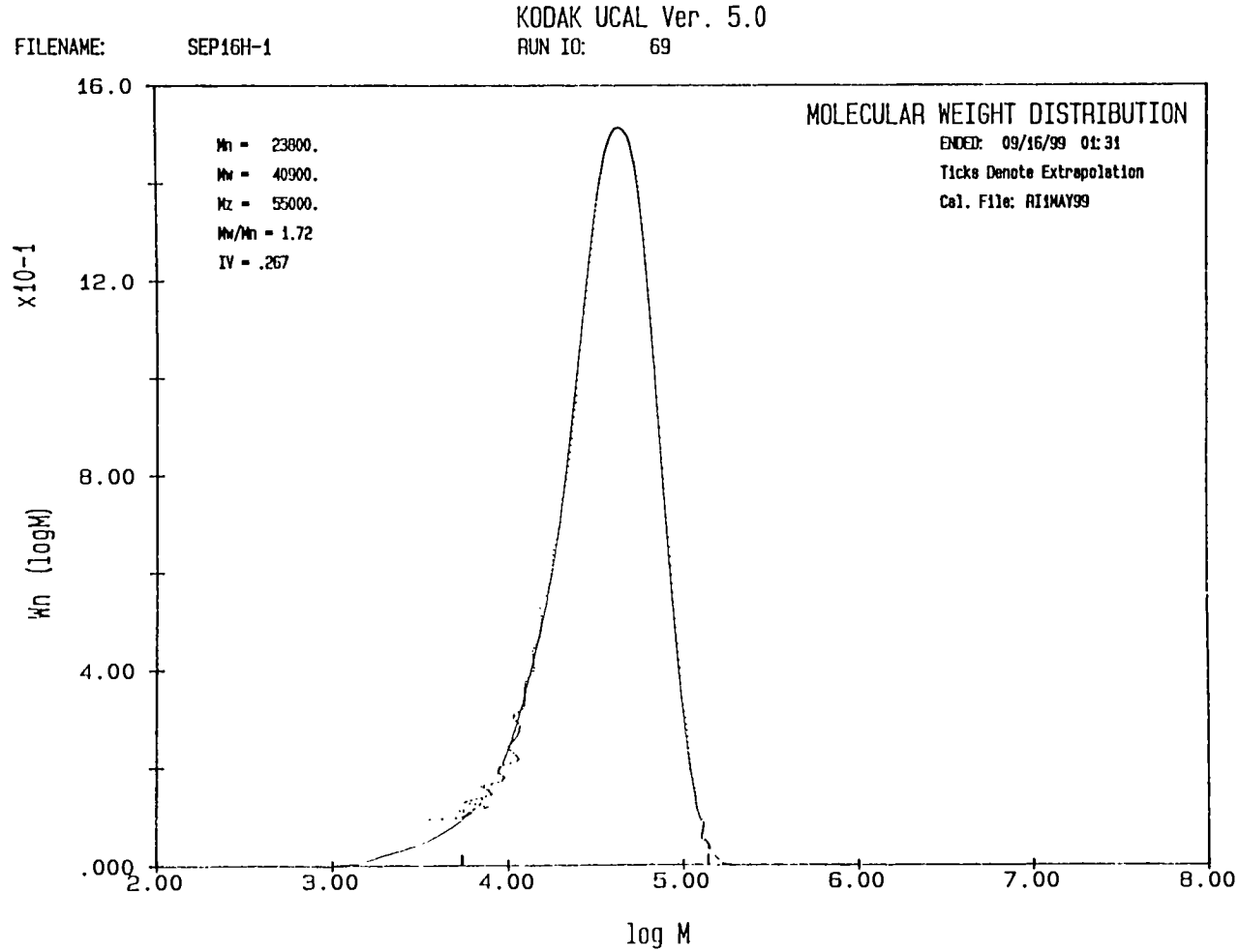
KODAK UCAL Ver. 5.0
FILENAME: SEP16H-1
RUN IO: 69
MOLECULAR WEIGHT DISTRIBUTION
ENDED: 09/16/99 01:31
Ticks Denote Extrapolation
Cal. File: RI1MAY99
Mn = 23800.
Mw = 40900.
Mz = 55000.
Mw/Mn = 1.72
IV = .267
x10-1
Wn (logM)
16.0
12.0
8.00
4.00
.000
2.00
3.00
4.00
5.00
6.00
7.00
8.00
log M

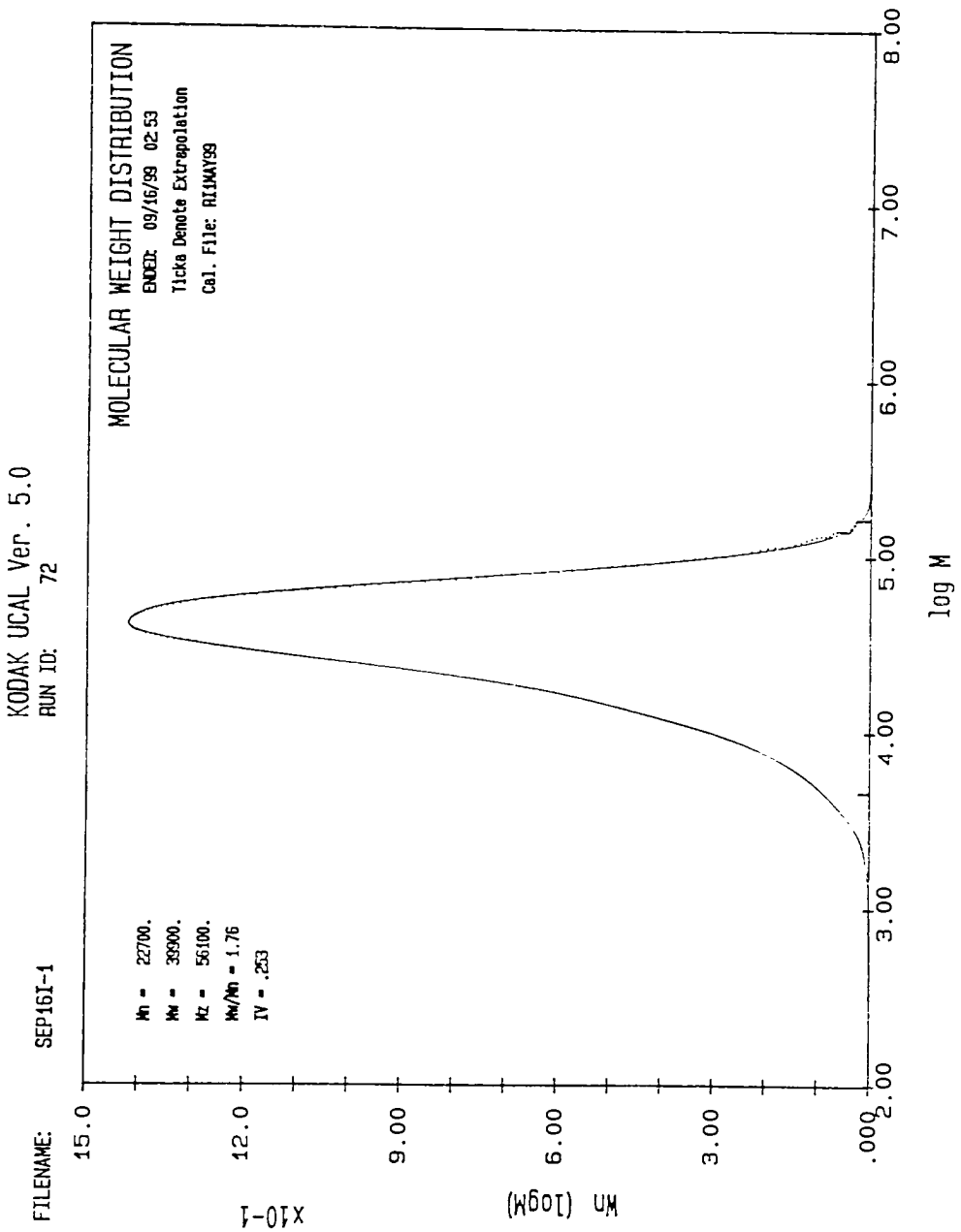
KODAK UCAL Ver. 5.0
RUN ID: 72
FILENAME: SEP16I-1
MOLECULAR WEIGHT DISTRIBUTION
ENDED: 09/16/99 02:53
Ticks Denote Extrapolation
Cal. File: RIIWAY99
Mn = 22700.
Mw = 39900.
Mz = 56100.
Mw/Mn = 1.76
IV = .253
X10-1
Wn (logM)
log M
15.0
12.0
9.00
6.00
3.00
.000
2.00
3.00
4.00
5.00
6.00
7.00
8.00

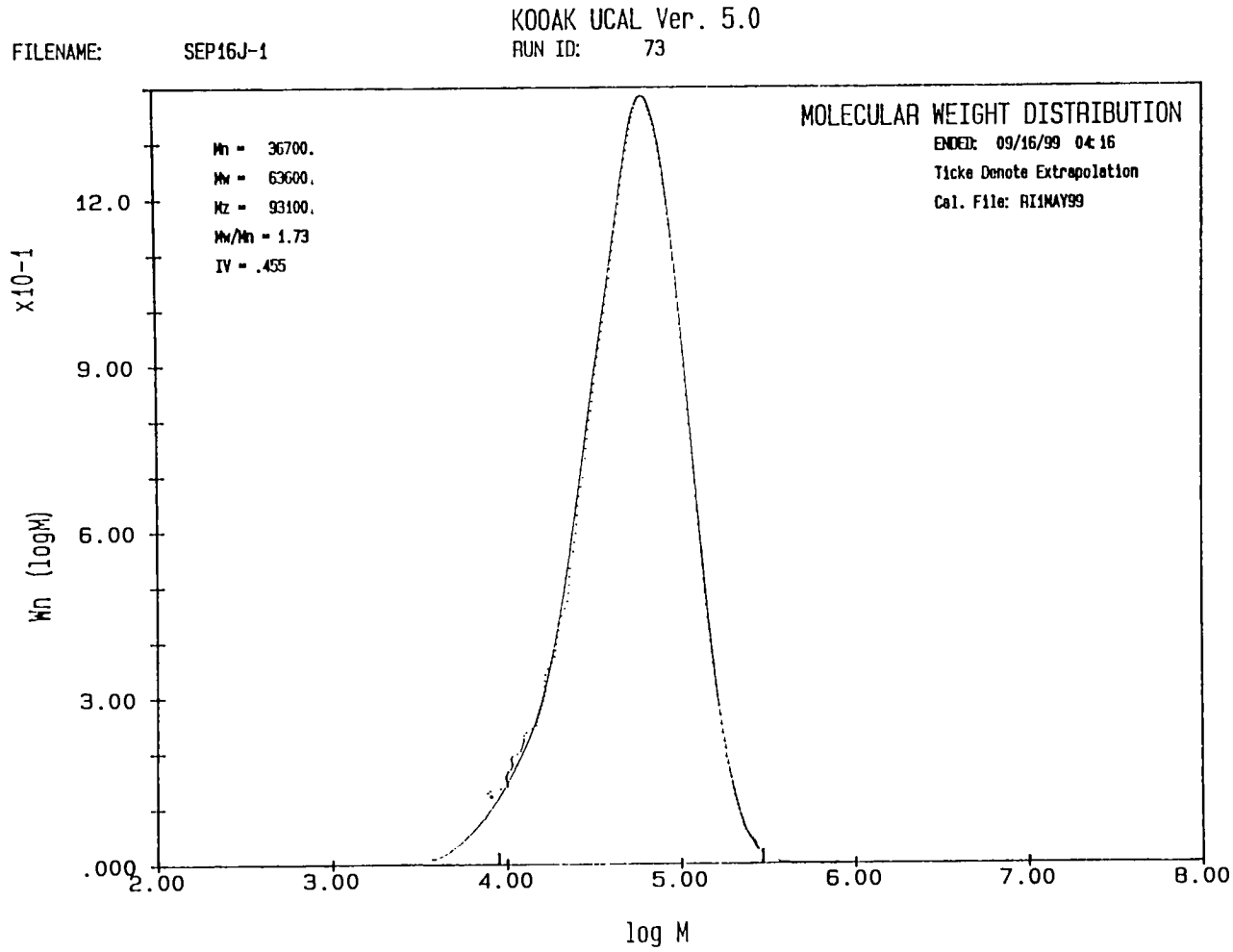
KOOAK UCAL Ver. 5.0
FILENAME: SEP16J-1
RUN ID: 73
MOLECULAR WEIGHT DISTRIBUTION
ENDED: 09/16/99 04:16
Ticke Denote Extrapolation
Cal. File: RI1MAY99
Mn = 36700.
Mw = 63600.
Mz = 93100.
Mw/Mn = 1.73
IV = .455
x10-1
Wn (logM)
12.0
9.00
6.00
3.00
.000
2.00
3.00
4.00
5.00
6.00
7.00
8.00
log M

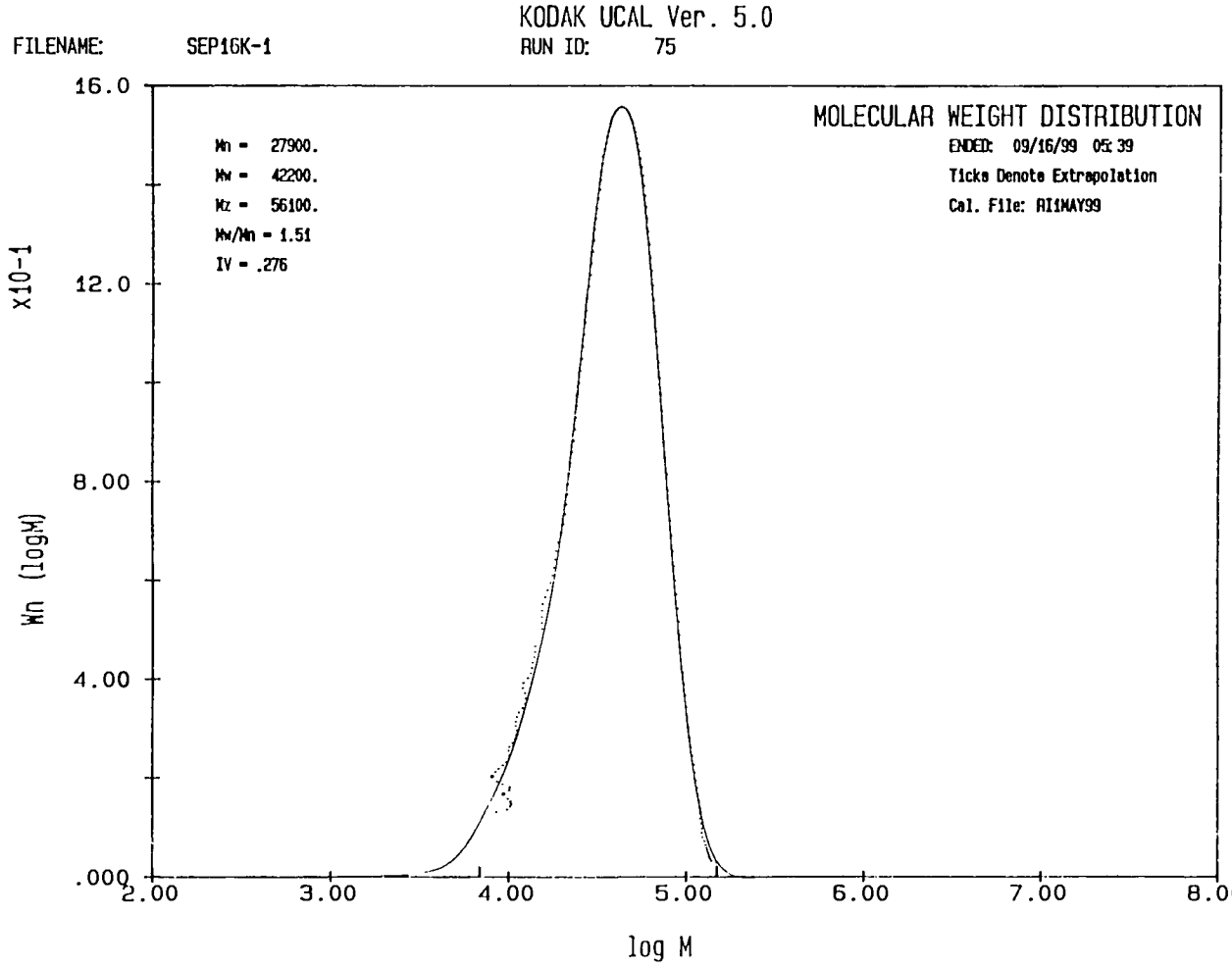
KODAK UCAL Ver. 5.0
FILENAME: SEP16K-1
RUN ID: 75
MOLECULAR WEIGHT DISTRIBUTION
Mn = 27900.
Mw = 42200.
Mz = 56100.
Mw/Mn = 1.51
IV = .276
ENDED: 09/16/99 05:39
Ticks Denote Extrapolation
Cal. File: AI1MAY99
16.0
12.0
8.00
4.00
.000
X10-1
Wn (logM)
2.00
3.00
4.00
5.00
6.00
7.00
8.00
log M

Appendix F: Luminescence Spectra of Blends

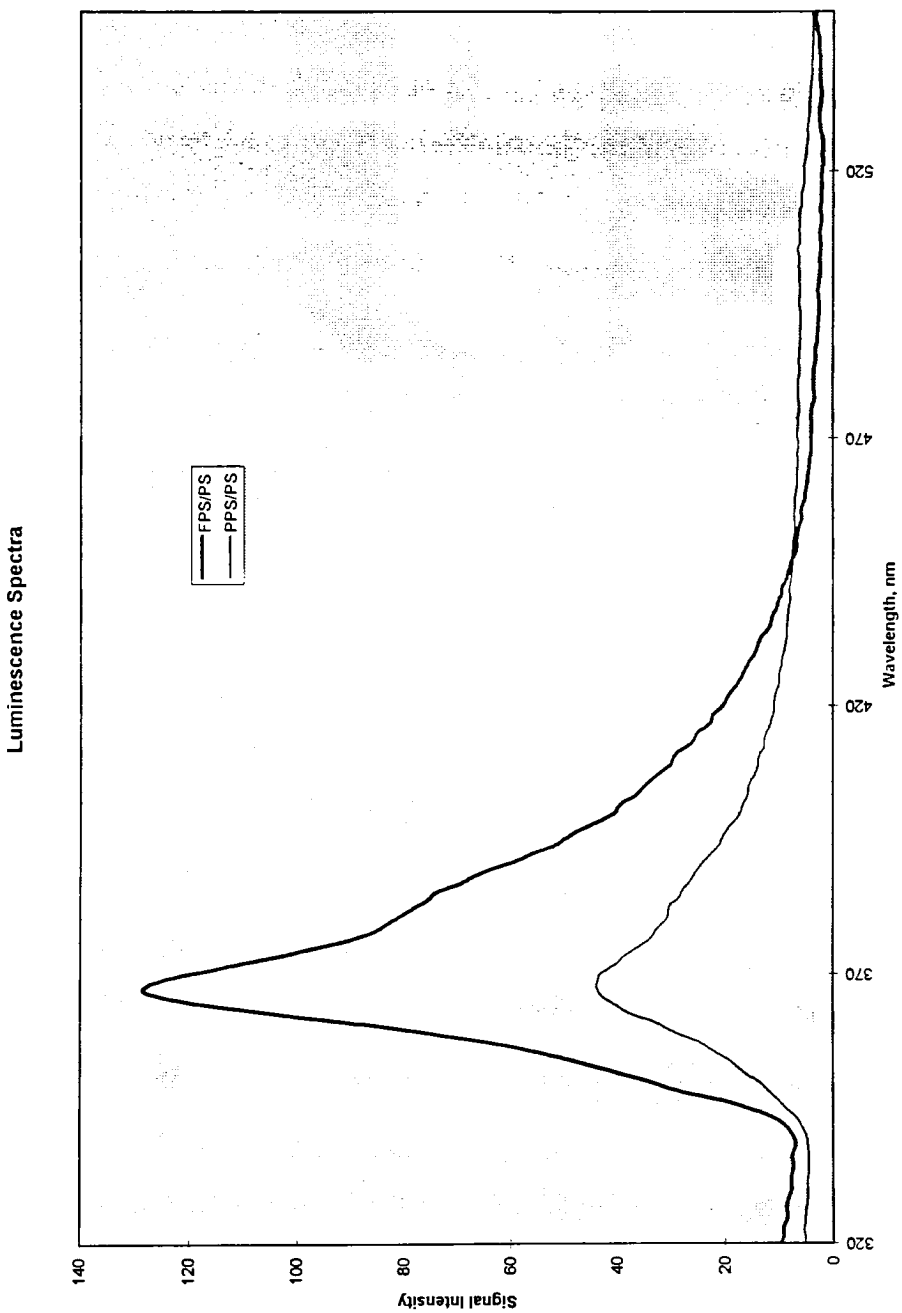
Luminescence Spectra
FPS/PS
PPS/PS
Signal Intensity
Wavelength, nm
0
20
40
60
80
100
120
140
320
370
420
470
520

F1

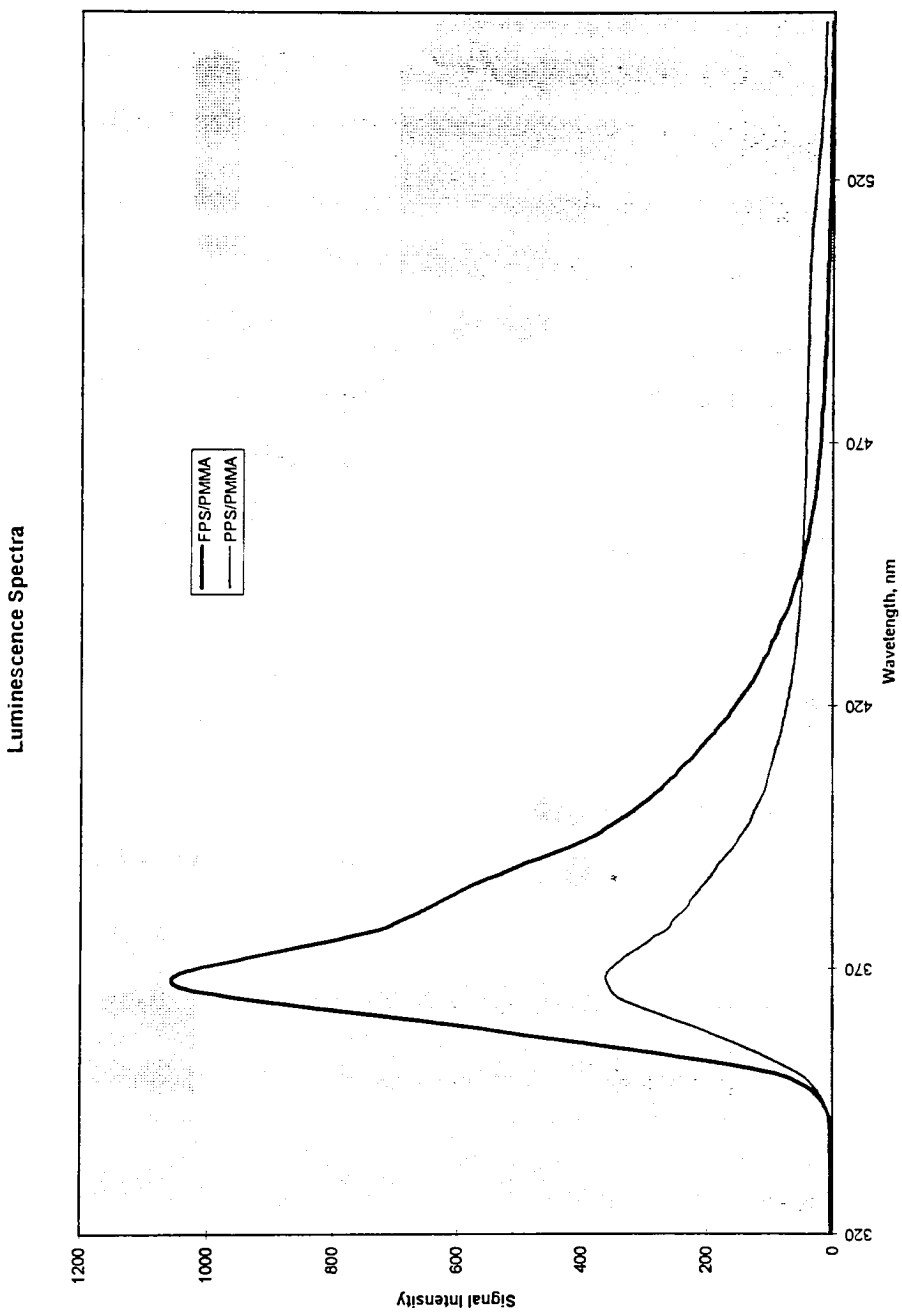
Luminescence Spectra
FPS/PMMA
PPS/PMMA
Signal Intensity
0
200
400
600
800
1000
1200
320
370
420
470
520
Wavelength, nm

F2

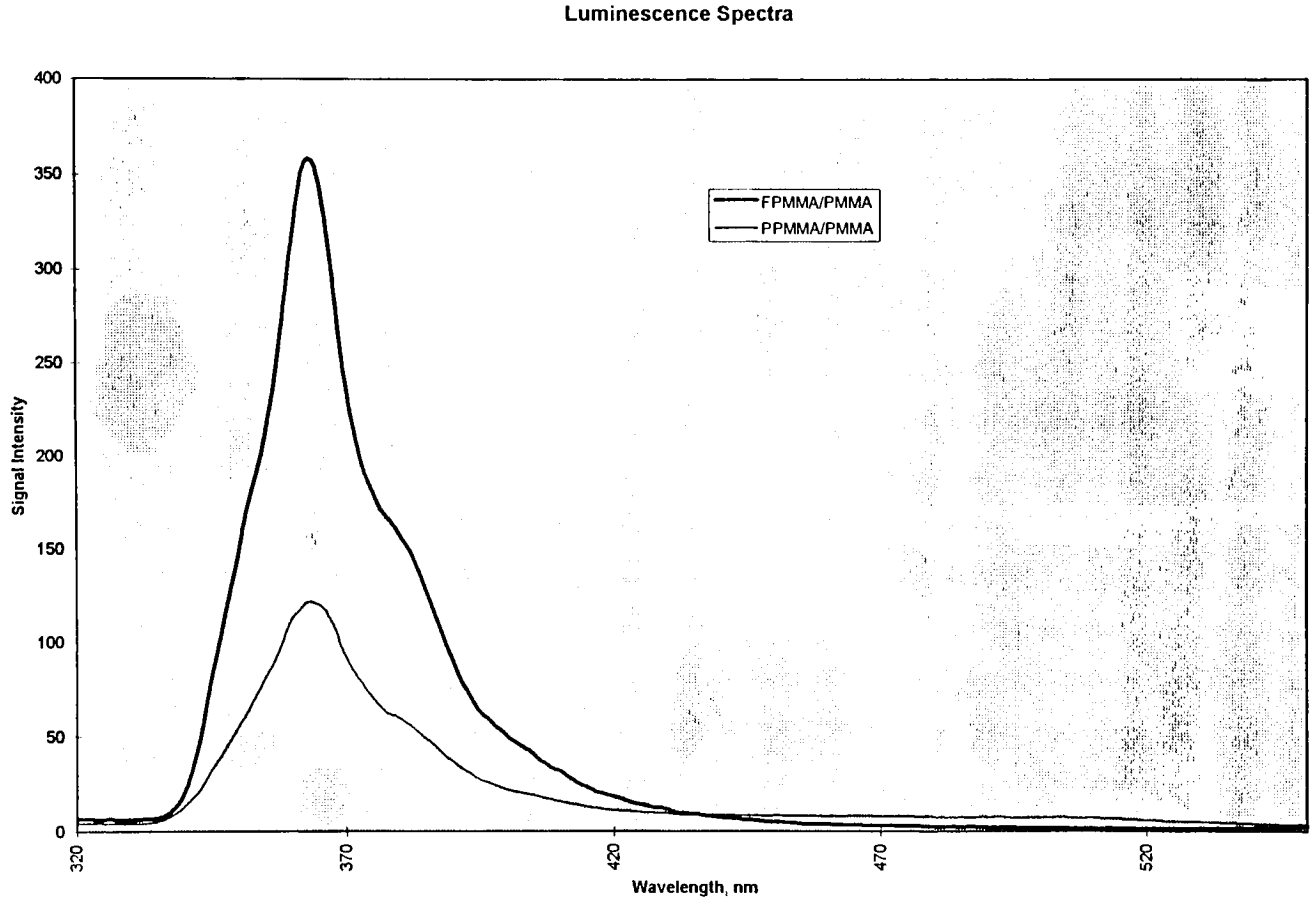
Luminescence Spectra
FPMMA/PMMA
PPMMA/PMMA
Signal Intensity
Wavelength, nm
400
350
300
250
200
150
100
50
0
320
370
420
470
520

F3

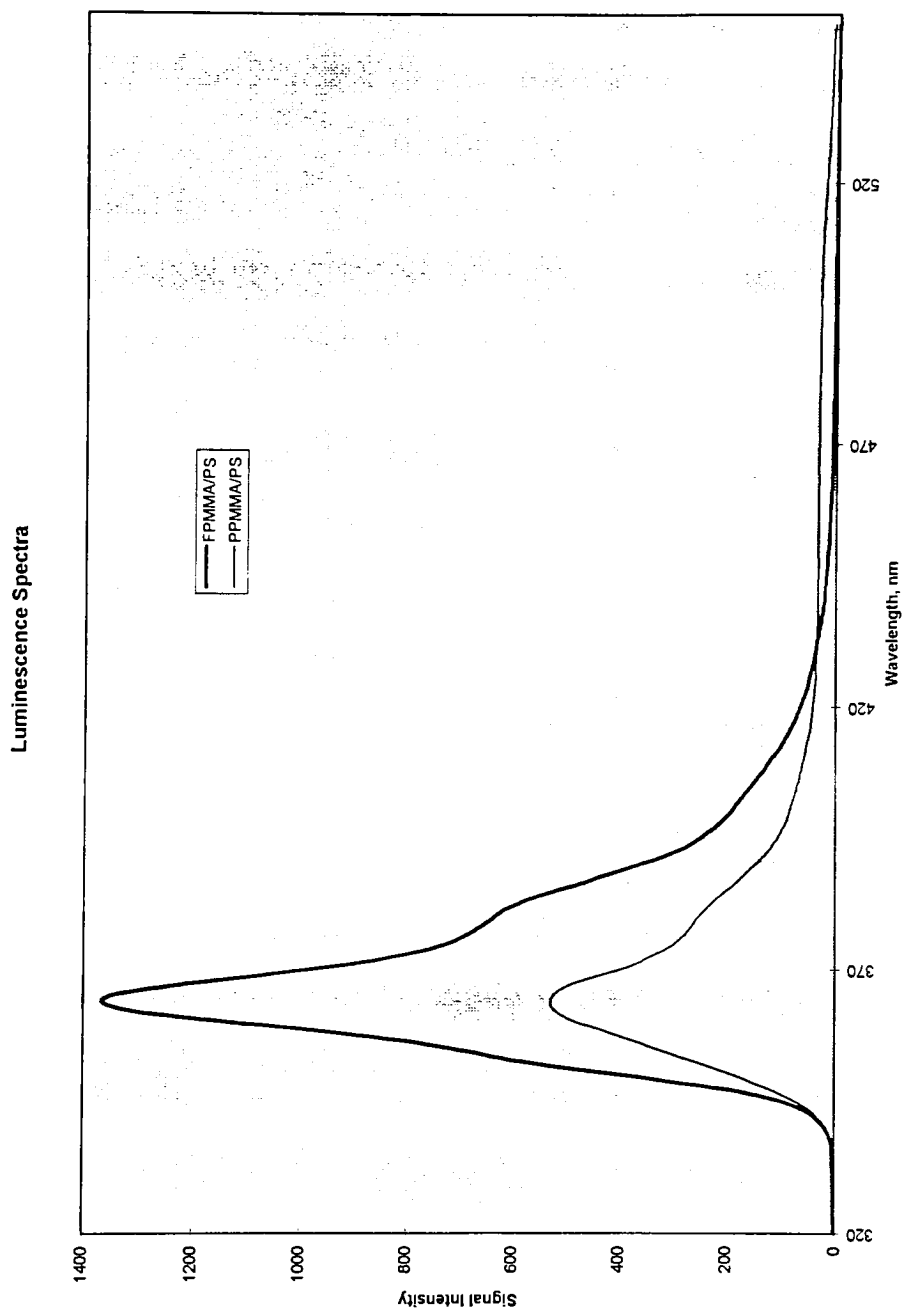
Luminescence Spectra
FPMMA/PS
PPMMA/PS
Signal Intensity
0
200
400
600
800
1000
1200
1400
320
370
420
470
520
Wavelength, nm

Luminescence Spectra
F50/50
P50/50
Signal Intensity
0
100
200
300
400
500
600
320
370
420
470
520
Wavelength, nm

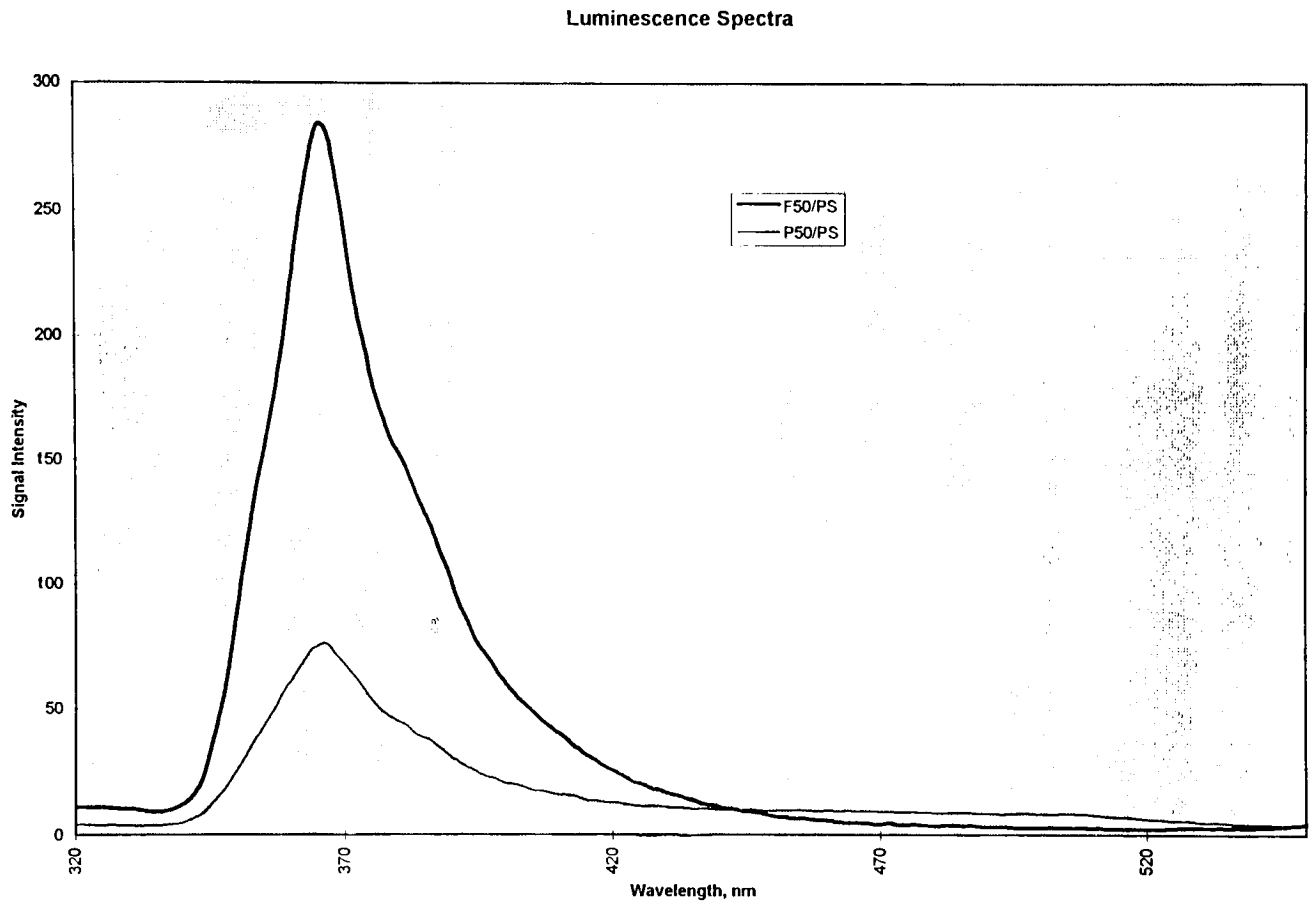
Luminescence Spectra
300
250
200
150
100
50
0
Signal Intensity
F50/PS
P50/PS
320
370
420
470
520
Wavelength, nm

Fig

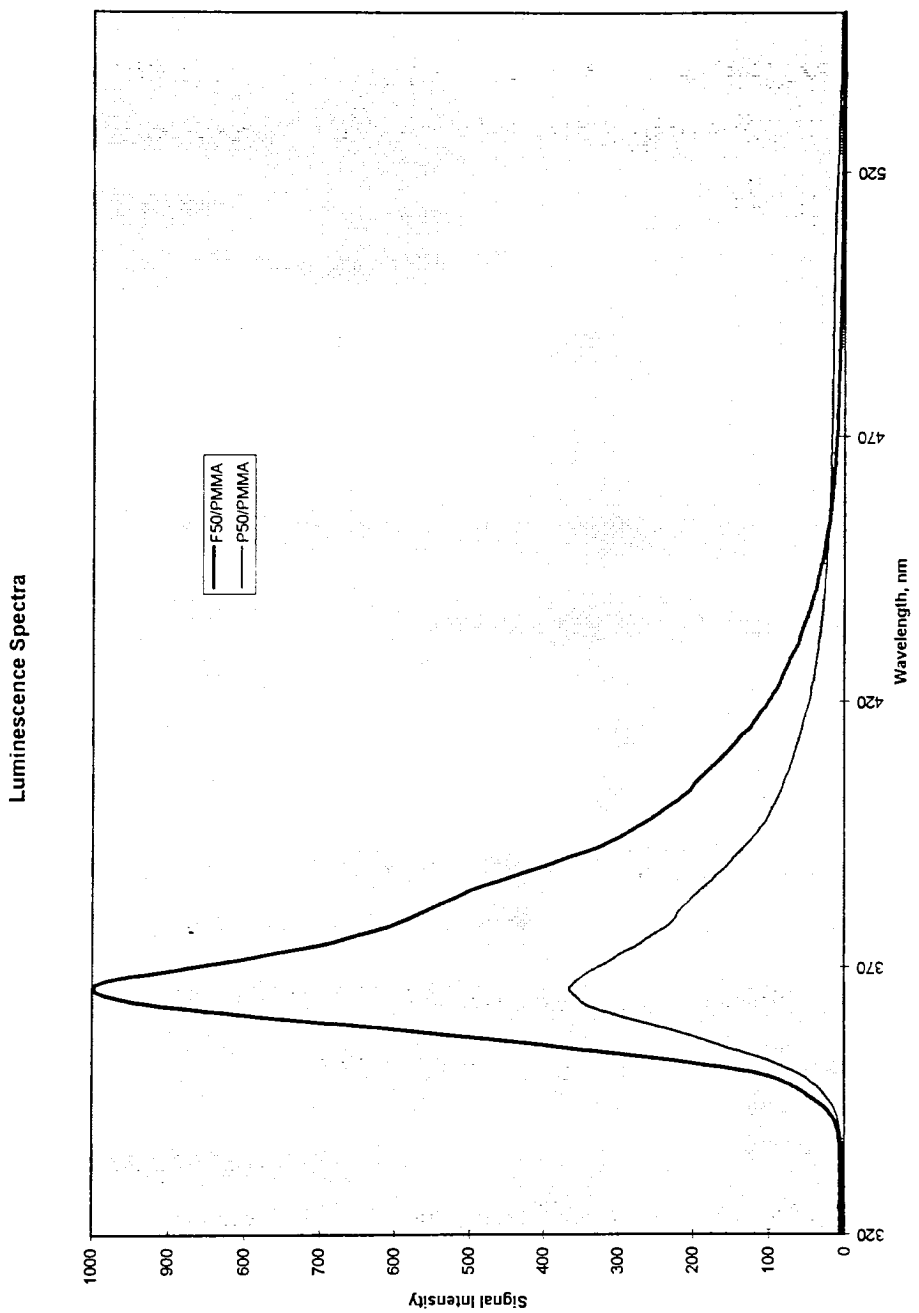
Luminescence Spectra
F50/PMMA
P50/PMMA
Signal Intensity
1000
900
800
700
600
500
400
300
200
100
0
320
370
420
470
520
Wavelength, nm

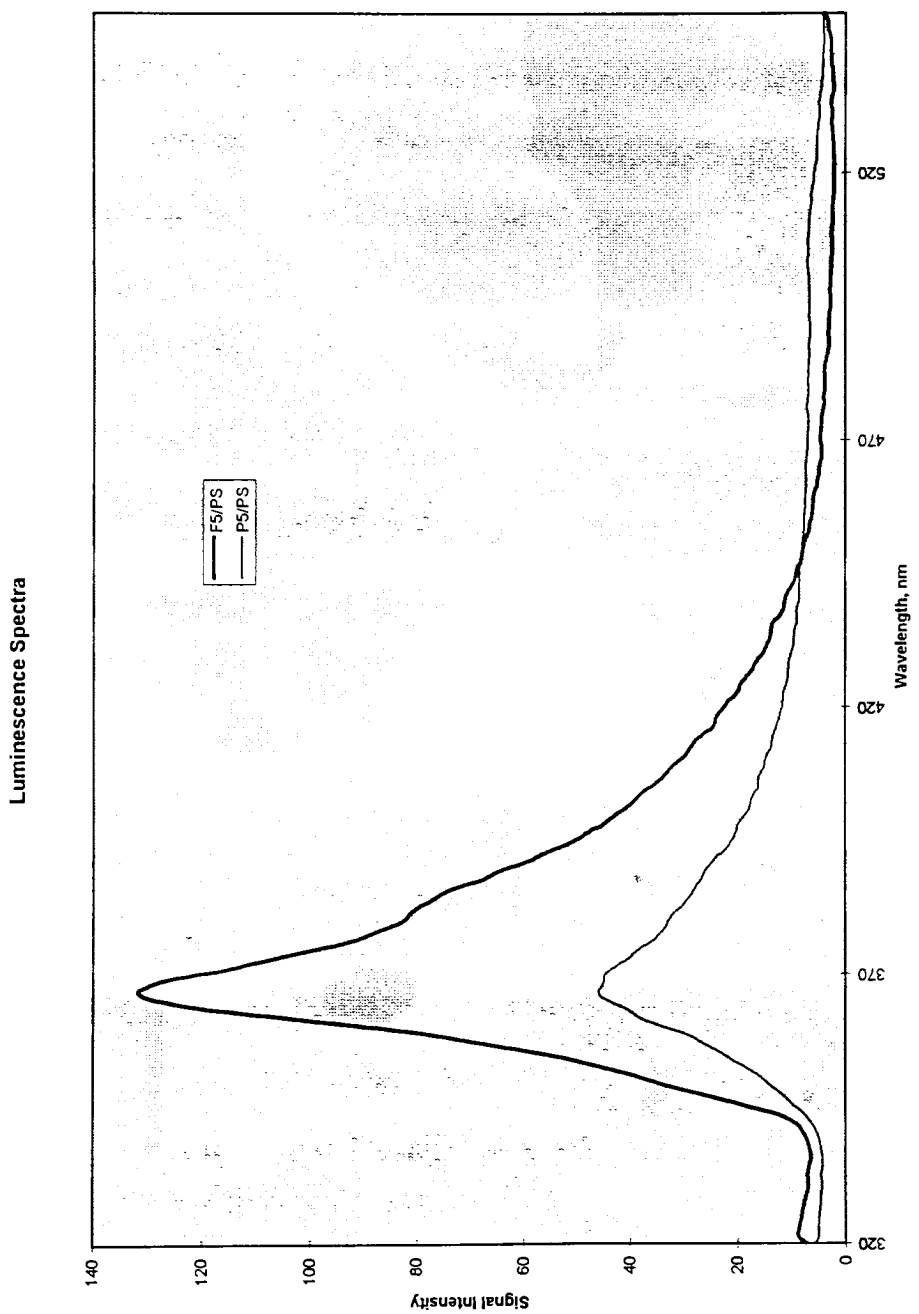
Luminescence Spectra
F5/PS
P5/PS
Signal Intensity
0
20
40
60
80
100
120
140
320
370
420
470
520
Wavelength, nm

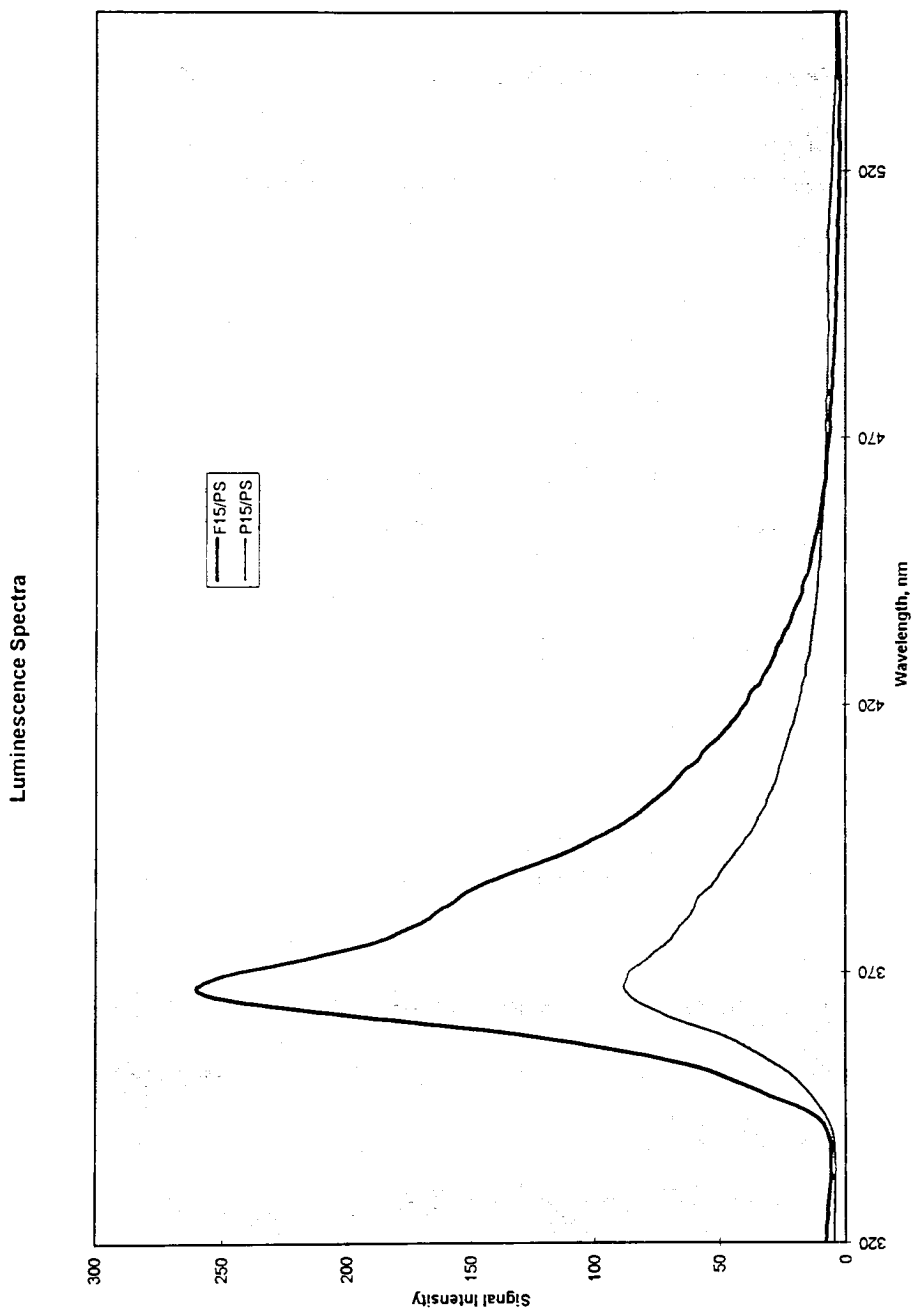
Luminescence Spectra
F15/PS
P15/PS
Signal Intensity
300
250
200
150
100
50
0
320
370
420
470
520
Wavelength, nm

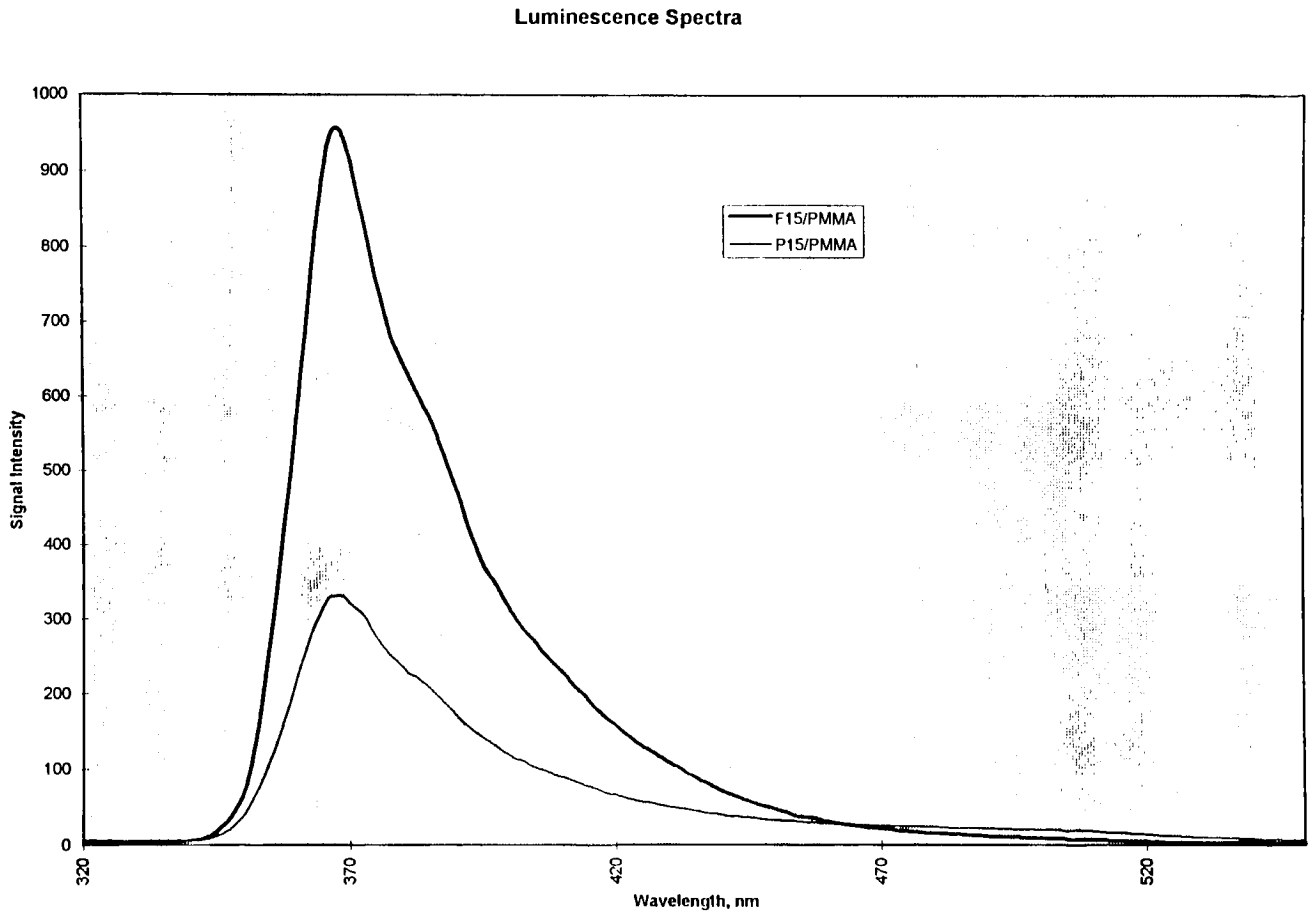
Luminescence Spectra
F15/PMMA
P15/PMMA
Signal Intensity
Wavelength, nm
0
100
200
300
400
500
600
700
800
900
1000
320
370
420
470
520

F10

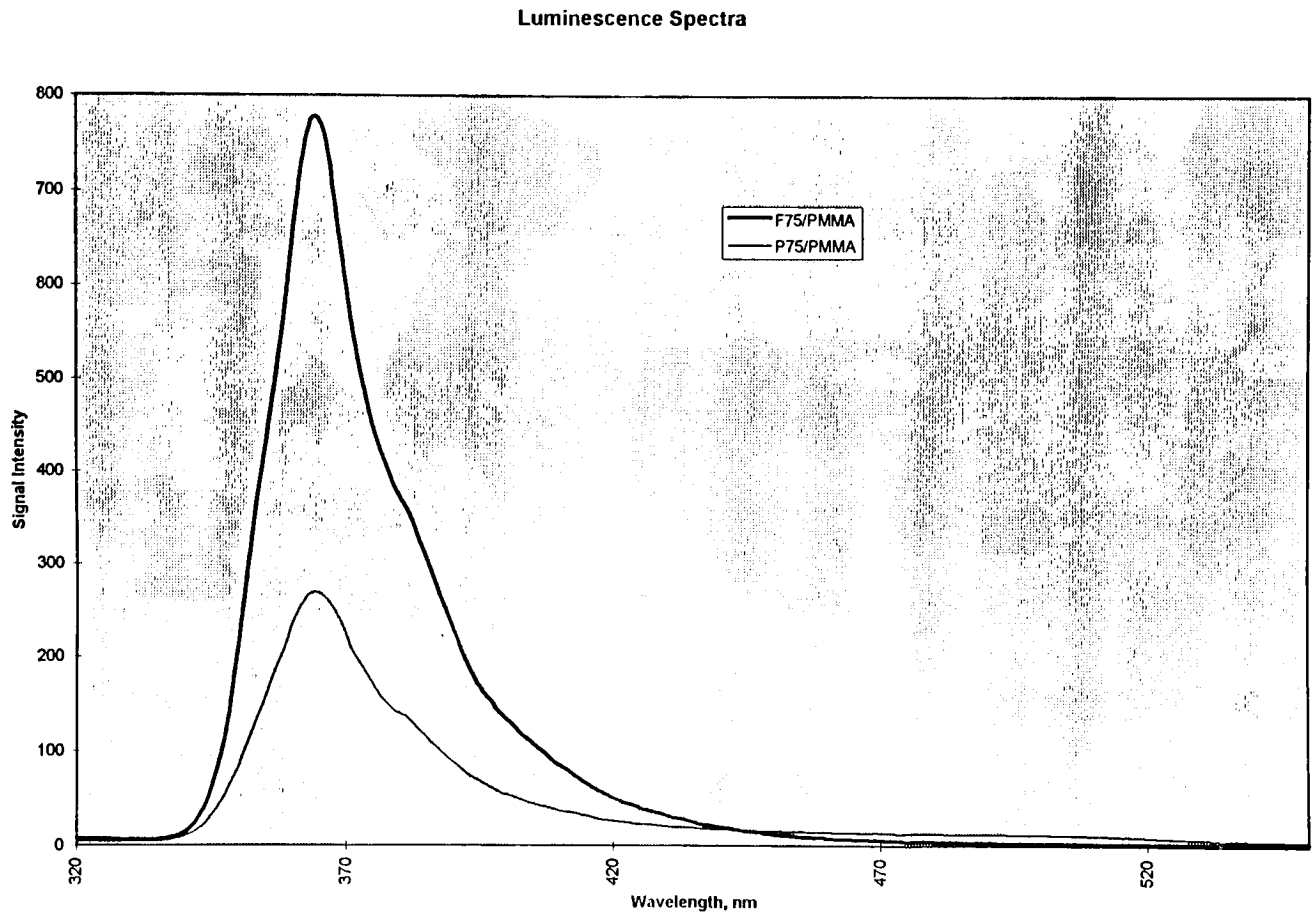
Luminescence Spectra
F75/PMMA
P75/PMMA
Signal Intensity
Wavelength, nm
800
700
600
500
400
300
200
100
0
320
370
420
470
520

F11